

ULTRASONIC DECROSSLINKING
OF CROSSLINKED POLY (ETHYLENE)

A Thesis

Presented to

The Graduate Faculty of The University of Akron

In Partial Fulfillment
of the Requirements for the Degree
Master of Science

John Allen Jenkins Junior

May, 2007

ULTRASONIC DECROSSLINKING
OF CROSSLINKED POLY (ETHYLENE)

John Allen Jenkins Junior

Thesis

Approved:

Accepted:

Advisor
Dr. Avraam I. Isayev

Department Chair
Dr. Sadhan C. Jana

Faculty Reader
Dr. Kyonsuku Min

Associate Dean of the College
Dr. Ernst Von Meerwall

Faculty Reader
Dr. Thein Kyu

Dean of the Graduate School
Dr. George R. Newkome

Department Chair
Dr. Sadhan C. Jana

Date

ABSTRACT

Decrosslinking of crosslinked polyethylene with the aid of ultrasonics is considered in this study. Polyethylene is crosslinked with peroxide by heating and compression molding and then subjected to various levels of ultrasonic energies to break the bonds in the crosslinked polyethylene network. Properties of the resulting materials are then compared to original properties to determine the usefulness of the process. Apparatus used to perform continuous decrosslinking includes a one-inch single screw Killion extruder for pumping of the crosslinked polyethylene into a die fitted with the ultrasonic device. The die is designed to allow the material to pass through an area where it is uniformly subjected to ultrasonic energies of various levels. The ultrasonic energy is introduced to the material through a stepped horn using a Branson power source. During processing, conditions were set that included pressures and time for the static experiments, barrel temperatures, flow rates, and ultrasonic power consumption for the continuous experiment.

Static experiments on crosslinked polyethylene were performed where specific amounts of crosslinked material were exposed to controlled ultrasound energy. This apparatus used the same power source but was discontinuous.

Properties of treated and untreated material such as gel fraction, crosslink density, viscosity, and mechanical properties were measured. Comparisons of collected samples showed that the process is highly effective for decreasing linking of crosslinked polyethylene at specific processing conditions. Further study of this process will surely be beneficial.

ACKNOWLEDGEMENTS

The author dedicates this work to his dear wife Dr. Sirarpi Bicakci Jenkins. Without her gentle encouragement, this work would have surely remained undocumented.

The author would like to thank first, his advisor Prof. A. I. Isayev, for his valuable advice. Especially since at the time the advice was given, its value was not fully appreciated.

Thanks should also go to the friends made at The University of Akron's Polymer Engineering Department who continued to relentlessly remind and embarrass the author until the work was finished.

Finally, the author would like to thank his Mother and Father, Sonja and John Jenkins Senior who put up with everything during the memorable grad-school experience.

TABLE OF CONTENTS

	Page
LIST OF TABLES.....	vii
LIST OF FIGURES	viii
LIST OF SCHEMATICS.....	xiv
CHAPTER	
I. INTRODUCTION.....	1
II. LITERATURE SURVEY	3
2.1 State of Recycling.....	3
2.2 Problems in Recycling.....	7
2.3 Chemical Structure of Polyethylene	10
2.4 Crosslinking methods	11
2.4.1 Crosslinking by means of irradiation	11
2.4.2 Crosslinking by means of peroxides	13
2.4.3 Crosslinking by means of moisture.....	14
2.5 Degradation of Polyethylene	15
2.6 Recycling Polyethylene using Ultrasound.....	17
III. EXPERIMENTAL.....	19
3.1 Preparation of Crosslinked Polyethylene Samples.....	19
3.2 Continuous De-crosslinking	20
3.3 Static De-crosslinking	24

3.4 Determination of Gel Fraction.....	24
3.5 Tensile Test	29
3.6 Rheological Measurements by RMS-800.....	29
IV. RESULTS AND DISCUSSION.....	31
4.1 General	31
4.2 Static Experiments.....	32
4.3 Continuous Extrusion Experiments.....	44
4.3.1 Gel Fraction and Crosslink Density	44
4.4 Rheological Behavior	81
4.4.1 Tensile Properties.....	114
V. CONCLUSIONS.....	120
REFERENCES	125
APPENDIX.....	127

LIST OF TABLES

Table		Page
3.1	Residence time.....	23
4.1	Viscosity Slope Table of Continuous Samples	113

LIST OF FIGURES

Figure		Page
4.1	Gel fraction versus exposure time for different thickness samples. Samples are exposed to ultrasound at a temperature of 150°C, horn amplitude of 8.5 μm and pressures of 0.35 MPa (filled symbols) and 0.69 MPa (open symbols).....	33
4.2	Gel fraction versus exposure time for different thickness samples. Samples are exposed to ultrasound at a temperature of 150°C, horn amplitude of 10 μm and pressures of 0.35 MPa (filled symbols) and 0.69 MPa (open symbols).	34
4.3	Gel fraction versus exposure time for different thickness samples. Samples are exposed to ultrasound at a temperature of 150°C, horn amplitude of 12 μm and pressures of 0.35 MPa (filled symbols) and 0.69 MPa (open symbols).	35
4.4	Crosslink density versus exposure time for different thickness samples. Samples are exposed to ultrasound at a temperature of 150°C, horn amplitude of 8.5 μm and pressures of 0.35 MPa (filled symbols) and 0.69 MPa (open symbols)..	37
4.5	Crosslink density versus exposure time for different thickness samples. Samples are exposed to ultrasound at a temperature of 150°C, horn amplitude of 10 μm and pressures of 0.35 MPa (filled symbols) and 0.69 MPa (open symbols).	38
4.6	Crosslink density versus exposure time for different thickness samples. Samples are exposed to ultrasound at a temperature of 150°C, horn amplitude of 12 μm and pressures of 0.35 MPa (filled symbols) and 0.69 MPa (open symbols).	39
4.7	Crosslink density versus specimen thickness for different exposure times. Samples are exposed to ultrasound at 150°C, horn amplitude of 8.5 μm and pressures of 0.35 MPa (filled symbols) and 0.69 MPa (open symbols).	41

4.8	Crosslink density versus specimen thickness for different exposure times. Samples are exposed to ultrasound at 150°C, horn amplitude of 10 μm and pressures of 0.35 MPa (filled symbols) and 0.69 MPa (open symbols).....	42
4.9	Crosslink density versus specimen thickness for different exposure times. Samples are exposed to ultrasound at 150°C, horn amplitude of 12 μm and pressures of 0.35 MPa (filled symbols) and 0.69 MPa (open symbols).....	43
4.10	Gel fraction versus crosslink density for different exposure time and sample thicknesses. Samples are exposed to ultrasound at 150°C and pressure of .35 MPa.	45
4.11	Gel fraction versus crosslink density for different exposure time and sample thicknesses. Samples are exposed to ultrasound at 150°C and pressure of .69 MPa.	46
4.12	Gel fraction versus crosslink density for all exposure times and thicknesses. Samples are exposed to ultrasound at 150°C and pressures of .35 MPa and .69 MPa.....	47
4.13	Gel fraction versus crosslink density for different flow rates and 1 mm gap in continuous decrosslinking.....	49
4.14	Gel fraction versus crosslink density for different flow rates and 2 mm gap in continuous decrosslinking.....	50
4.15	Gel fraction versus crosslink density for different flow rates and 4 mm gap in continuous decrosslinking.....	51
4.16	Gel fraction versus crosslink density for all gaps in continuous decrosslinking.	53
4.17	Gel fraction versus crosslink density for all samples.....	54
4.18	Crosslink density as a function of amplitude at various gaps and a flow rate of 23.2 g/min.....	55
4.19	Crosslink density as a function of amplitude at various gaps and a flow rate of 15.8 g/min.....	56
4.20	Crosslink density as a function of amplitude at various gaps and a flow rate of 8 g/min.....	57

4.21	Crosslink density as a function of amplitude at various gaps and a flow rate of 4.2 g/min.....	58
4.22	Crosslink density as a function of gap at various throughput rates and at an amplitude of 16.5 μm	59
4.23	Crosslink density as a function of gap at various throughput rates and at an amplitude of 20 μm	60
4.24	Crosslink density as a function of gap at various throughput rates and at an amplitude of 25 μm	61
4.25	Crosslink density as a function of flow rate at various amplitudes and at a sample thickness of 1 mm.	63
4.26	Crosslink density as a function of flow rate at various amplitudes and at a sample thickness of 2 mm.	64
4.27	Crosslink density as a function of flow rate at various amplitudes and at a sample thickness of 4 mm.	65
4.28	Gel Fraction as a function of amplitude at various gaps and at a flow rate of 23.2 g/min.....	66
4.29	Gel Fraction as a function of amplitude at various gaps and at a flow rate of 15.8 g/min.....	67
4.30	Gel Fraction as a function of amplitude at various gaps and at a flow rate of 8 g/min.....	68
4.31	Gel Fraction as a function of amplitude at various gaps and at a flow rate of 4.2 g/min.....	69
4.32	Gel Fraction as a function of gap at various flow rates and at an amplitude of 16.5 μm	70
4.33	Gel Fraction as a function of gap at various flow rates and at an amplitude of 20 mm.....	71
4.34	Gel Fraction as a function of gap at various flow rates and at an amplitude of 25 mm.	72
4.35	Gel fraction as a function of flow rate at various amplitudes and at a constant gap of 1 mm.	74

4.36	Gel fraction as a function of flow rate at various amplitudes and at a constant gap of 2 mm.	75
4.37	Gel fraction as a function of flow rate at various amplitudes and at a constant gap of 4 mm.	76
4.38	Viscosity versus shear rate for samples treated at various amplitudes. Gap is 4 mm and flow rate is 4.2 g/min.	77
4.39	Viscosity versus shear rate for samples treated at various amplitudes. Gap is 4 mm and flow rate is 8 g/min.	78
4.40	Viscosity versus shear rate for samples treated at various amplitudes. Gap is 4 mm and flow rate is 15.8 g/min.	79
4.41	Viscosity versus shear rate for samples treated at various amplitudes. Gap is 4 mm and flow rate is 23.2 g/min.	80
4.42	Viscosity versus shear rate for samples treated at various amplitudes. Gap is 2 mm and flow rate is 4.2 g/min.	82
4.43	Viscosity versus shear rate for samples treated at various amplitudes. Gap is 2 mm and flow rate is 8 g/min.	83
4.44	Viscosity versus shear rate for samples treated at various amplitudes. Gap is 2 mm and flow rate is 15.8 g/min.	84
4.45	Viscosity versus shear rate for samples treated at various amplitudes. Gap is 2 mm and flow rate is 23.2 g/min.	85
4.46	Viscosity versus shear rate for samples treated at various amplitudes. Gap is 1 mm and flow rate is 4.2 g/min.	86
4.47	Viscosity versus shear rate for samples treated at various amplitudes. Gap is 1 mm and flow rate is 8 g/min.	87
4.48	Viscosity versus shear rate for samples treated at various amplitudes. Gap is 1 mm and flow rate is 15.8 g/min.	88
4.49	Viscosity versus shear rate for samples treated at various amplitudes. Gap is 1 mm and flow rate is 23.2 g/min.	89
4.50	Viscosity versus shear rate for samples obtained at various throughput rates. Gap is 4 mm and amplitude is 16.5 μm	91

4.51	Viscosity versus shear for samples obtained rate at various flow rates. Gap is 4 mm and amplitude is 20.0 μm	92
4.52	Viscosity versus shear rate for samples obtained at various flow rates. Gap is 4 mm and amplitude is 25 μm	93
4.53	Viscosity versus shear rate for samples obtained at various flow rates. Gap is 2 mm and amplitude is 16.5 μm	94
4.54	Viscosity versus shear rate for samples obtained at various flow rates. Gap is 2 mm and amplitude is 20.0 μm	95
4.55	Viscosity versus shear rate for samples obtained at various flow rates. Gap is 2 mm and amplitude is 25 μm	96
4.56	Viscosity versus shear rate for samples obtained at various flow rates. Gap is 1 mm and amplitude is 16.5 μm	97
4.57	Viscosity versus shear rate for samples obtained at various flow rates. Gap is 1 mm and amplitude is 20.0 μm	98
4.58	Viscosity versus shear rate for samples obtained at various flow rates. Gap is 4 mm and amplitude is 25 μm	99
4.59	Viscosity versus shear rate for samples obtained at various gaps. Flow rate is 4.2 g/min and amplitude is 16.5 μm	100
4.60	Viscosity versus shear rate for samples obtained at various gaps. Flow rate is 4.2 g/min and amplitude is 20.0 μm	101
4.61	Viscosity versus shear rate for samples obtained at various gaps. Flow rate is 4.2 g/min and amplitude is 25.0 μm	102
4.62	Viscosity versus shear rate for samples obtained at various gaps. Flow rate is 8 g/min and amplitude is 16.5 μm	104
4.63	Viscosity versus shear rate for samples obtained at various gaps. Flow rate is 8 g/min and amplitude is 20.0 μm	105
4.64	Viscosity versus shear rate for samples obtained at various gaps. Flow rate is 8 g/min and amplitude is 25.0 μm	106
4.65	Viscosity versus shear rate at various gaps. Flow rate is 15.8 g/min and amplitude is 16.5 μm	107

4.66	Viscosity versus shear rate at various gaps. Flow rate is 15.8 g/min and amplitude is 20.0 μm	108
4.67	Viscosity versus shear rate at various gaps. Flow rate is 15.8 g/min and amplitude is 25.0 μm	109
4.68	Viscosity versus shear rate at various gaps. Flow rate is 23.2 g/min and amplitude is 16.5 μm	110
4.69	Viscosity versus shear rate at various gaps. Flow rate is 23.2 g/min and amplitude is 20.0 μm	111
4.70	Viscosity versus shear rate at various gaps. Flow rate is 23.2 g/min and amplitude is 25.0 μm	112
4.71	Elongation at break as a function of crosslink density for samples treated in continuous decrosslinking process.....	116
4.72	Elongation at break as a function of % gel for samples treated in continuous decrosslinking process.....	117
4.73	Tensile strength at break as a function of crosslink density for samples treated in continuous decrosslinking process.....	118
4.74	Tensile strength at break as a function of % gel for samples treated in continuous decrosslinking process.....	119

LIST OF SCHEMATICS

Schematic		Page
3.1	Schematic of decrosslinking reactor with an external ultrasonic horn/die configuration.....	21
3.2	Die of an ultrasonic extruder along its longitudinal axis. d_e is the extruder exit bore of 6.1 mm. d_r is the die exit bore of 6.1 mm, d_h is ultrasonic horn diameter of 25.4 mm	22
3.3	Schematic of static decrosslinking device	25

CHAPTER I

INTRODUCTION

Plastics are made from hydrocarbon feedstock for the most part and should be recycled as a means of energy conservation. Most plastics can be easily included in waste-derived fuels; however more energy conservation may be achieved by recycling as plastic materials. The rubber industries recycling efforts have been in place in varying degrees for some time. Many industrial waste-plastic streams are recycled, but not nearly to the same level as that of the rubber industry. Some plastics are difficult or impossible to recycle because of inherent limitations in the nature of plastics or because they are often intimately combined with other non-plastic materials. One of the inherent limitations to crosslinked plastics is that it cannot be remelted and re-introduced into the initial process.

Decrosslinking crosslinked polyethylene with the aid of ultrasound is a possible solution. This is because the introduction of ultrasound to the material is a mechanical phenomenon and can be delivered at a controlled rate. The introduction of this mechanical energy leads to stress-induced chemical changes that are capable of transforming the material into something new and perhaps more useful than discarded crosslinked polyethylene. Isayev and coworkers have performed extensive research and experimentation on the application of ultrasound to the polymer extrusion process^{1,2,3,4}. The application of ultrasonic energy to crosslinked polymers in an attempt to decrosslink the material will be studied in this work. If the amount of energy that the crosslinked

material is exposed to by ultrasound is controlled properly, the materials crosslink's should be broken without the material arriving at the point of degradation. Degradation shall be defined as chain scission that renders the polymer material useless in typical polymer applications for this discussion. While chain scission occurs during any processing, if the material retains useful properties it is not referred to as degraded. Therefore, if crosslinked polyethylene is decrosslinked, or in other words, if the materials molecular weight is reduced so that it is processable and no longer a thermoset, then it can be said to be recycled.

In this study polyethylene is crosslinked with organic peroxide. Then, the material is subjected to varying levels of ultrasound under static and continuous conditions. The details of the operations conditions and experimental procedures are given in the Experimental Part. The properties of the resulting specimens subjected to ultrasound are evaluated by viscosity measurements and the determination of crosslink density through gel fraction and swell ratio measurements. These results are then compared with the results of the experiments performed on untreated crosslinked specimens to evaluate the usefulness of the ultrasound process for decrosslinking crosslinked polyethylene.

CHAPTER II

LITERATURE SURVEY

2.1 State of Recycling

Several methods for rubber recycling exist today, grinding, cryogenic, digester process, all with their limitations^{5,6}. Ground rubber is used as filler in an existing rubber matrix. However, the addition of this filler comes at the expense of properties that make the resulting materials less useful. Plastics' recycling has made some progress in recent years. The American Plastics Council reported that recycled plastic packaging hit 1.2 billion lbs in 1995, and the recycling rate for plastic bottles and containers was 30% for PET and 19% for HDPE. With public attention fixed on the environment and solid waste issues', recycling has high public relations value and offers some solid marketing advantages, contributing to anticipated annual growth greater than the general plastics industry.

The North American market consisted of 9.7 million tons demand in 1990 with LLDPE/LDPE having a share of 5.5 million tons and HDPE 3.9 million tons. The amount of recycled PE amounts to only 1.5% of total consumption. This situation clearly will not be acceptable to the public or industry itself.⁷

In the U.S., more that 85% of solid waste is disposed of in landfills. The numbers of landfills are being reduced rapidly. Plastics represent 7-8% of landfill by

weight yet 18-20% by volume. There is terrific pressure from all angles to reduce the amount of plastic waste in our landfills.

Industry has found many uses for ultrasound. Ultrasound is used in areas from medical applications to mechanical welding devices¹². High intensity ultrasonics can be used in industry to take advantage of the mechanical and chemical effects that ultrasound has when it is used correctly.

The mechanical benefits of ultrasound can be seen in several different industrial arenas. The measurement of mixing in polymer melts can be measured by focused ultrasound as explained by Erwin and Dohner⁸. In this experiment, an acoustical system produces an interrogation zone in the region of poorest dispersion by using focused waves. The degree of mixing in a melt was signified by fluctuations in the melt's properties.

Machining and metal forming also find benefit from the use of ultrasound^{9,10}. Abrasive slurry is flooded over the end of a tool in the desired end shape. The ultrasonic motion of the tool tip and the resulting cavitations erode material away until the desired shape is formed. Ultrasonic energy can also be used in conjunction with drawing dies to form some metals such as copper¹¹. In this case the ultrasound is helpful by softening the crystals in the metal and by reducing frictional forces between the work piece and the tool.

The use of ultrasound for combining thermoplastics in near and far field welding is widely accepted because it is easy to use, very fast, clean, and does not require a skillful operator. Near field refers to when the two surfaces are within 4 mm at 20 kHz, and anything greater than this is considered far field welding¹². Ultrasonic welding has another advantage over the use of adhesives for plastic part welding in that there is not additional material added for the weld.

Liquid atomization and droplet formation by means of ultrasound is used in the medical inhalant industry, and for atomizing fuels for more efficient combustion, industrial paints for use with electrostatic painting, dispersing cleaners, and producing metallic powders¹³.

Ultrasound can be used in conjunction with a cleaning fluid to properly clean a contaminated surface¹³. The effectiveness of the combination of the cleaning fluid with the ultrasound can be attributed to cavitations. These cavitations are responsible for phenomena that increase the effectiveness of a cleaning solution. The development of stresses between the cleaning fluid and the contaminated surface, agitation and dispersion of the contaminant throughout the cleaning fluid, an increase in attractive forces between the contaminant and the cleaning fluid, promotion of chemical reactions, and effective penetration into pore and crevices are all benefits of ultrasonic cleaning.

Several other instances exist where the chemical benefit of the application of ultrasonic energy is used. The curing of epoxy resins modified by diols was monitored by longitudinal ultrasonic velocity and attenuation measurements¹⁴.

The use of ultrasonics can also be found in the field of combining metals through soldering and welding¹³. Ultrasound vibrations erode the oxide coating and bring solder into direct contact with the base metal¹⁵. In the field of welding, two metals can be placed in contact and with the correct pressure ultrasound will produce shearing stresses that will weld the two metals together¹³.

Although it is an expensive method for drying, it is practical to use ultrasonics when drying heat sensitive materials. The ultrasound has the effect of producing gas turbulence above the liquid interface and at low temperatures it will boil off liquid vapors¹³. The main use of this process is in the pharmaceutical industry.

Agriculture has also found a couple of uses for ultrasonic energy including tomato pollination, and the germination of seeds¹². A mass of dust particles can be produced using ultrasound and dispersed into a large cloud¹⁶. This cloud will then equally pollinate all of the tomatoes without the need for direct human contact. The germination of seeds can be aided by ultrasound through the production of heat, transfer of moisture into the seed, and rupture of the seed coat¹⁶.

Another chemical application of ultrasound is accelerated etching. When ultrasound is applied during chemical or electrolytic etching it increases the rate of material removal¹³. Below cavitation levels the ultrasound is used to help maintain close contact between the work surface and the etchant. Above the cavitation levels etching may proceed at an accelerated rate.

The beverage and oil industries also have applications for ultrasound. When ultrasound is applied to a newly fermented alcoholic beverage, it produces the effects of aging over a long period of time. This effect was tested on several different types of wines by Singleton. The cavitations produced by ultrasound have also been used to change the odor produced by some fragrances¹³.

Isayev and co-workers have developed a process using high power ultrasonics to continuously devulcanize crosslinked elastomers^{17,18}. These previous studies in this area were performed on SBR and NBR where the original composition and properties were known^{17,18}. This technology will be applied to polyethylene that has been chemically crosslinked. The materials original properties were measured and then compared to properties of processed material.

2.2 Problems in Recycling

Three major obstacles stand between the plastics industry and recycling efforts: collection, quality, and markets¹⁹. A number of plastic recycling efforts have failed because they did not meet four essential criteria necessary for a successful program, a continuous source of suitable scrap, technology for recycling, applications and markets for the products based on the wastes, and an economical enterprise²⁰. The technology for recycling is the focus of this thesis.

Process engineering is important to this dynamic growth area, as regrind and post-consumer waste must be reworked and modified to yield solid recycled products. It should be pointed out that for the purposes of this thesis, the term “recycling” will include both material known in the industry as in house reclaim and post consumer material known as recycle²².

Broadly, plastics are of two types: thermoplastic and thermosetting. Thermoplastic materials can be reheated and reformed, often several times. Thermosetting materials cannot; the initial heating and fabrication cause permanent chemical changes (crosslinking) and subsequent reheating can cause degradation. Most plastics used either in durable goods or single-service items are thermoplastic. Thermosetting plastics are used mostly in durable goods and in much lower quantity than thermoplastics. Thermosetting plastic waste arises during manufacture and when obsolete items or capital goods, e.g., automobiles or buildings, are scrapped. Thermosetting materials at this point have not been identified as a suitable source for post consumer recycling. This is primarily because the crosslinking that occurs during the thermosetting process produces a molecular network. This network gives very good physical properties and a higher temperature range that the material can be used within,

but does not allow the material to flow at elevated temperature before thermal degradation.

A commercial plastic item is likely to consist of a base resin or polymer mixed with additive ingredients to enhance properties or resistance to degradation²¹. Other ingredients include colorants or even a foaming ingredient. The reprocessor must take into account the presence of these additives. In the work that follows, these were not considered within the scope of the project.

This leaves the recycling industry with the challenge of finding a technology that will allow the thermoset plastic to be recycled instead of thrown away. While the purpose of the project is not to put into place an entire recycling program, some thought should be given to the recycling process in order to properly understand where the project fits into the big picture. The first major obstacle is collection of material that is suitable for recycling. Curbside collections that are in place in some communities are still largely subsidized and do not currently justify themselves economically by the resale of processed materials. On the industrial front, the cost of transportation usually outweighs by itself the cost of virgin material so the interest in recycling is largely from a public relations or marketing point of view. Since prices for virgin resin are at roughly \$0.50 per pound, the cost for collection and transportation of materials to recycling sites must be significantly lower to justify recycling programs. Virgin resin is usually received at high volume users by railcar or at lower volume users by gaylord size. The bulk density of the entire containers filled with resin is quite close to that of the material itself. The problem is that when the resin is processed into a useable product, its bulk density is typically decreased drastically. This makes shipping costs increase on the basis of area taken up by relatively small volumes of plastic. Also there is the issue of separation after collection. For example, a material that is intended for extrusion as film is not well suited

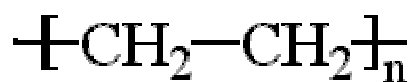
for injection molding. In recycling any material, the end users' specifications must be met and in turn, the specifications determine the separation and recycling technology to be used. When plastics are separated from a mixture of materials, especially if they are separated as a mixture of different kinds of plastics, the final properties must be predictable within a consistent and useful range. Most buyers of recycled resins, while not so choosy as virgin resin buyers, usually want to be able to know that the material is of some specification, adding a separation cost. This brings us to the question of the quality of recycled resin. By the nature of polymer manufacture in reactors usually at large chemical plants, the base resins are quite clean. These processes are usually tightly controlled so that the material can be sold according to the specific properties attained during polymerization. Therefore, any type of a process that would reclaim crosslinked polyethylene would have to be of a predictable nature enough that one could determine the materials properties after processing. Resins prices are on the rise but a substantial price increase would have to occur to justify recycling based on cost effectiveness alone. This situation would change drastically if governing body's mandate recycling efforts.

Despite environmentalism, the so-called green consumer who demands and pays for recycled materials has not surfaced in great enough numbers. The future of recycling depends on firming prices and demand-pull.

Solutions to these recycling problems may come from current activities. Some promising ones are molecular "markers" into PET so that it may be electronically sorted. Another encouraging technology removes contaminants, such as paper and dirt, from post-consumer polyethylene grocery sacks and stretch film. Since 1994, the Annual Recycling Conference has been organized by the Society of Plastics Engineers and held in Dearborn Michigan. These conferences and other solutions will help to meet the challenge of plastics recycling.

In addition, recycling plastic will likely soon be imposed on the industry rather than done by choice. At this point there will be no marketing advantages since everyone would be involved in the same process. With the proper attention and solid engineering practices, recycling plastic can be a large contributor to the somewhat tarnished image that the public currently has of plastic material. With this sort of conscientious recycling practice, that image can not only be removed but also turned completely around. Any raw material that can be completely recycled is a benefit to consumers and manufacturers and should be considered as a very good part of the “big picture”.

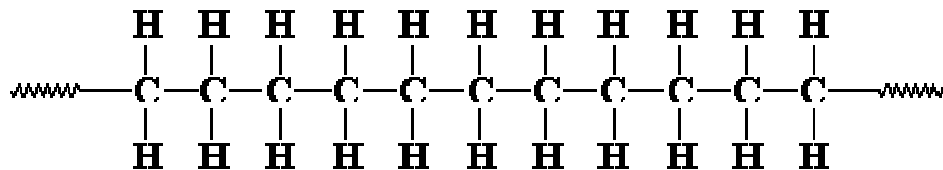
2.3 Chemical Structure of Polyethylene



Ethylene (a gas) at a molecular level is formed of two carbon atoms with two hydrogen atoms attached to each carbon atom²¹. The chemical representation is C₂H₄. Carbon has a valence of four, which requires a tetrahedral structure for the atoms bonded to it including other carbon atom. The four atoms will be at opposing corners leaving every other corner open. This structure requires a rigid angle of 109 degrees between each atom. Of the six electrons in the carbon atom, four of them are in the outer energy level. The filled outer energy level would have eight electrons. To this end, each carbon atom shares two of its electrons with another carbon atom resulting in a double ‘covalent’ bond between carbons in the ethylene molecule. The other two electrons come from the hydrogen atoms connected to each carbon. Each instance of electron sharing represents one covalent bond. The carbon atoms are bonded together with this unsaturated double

bond for the individual molecule. It is because of this unsaturated bond that polymerization is possible²².

The polyethylene chain is formed by addition polymerization. In this type of polymerization, using heat, pressure, or a catalyst, the double bond between the carbon atoms is broken leaving a single covalent bond between carbon atoms. This leaves the ethylene molecule with seven electrons in its outer energy level and the molecule is now referred to as a mer. The mer will bond with adjacent mers to fulfill the requirement for the outer energy level of each carbon atom. Once the chain is initiated the reaction proceeds spontaneously. This process continues until the chain is terminated with an initiator or in bonding with another chain. The long carbon back boned molecular chain is called polyethylene²².



2.4 Crosslinking methods

In general the following crosslinking technologies are applied commercially in industries, such as wire and cable, foam, pipe, film and heat-shrinkable products:

2.4.1 Crosslinking by means of irradiation

When atomic radiation passes through materials, a large fraction of energy is dissipated through ionization and electronic excitation. This process may have several effects, but for polymers, the most important one is breaking chemical bonds, which

results in the formation of free radicals. For PE, the result of the irradiation is the formation of C-C crosslinks, while in polypropylene, chain-scission occurs. At this time, the most common commercial sources of ionizing radiation are ^{60}Co and ^{137}Cs for gamma irradiation, and electron accelerators for e-beam (beta) irradiation²³.

In order to predict the behavior of carbon-chain polymers exposed to ionizing radiation, an empirical rule can be used. According to this rule, polymers containing a hydrogen atom at each carbon atom predominantly undergo crosslinking, whereas those polymers containing quaternary carbon atoms and polymers of the -CX₂-CX₂- type (where X is a halogen), chain scission predominates. Aromatics, like polystyrene (PS) and polycarbonate (PC) are relatively resistant to electron beam processing and are thus well suited to serve as packaging materials for medical disposables, which are slated to be radiation sterilized.

During irradiation, chain scission occurs simultaneously and competitively with crosslinking, the end result being determined by the ratio of the yields of the two reactions. For some polymers, such as polyvinyl chloride (PVC), polypropylene (PP), and polyethylene terephthalate (PET), both directions of transformation are possible, and certain conditions exist for the predominance of each one.

The ratio of crosslinking to scission depends on factors including total irradiation dose, dose rate, the presence of oxygen, stabilizers, and radical scavengers, and steric hindrances derived from structural or crystalline forces.

Overall property effects of crosslinking can be complex and contrary, especially in copolymers and blends. For example, after electron beam processing, highly crystalline polymers like high-density polyethylene (HDPE) may not show significant changes in tensile strength, a property derived from the crystalline structure, but a significant improvement in properties associated primarily with behavior on the

amorphous regions, like impact and stress-crack resistance. The main application of irradiation crosslinking is in the low voltage cable area, where the insulating layer is not too thick and high output extrusion can be used because there is no risk of premature curing in the extruder. Compared to peroxide and silane crosslinking, irradiation crosslinking is not as economical and as a result, it has not been used as extensively.

2.4.2 Crosslinking by means of peroxides

Peroxide crosslinking is basically a two-step process. A crosslinkable polymer is initially obtained in the processing equipment by melt incorporation of suitable peroxides into the polymer matrix, followed by processing into finished articles, such as cable insulations and pipes, under conditions that avoid unwanted, premature crosslinking.

The crosslinked structure is then obtained by heat treatment applied on the finished article, normally made in-line directly after the extrusion step. In this case, the powdered peroxide was mixed with powdered polyethylene thoroughly and then compression molded into plaques.

The peroxide is a key factor in this technology and from a multitude of peroxides only a limited number are suitable for crosslinking purposes. The overall crosslinking reaction of polyolefin's by organic peroxides can be divided into three successive stages:

- 1) Homolytic decomposition of the peroxide into primary free radicals.
- 2) Abstraction of hydrogen atoms by the free radicals from the polyolefin chain, resulting in stable peroxide decomposition products and polyolefin macro radicals.
- 3) Combination of two macro radicals to form a C-C crosslink.

While the first stage is the rate-determining step in the overall crosslinking reaction, its efficiency depends mainly on the types of primary free radicals created in this stage, as well as on the types of polyolefin macro radicals resulting from the second stage. The chemical structures of both the peroxide and the polyolefin play decisive roles in the crosslinking process.

Almost all commercial polymers bear secondary and/or tertiary H-atoms in the main chain. Therefore, nearly all thermoplastics, as well as natural and synthetic elastomers, can be crosslinked using peroxide via the H-abstraction pathway. For only a few polymers, such as PP, PVC, and homo/copolymers of butane-1 or isobutene, all of which are prone to chain scission, unaided peroxide crosslinking is uncommon or not possible.

Unlike sulfur vulcanization, peroxides exhibit no significant difference in their rate of reaction in the presence of two different polymers, which makes it possible to obtain homogeneous crosslinked materials starting from blends of different polymers. Because peroxide crosslinking does not depend on the presence of double bonds in the substrates, the peroxide crosslinks both components in blends of polymers and/or elastomers simultaneously. Polymer blends are crosslinked to optimize chemical and physical properties in final products²³.

2.4.3 Crosslinking by means of moisture.

This utilizes reactive silane groups, which will crosslink in a humid environment. The moisture crosslinkable polyolefin's are linked through a C-Si-O-Si-C moiety, rather than a C-C bond. The crosslinking usually takes place around 80 °C. Moisture crosslinking offers greater processing latitude, as the fabrication does not have

to take place below the peroxide decomposition temperature as required in the peroxide crosslinking process.

Additionally, the extruded tubing in the moisture crosslinkable process can be cooled quickly during the extrusion process, instead of beginning an increasing thermal cycle to decompose the peroxide²³.

2.5 Degradation of Polyethylene

The type of polymer bonding which is responsible for the thermosetting characteristics in polyethylene is crosslinking. In this reaction the hydrogen atom is stripped from some of the carbon atoms in the polymer chain to form free radicals, which combine with each other to form a crosslinked structure. This network makes the material much stronger with a higher useful temperature range. Unfortunately, this also makes the polymer into a thermoset and virtually eliminates it from being recycled or reshaped into another form when reheated. There are methods under investigation that are reported to 'undo' this reaction but at this point have been proven to be less than successful and when actually successful, less than economical. In one method, polyethylene is ground to a mesh size of 100 or more and then added to polyethylene up to 25%²⁴. Then, the mixture is subjected to crosslinking. It has been reported that the mechanical properties of this system were comparable to the mechanical properties of the unfilled PE. However, since the loading in the evaluation was only up to 25% this qualifies the reground material as filler, but not necessarily as recycled. If the ground material could be used at 100% and recrosslinked or at least melted and used again as a thermoplastic, then this would qualify as truly recycling. The paper²⁴ reports that crosslinks are broken by grinding and then reformed upon crosslinking. This is unlikely. It is much more likely that the strength of the crosslinked network is such that the

addition of 25% reground material simply does not lessen the strength of the entire network. Another examination should look at the elasticity of the material instead of simply the maximum physical properties.

Any sort of recycling process would not change the backbone atom of any polymer so this is not of concern. Also the number of branches doesn't change with reprocessing unless there is considerable stress placed on the molecule. However, the chain length does lessen with each processing step. This is known as degradation. Degradation that is of concern in recycling is primarily encountered as thermal and mechanical. Thermal degradation is the chain scission of the backbone that can occur at elevated temperatures because of the simple carbon chain backbone. Mechanical degradation is also encountered during each processing step. This chain breakdown occurs to a certain extent, because of the very mechanism that allows plastic to be so useful. Plastic is very suitable in so many applications because it can be shaped at elevated temperatures and when cooled below its melting point will retain that shape. However, while that shape is being taken, chains are sliding and bending, being pushed around either into a mold or in an extrusion device of some sort. This movement causes some of the chains to break more from shear in a processing device than from the simple heating of the material. Mechanical degradation refers to the molecular scission induced by the application of mechanical stresses. In a single screw extruder, which is essentially a drag flow device, large stresses are applied to the polymer melt in pushing the material through the device and between the flight tips and the barrel wall. Also by simply pushing material through a die, large mechanical stresses are put into the material. These stresses contribute to the molecule chains being broken simply by stretching them to a maximum length until they snap. It is unlikely that mechanical and thermal degradation exist separately in any process.

Ultrasonic degradation takes place in a significantly different manner than does shear induced degradation. Shear induced degradation relies on the polymer chain being constrained by entanglements or some method and stressed until the molecule snaps. Ultrasonic degradation takes place without the requirement of rigid constraint^{17,18} in plastic melts^{1,2,3}. Hydrodynamic shear and shear stress during cavitations play major roles in this type of degradation. Hydrodynamic forces are caused by shock waves from the cavitations bubble collapse. The ultrasonic vibration causes cavitations and upon the bubble collapse, molecules flow toward the center of the bubble at very high velocities. This flow causes breakage of bonds. In addition elongation stresses are imposed on the molecule as part of the molecule is moved toward the center of the collapsing bubble and more bonds are broken.

2.6 Recycling Polyethylene using Ultrasound

A desirable recycling program would not diminish (degrade) the properties of the polymer to the point that they are not useful in any other products. Polymer properties basically depend on the backbone atom of the polymer molecule, the primary chain length and the number of branches. After the polymer chain is formed in the polymerization step, the chain length can only go down as a result of chain scission by one means or another. The only way chain length can increase after polymerization is through crosslinking, which is not *exactly* the same as increasing chain length.

In the ultrasonic decrosslinking procedure, the network is broken mechanically at the highest stressed points when the cavitations bubbles collapse. Since the highest stress points are most likely at the crosslinked site, the resulting material from the decrosslinking step is more similar to the virgin polyethylene than a randomly

degraded material. This statement is described in greater detail in the results and discussion portion of this study.

CHAPTER III

EXPERIMENTAL

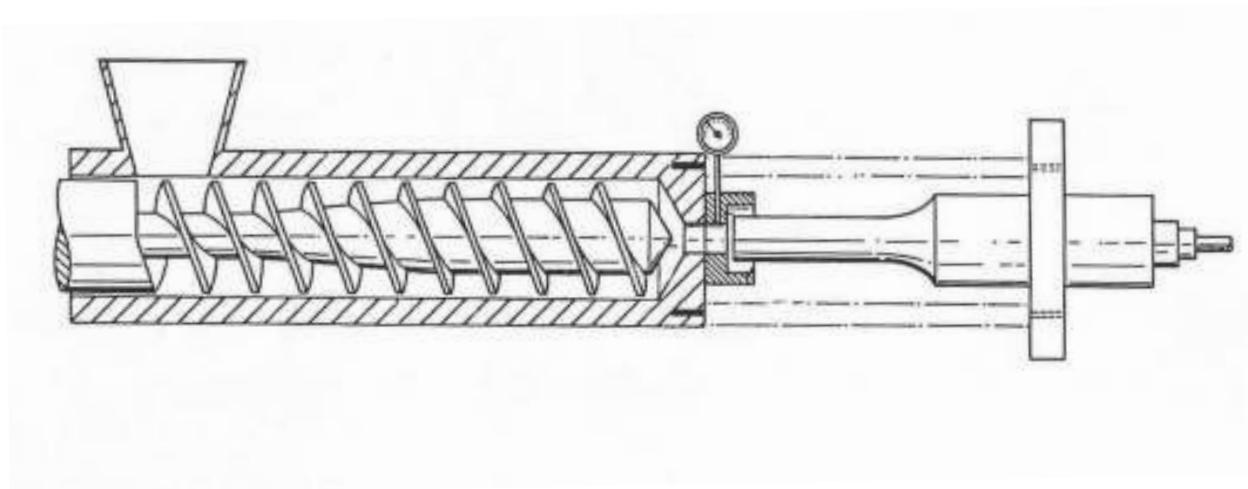
3.1 Preparation of Crosslinked Polyethylene Samples

In the present study, crosslinked polyethylene Paxon 7004 HDPE powder was used. Paxon 7004 is a UV-stabilized, 35 mesh crosslinkable HDPE powder intended for use in rotational molding. Density of the material is 0.944 g/cm^3 , tensile strength at yield is 3,000 psi (20.7 MPa). It has an elongation at break of 400%, tensile modulus of elasticity of 80,000 psi (552 MPa) and flexural modulus of 100,000 psi (690 MPa). Since the material is intended for rotational molding, no melt index is given. Injection molding was the first method attempted for producing crosslinked polyethylene. This operation proved to be unsuitable because the particular material did not release well from the mold even with the help of a mold release agent. It was later discovered that a likely reason for this is that the material was not crosslinking in the mold, as it should have. In the following attempts, organic peroxide was added to the polyethylene powder to insure that crosslinking took place. Two percent by weight of organic peroxide was added to the powder for crosslinking. The specific peroxide used was Lupersol 130 from ATOCHEM. Crosslinked material was successfully produced from compression molding polyethylene with the addition of organic peroxide into plaques. The polyethylene was in powdered form along with the peroxide. This powdered blend was measured and poured into a frame for compression molding. The dimensions of the steel frame used were

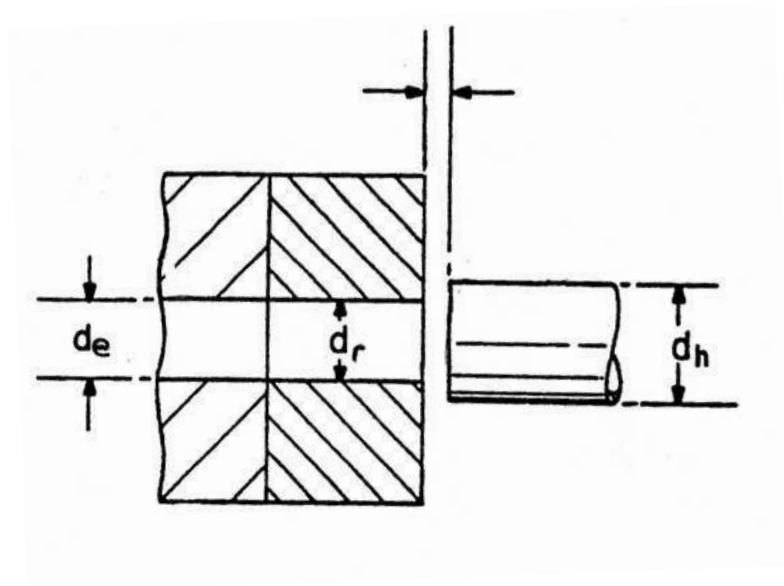
$L \times W \times H = 5 \times 5 \times 0.5 \text{ inch}^3$ ($12.7 \times 12.7 \times 1.27 \text{ cm}^3$). Heaping of the material in the middle of the frame was necessary because the bulk density of the material changed as it was melted. If the material was not heaped in the middle initially, voids were left in the plaque and leaking around the edges occurred. The blend was compression molded at 200 °C for 15 minutes. This was found to be the temperature and time that insured complete crosslinking of the material without degradation. Additional plaques were molded to a thickness of 3/32 inches (0.238 cm) in order to make samples for the static de-crosslinking operation. Disks with a 1-inch (2.54 cm) diameter were cut out of these plaques that matched the diameter cross section of the static horn.

3.2 Continuous De-crosslinking

After compression molding of an amount of material suitable for continuous decrosslinking experiments, the thick plaques were ground to a thirty-mesh size using the Gala grinder with a 30-mesh screen. While this operation reduced the particle size of the crosslinked material, it should not have significantly reduced the materials overall crosslink density since this is a macroscopic operation and crosslinking is on the microscopic level. This was done so that the material could be handled in the continuous decrosslinking operation. The ground material was fed into the feed-throat of the one-inch Killion extruder in the continuous decrosslinking operation. Screw speeds were 5, 10, 20 and 40 RPM with corresponding flow rates of 4.2, 8, 15.8, and 23.2 grams per minute. Material was transported with the one-inch extruder to the die. The exit of the die is where the decrosslinking takes place. The ultrasonic horn faces the exiting material directly as shown in Schematic 3.1. An exploded view is shown in Schematic 3.2. As the material exits the die, it is forced into close proximity (1, 2 and 4 mm) with the



Schematic 3.1 Schematic of decrosslinking reactor with an external ultrasonic horn/die configuration



Schematic 3.2 Die of an ultrasonic extruder along its longitudinal axis. d_e is the extruder exit bore of 6.1 mm. d_r is the die exit bore of 6.1 mm, d_h is ultrasonic horn diameter of 25.4 mm

ultrasonic horn and exposed to varying amounts of energies. After the material was processed, it was passed through a water bath and collected for testing. The water bath was used to bring the material back to a cooled state. The collected material was in similar physical condition as it was upon feeding to the device except for being somewhat stickier. Samples were again compression molded into plaques, this time a bit thinner so that they could be tested for mechanical properties, 5 x 5 x 0.08 inches (12.7 x 12.7 x .2032 cm) and specimens were cut out for tensile, shear and gel fraction testing. For shear testing a one-inch diameter disk was made. For gel fraction-testing samples were 0.500 grams +/- 0.020 grams and weighed to the nearest 0.001 gram. Tensile test specimens were 0.160 inches (0.4064 cm) wide, 0.08 inches (.2032 cm) thick, and used an extensometer gauge length of .75 inches (1.905 cm). The specimen gauge length was 2 inches (5.08 cm) and we used the extensometer in order to minimize the effect of specimen imperfections. The tensile tests were performed on an Instron series IX Automated Materials Testing System borrowed from Advanced Elastomer Systems. The sample rate was set at 20 pts/sec with a crosshead speed of .1969 in/min (5 mm/min).

The table below shows the residence times for the samples collected at the three gaps and four flow rates.

Table 3.1 Residence time

	Flow Rate			
Gap	4.2 g/min	8 g/min	15.8 g/min	23.2 g/min
1 mm	6.82 sec	3.59 sec	1.81 sec	1.23 sec
2 mm	13.62 sec	7.16 sec	3.62 sec	2.47 sec
4 mm	27.24 sec	14.33 sec	7.25 sec	4.94 sec

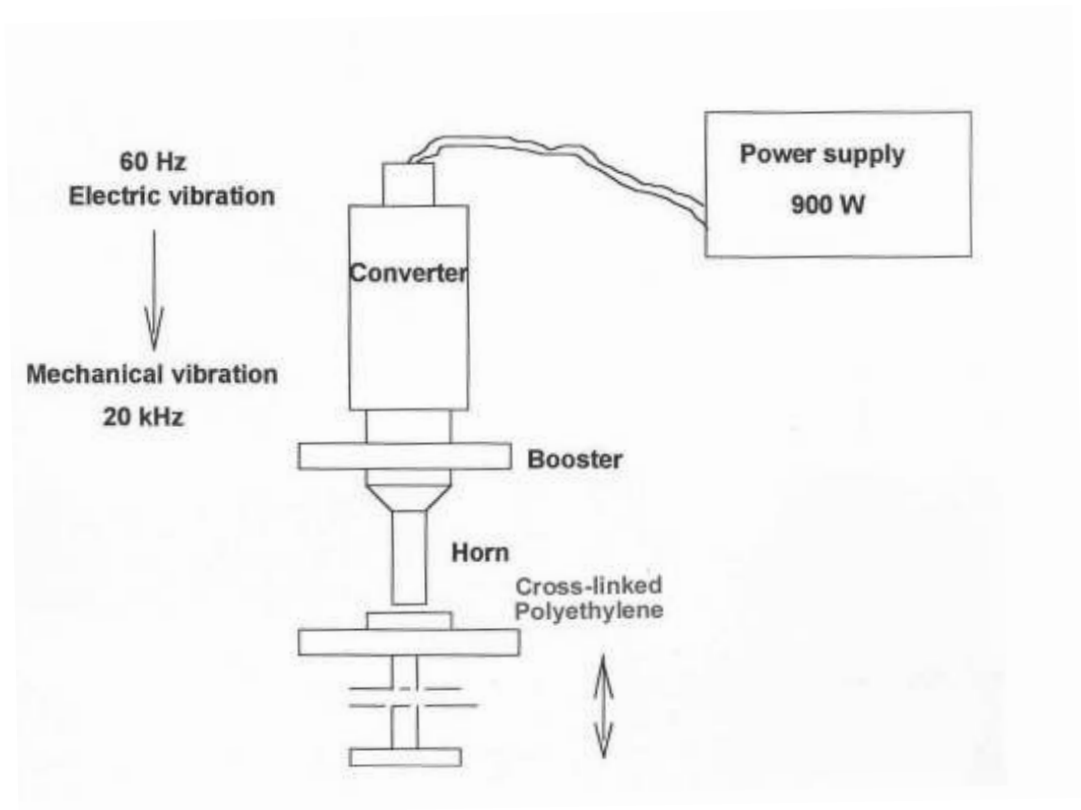
3.3 Static De-crosslinking

Thinner crosslinked plaques (1, 2.1 and 3.9 mm) were compression molded and disks that matched the cross section of the ultrasonic horn were cut from the plaques. These disks of crosslinked polyethylene were subjected to ultrasound in a static device as shown in Schematic 3.3. Static experiments were carried out at 150°C. The amount of material that could be subjected to this at one time was limited by the cross section of the ultrasonic horn. The advantage of this system is that the amount of energy and pressure could be controlled precisely. The samples were pressed against the end of the horn for different pressures and amounts of time. Pressures used were .35 and .69 MPa with exposure times of 2, 5, and 10 seconds.

The specimens were then measured for gel fraction in a Soxhlet extraction experiment. Gel fraction and extract percent measurements were used for the determination of crosslink densities. Since the amount of material was limited, experimentation on the specimens from static sonication experiments was limited to gel fraction measurements.

3.4 Determination of Gel Fraction

Using ASTM designation D 2765– 90, test method C, gel content and swell ratio of the treated and untreated materials was determined. Degree of crosslinking is determined by measuring the swell and extraction occurring in a solvent that dissolves that portion of the polymer which is not crosslinked. Both measurements are obtained in one test. The degree of crosslinking is not expressed as a percent of total crosslinkability or similar expression, but is judged from swell ratio and percent extract based on experience with the particular polymer-solvent system under consideration. Gel content



Schematic 3.3 Schematic of static decrosslinking device

is the insoluble fraction produced in ethylene by crosslinking. Specimens of the crosslinked/decrosslinked ethylene plastic are weighed and then immersed in a one-ounce glass vessel with a screw on sealing cap containing the extracting solvent (xylene). The entire vessel is then immersed in an oil bath at 110 degrees Celsius for 24 hours, removed, weighed in the swollen state, and dried and reweighed. The amount of material extracted is measured and swell ratio is determined. The percent extract is a measure of the amount of polymer that is soluble or is not entrapped in the main gel phase, or both, at the end of the immersion period. When there is no chemical degradation, a lower swell ratio indicates greater crosslinking and a lower molecular weight between crosslinks. The following procedures²⁵ were used to calculate swell ratio and gel fraction:

Swell ratio = (volume of polymer in gel + volume of absorbed xylene)/volume of polymer in gel

$$\begin{aligned}
 \text{Swell ratio} &= (V_p + V_x)/V_p = ((W_p/\rho_p) + (W_x/\rho_x))/(W_p/\rho_p) & (3.1) \\
 &= 1 + (\rho_p/W_p)(W_x/\rho_x) \\
 &= 1 + (\rho_p/\rho_x)(W_x/W_p) = 1 + K(W_x/W_p) \\
 &= 1 + K((W_g - W_d)/(W_o - W_e)) \\
 &= 1 + K[(W_g - W_d)/(W_d - (1-f)W_s)]
 \end{aligned}$$

Extract % = (weight of extract/original polymer weight) x 100

$$\begin{aligned}
 &= (W_e/W_o) \times 100 = [(W_s - W_d)/W_o] \times 100 & (3.2) \\
 &= [(W_s - W_d)/fW_s] \times 100
 \end{aligned}$$

where:

K is the ratio of density of polymer, ρ_p , to that of the solvent, ρ_s , at the immersion temperature. This ratio is approximately 1.07 for low-density polyethylene at 80 °C and 1.17 for high-density polyethylene at 110 °C²⁵.

f is the polymer factor (the ratio of the weight of the polymer in the formulation to the total weight of the formulation. Formulation may contain various plasticizers, etc.) In these measurements we used a polymer factor of 1.

W_o is the original polymer weight (the amount of polymer in the specimen being tested)

W_s is the weight of specimen being tested

$$W_o = fW_s \quad (3.3)$$

W_e is the weight of extract (amount of polymer extracted from specimen in the test)

W_g is the weight of swollen gel after the immersion period

W_d is the weight of dried gel

$$W_e = W_s - W_d \quad (3.4)$$

W_p is the weight of insoluble polymer in swollen gel

$$W_p = W_o - W_e \quad (3.5)$$

ρ_p is the density of polymer at the immersion temperature (assumed to be same as density at room temperature for these calculations)

V_p is the volume of polymer in gel

$$V_p = (W_o - W_e) / \rho_p = W_p / \rho_p \quad (3.6)$$

$$W_x = W_g - W_d \quad (3.7)$$

ρ_x is the density of solvent at the immersion temperature

V_x is the volume of solvent in gel

$$V_x = (W_g - W_d) / \rho_x = W_x / \rho_x \quad (3.8)$$

The swelling technique is based on the fact that a crosslinked polymer will absorb a certain amount of solvent based on the crosslink density in the polymer and the solvent used. The solvents will fill the network and the crosslinks will create a force operating against swelling. A given crosslinked polymer will reach a point where maximum swelling has occurred. The effective number of crosslinks in the polymer can then be found using the Flory-Rehner equation²⁶.

$$v_e = - \frac{\ln(1 - v_{ro}) + v_{ro} + \chi v_{ro}^2}{v_1 (v_{ro}^{\frac{1}{3}} - \frac{1}{2} v_{ro})} \quad (3.9)$$

where v_1 is the molecular volume of the solvent, χ is the parameter expressing the first neighbor interaction free energy, v_e is the effective number of chains in a real network per unit of volume, and v_{ro} is the volume fraction of the polymer in the swollen network that is in equilibrium with the solvent. An average value of $\chi = 0.28$ was used in the calculations using xylene as the solvent²⁷. This value is based on values found for xylene in the CRC Handbook of Polymer-Liquid Interaction Parameters and Solubility Parameters. The molecular weight of xylene is 104 g/mol and its density is 0.81 g/cm³.

$$v_{ro} = \frac{\frac{\text{Plastic Dry Weight}}{\text{Plastic Density}}}{\frac{\text{Plastic Dry Weight}}{\text{Plastic Density}} + \frac{\text{Solvent Weight}}{\text{Solvent Density}}} \quad (3.10)$$

The molecular volume of the solvent is given by the following equation:

$$v_1 = \frac{\text{Molecular Weight of Solvent}}{\text{Density of Solvent}} \quad (3.11)$$

The calculated value for v_1 used in all calculations was 128.4 cm³/mol because the solvent was the same in all experiments.

3.5 Tensile Test

Tensile tests were performed on material collected from the continuous decrosslinking process. Testing in the ranges of zero to 40% elongation was carried out on tensile testing equipment later borrowed from Advanced Elastomer Systems. The equipment used was an Instron series IX interface 4200 automated testing system. Initial testing at ASTM standard D 638 produced results that were not useful because the crosshead speed was too high. All of the samples are somewhat brittle so the differences were not measurable at the ASTM crosshead speed. Tests were modified using a slower crosshead speed (5mm/min) to show more subtle differences in properties. A sample with dimensions of 0.16 inches (.4064 cm) width, 0.08 (.2032 cm) inches thickness and 2.0 inches (5.08 cm) gauge length was prepared using dies borrowed from Advanced Elastomer Systems. Maximum stress, and elongation at break were measured and used to compare specimens that were subjected to varying decrosslinking conditions.

3.6 Rheological Measurements by RMS-800

Disks with a 1-inch (2.54 cm) diameter and a thickness of 0.08 inches (.2032 cm) were cut from plaques made up of material collected from the continuous decrosslinking procedure. These disks were all the same diameter as the RMS 800 plate

and were tested under the same conditions in the RMS-800 tester. Initially the cone and plate procedure was attempted but failed. This was because the material could not be tested under the same conditions. Since the specimens were of a different crosslink density, when the cone was placed at the same position in each test, the pressure on samples was different. The method for that reason was changed to the parallel plate method. Specimens were tested at 150 °C in steady shear. Viscosity at each shear rate was compared for the different samples.

CHAPTER IV

RESULTS AND DISCUSSION

4.1 General

The question now arises as to whether or not the decrosslinking in crosslinked networks would be crosslink site specific. In order for this to be possible in the purely mechanical system, the crosslinked sites would have to be somehow the weakest or most pre-stressed links in the chain. Chemically, this is not the case. The crosslinked sites should have the same chemical strength as the backbone of the polyethylene chain. Mechanically however, the story could be somewhat different. When the chains are originally formed by addition polymerization, chain shape is determined by locations of the ethylene mers and surrounding physical parameters (temperature, pressure, etc.). The chain is not stressed upon chain formation. When the crosslinks between chains occur, there is invariably some chain movement in order to allow the chains to move physically close enough to become crosslinked. This would make the chains slightly stressed at those locations. When ultrasound is introduced to the molecular network and the entire structure is in motion, the locations of chain scission will be those that have the highest stress and moment. In this case, moment is the sum of the product of stresses on the molecular chain that are transmitted through the point of crosslinking. In the network, the chains are somewhat bound by their crosslinked sites, more so than they would be if they were not crosslinked. At these sites, the crosslinking

points, the moment will be highest when the network is agitated. A moment diagram of any cantilever beam will show that the moment is the highest at the point of restricted movement. A crosslink would serve as restriction to movement and would therefore be the point of the highest moment. Because of this, the likelihood of chain scissions at these points is thought to be higher than less constrained regions of the polymer. Some scissions will invariably occur at other locations, but the locations that serve as points of restricted movement and have additionally been pre-stressed by crosslinking, will most likely have a higher occurrence of scission.

4.2 Static Experiments

Experimentation with static sonication was carried out using four factors: exposure time, specimen thickness, ultrasonic power, and pressure. Levels for the factors were: exposure times, t , of 2, 5, and 10 seconds, specimen thickness, δ , of 1, 2.1, and 3.9 mm, ultrasound power levels of 60, 80, and 100 percent which corresponded to amplitudes of 8.5, 10, and 12 μm , and pressures, P , of .35 and .69 MPa. The samples sonicated at these conditions were used for gel fraction measurement.

Graphs of gel fraction versus time show that in each case, gel fraction is reduced with an increased exposure time to ultrasound. In Figure 4.1, the 1 mm thick specimens show the most response to the time factor. The 3.9 mm thick sample shows a reduced response to exposure time. Indeed, Figures 4.1 through 4.3 show that the thicker specimens are less responsive to ultrasound than the thinner ones. This perhaps shows the effect of applying strain amplitude over a thicker sample. Since the amplitude that the thicker samples is subjected to from the movement of the ultrasonic horn is the same amplitude that the thinner samples are subjected to, its effect on the entire network is diminished. Additionally, if the crosslinks are broken on the surface of the specimen and

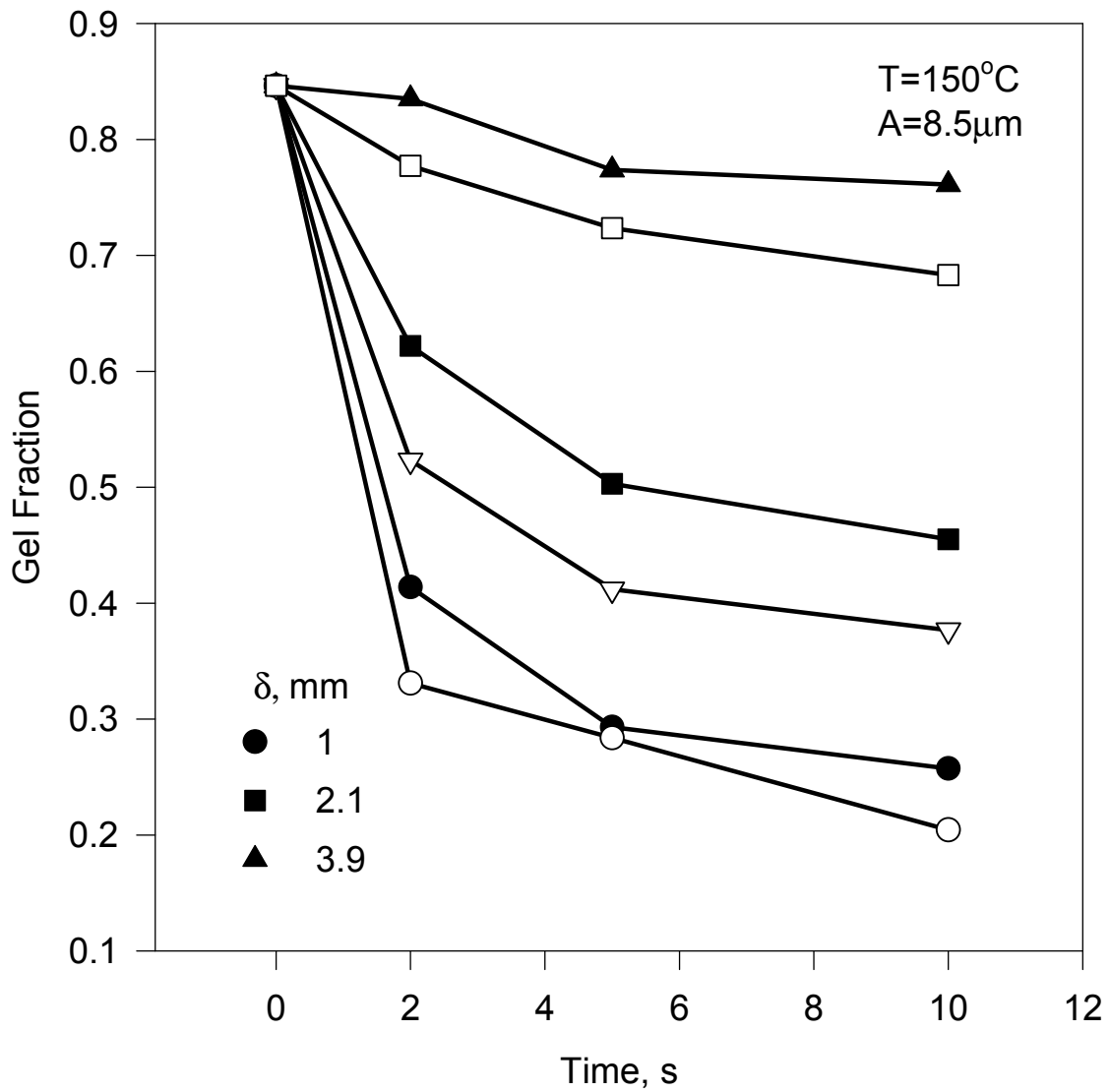


Figure 4.1 Gel fraction versus exposure time for different thickness samples. Samples are exposed to ultrasound at a temperature of 150°C , horn amplitude of $8.5\mu\text{m}$ and pressures of 0.35 MPa (filled symbols) and 0.69 MPa (open symbols).

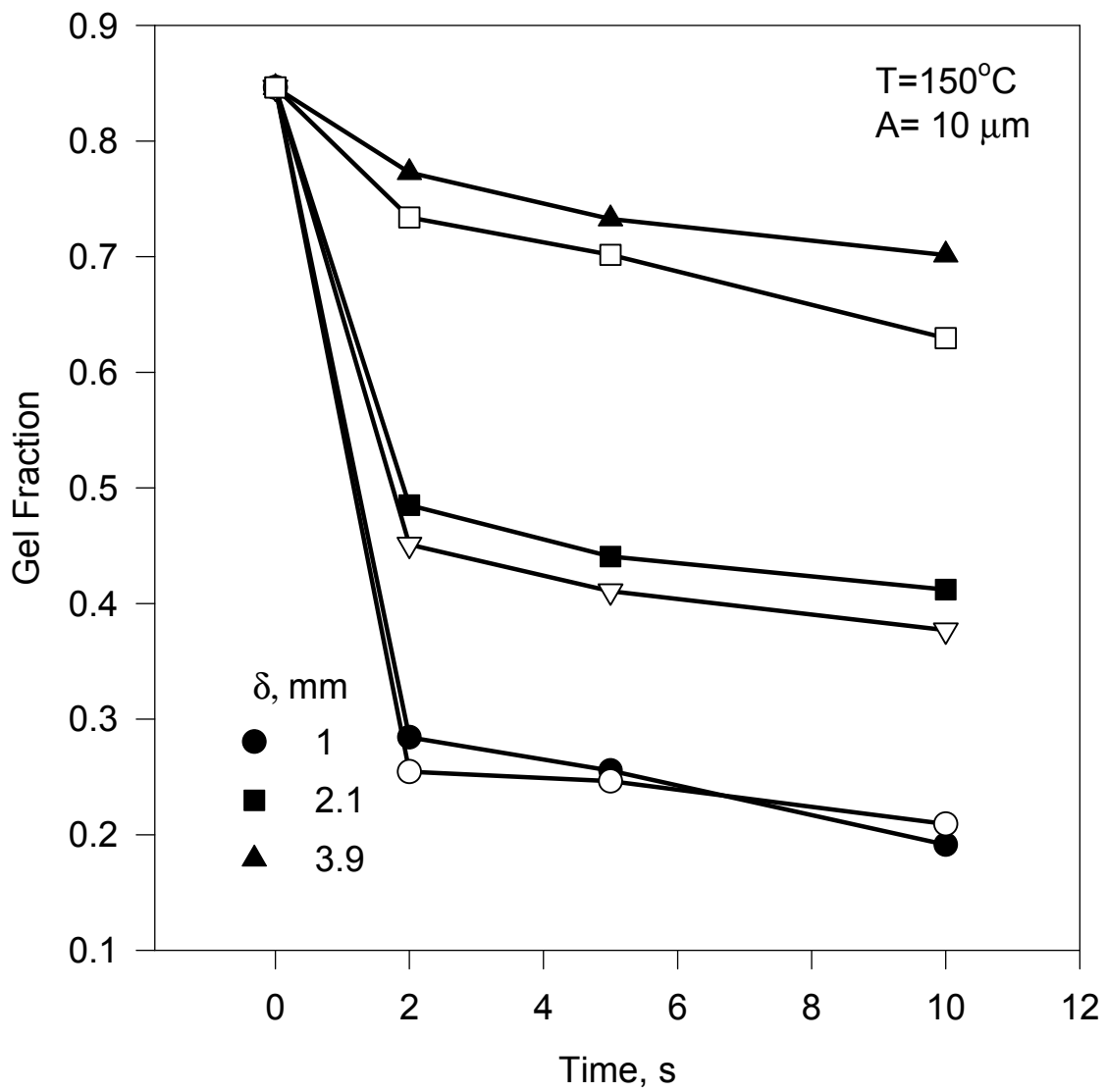


Figure 4.2 Gel fraction versus exposure time for different thickness samples. Samples are exposed to ultrasound at a temperature of 150°C, horn amplitude of 10 μm and pressures of 0.35 MPa (filled symbols) and 0.69 MPa (open symbols).

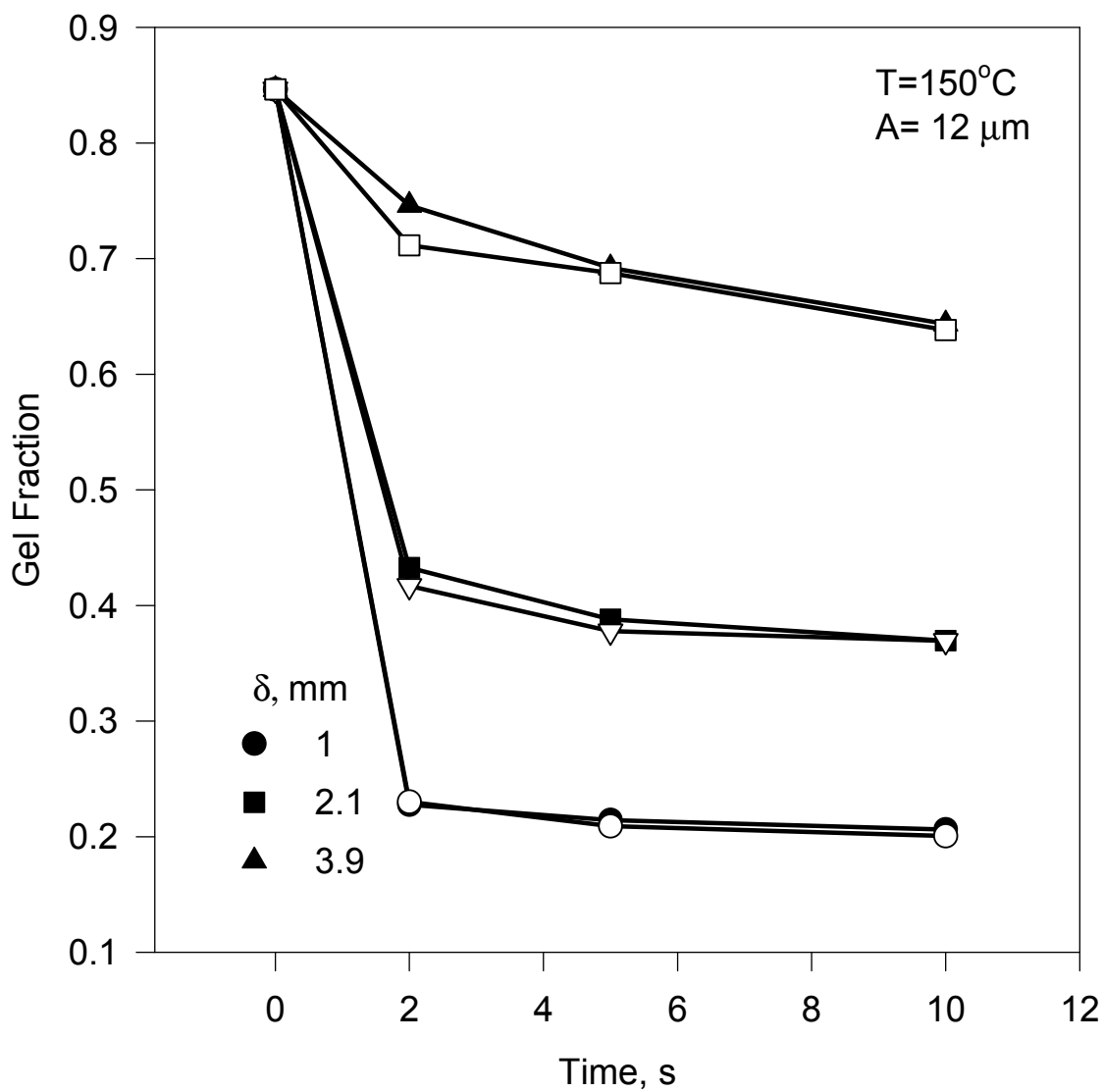


Figure 4.3 Gel fraction versus exposure time for different thickness samples. Samples are exposed to ultrasound at a temperature of 150°C, horn amplitude of 12 μm and pressures of 0.35 MPa (filled symbols) and 0.69 MPa (open symbols).

the viscosity is reduced such that the material network is no longer rigid enough to transport ultrasound, then it is reasonable to say that the material below this decrosslinked region remains unaffected by the process. In Figure 4.1 the pressure to which the filled symbol specimens are exposed is double that of the pressure which specimens represented by open symbols. The same trend is seen with the thicker sample showing more reaction, but still to a much lower level than the thinner ones.

Figure 4.1 shows the specimens at the lowest ultrasound levels they were tested. The remaining Figures, 4.2 and 4.3, which use higher levels of ultrasound, have much flatter slopes from 2 to 10 seconds indicating that the effect of the process at those energy levels is essentially complete in 2 seconds. With this information, it is clear that strain amplitude is more important than the total energy the material is exposed to. Additionally, in Figure 4.2, which use pressures of .35 and .69 MPa, it appears that when the ultrasound level is high enough the pressure is less of a factor in decrosslinking the material. Figure 4.3, gel fraction versus exposure time, represent the highest amplitudes that the samples were exposed. The figure shows very flat slopes, especially for the thin specimens.

From these graphs it is apparent that there is a limitation to the thickness that the ultrasound will affect the material. They also show that pressure and time are only controlling factors when the ultrasound amplitude is at its smallest value. When the amplitude is high enough, the specimens seem to reach their final gel fraction quickly and that increased exposure time yields diminishing returns.

Figures 4.4 through 4.6 show crosslink density versus exposure time. The original crosslink density of the specimen before being exposed to the de-crosslinking process was $1.93 \times 10^{-4} \text{ mol/cm}^3$. In each graph it is shown that exposure time is not a controlling factor of the resulting crosslink density with increased exposure time. Figure

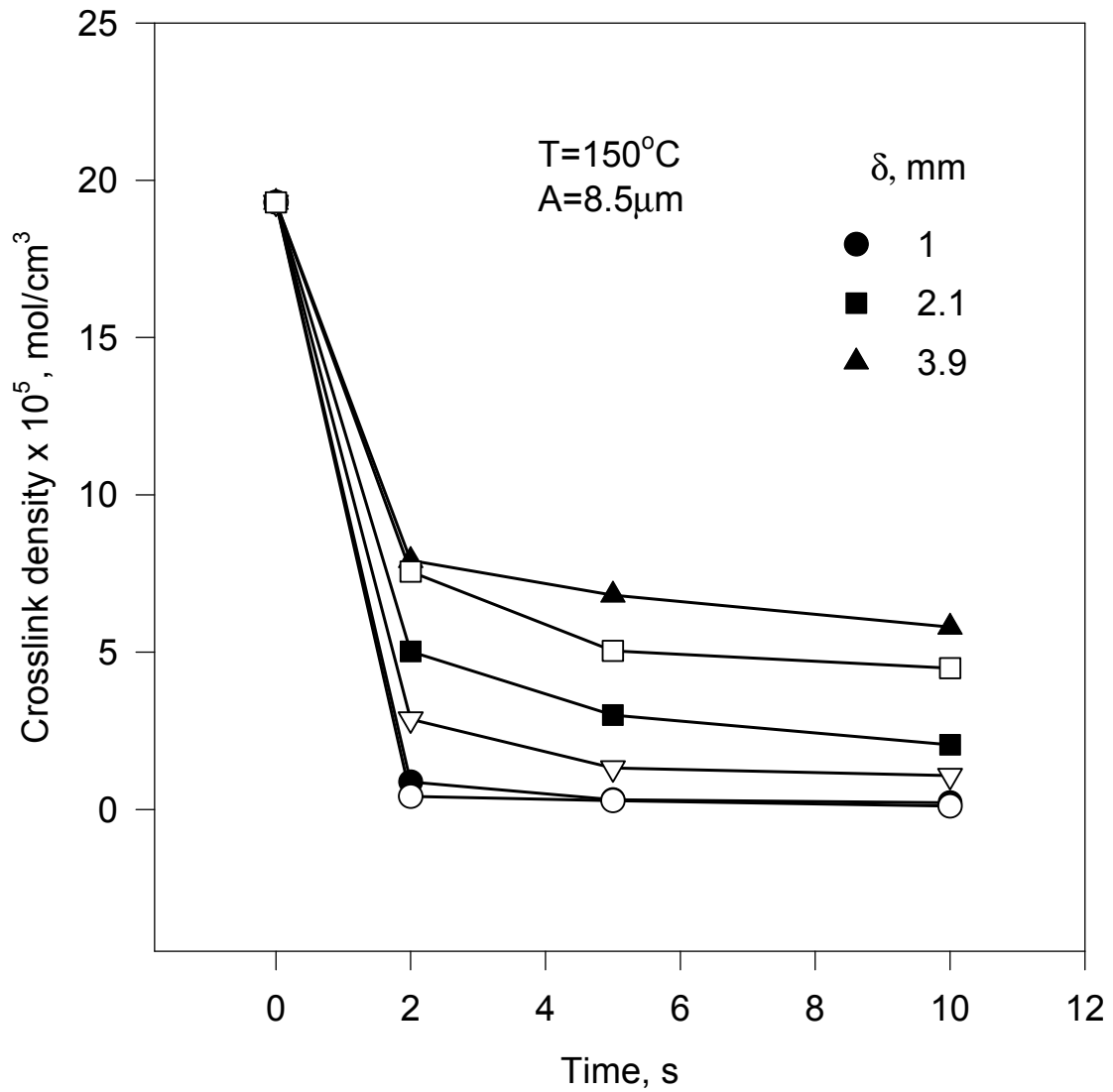


Figure 4.4 Crosslink density versus exposure time for different thickness samples. Samples are exposed to ultrasound at a temperature of 150°C , horn amplitude of $8.5 \mu\text{m}$ and pressures of 0.35 MPa (filled symbols) and 0.69 MPa (open symbols)..

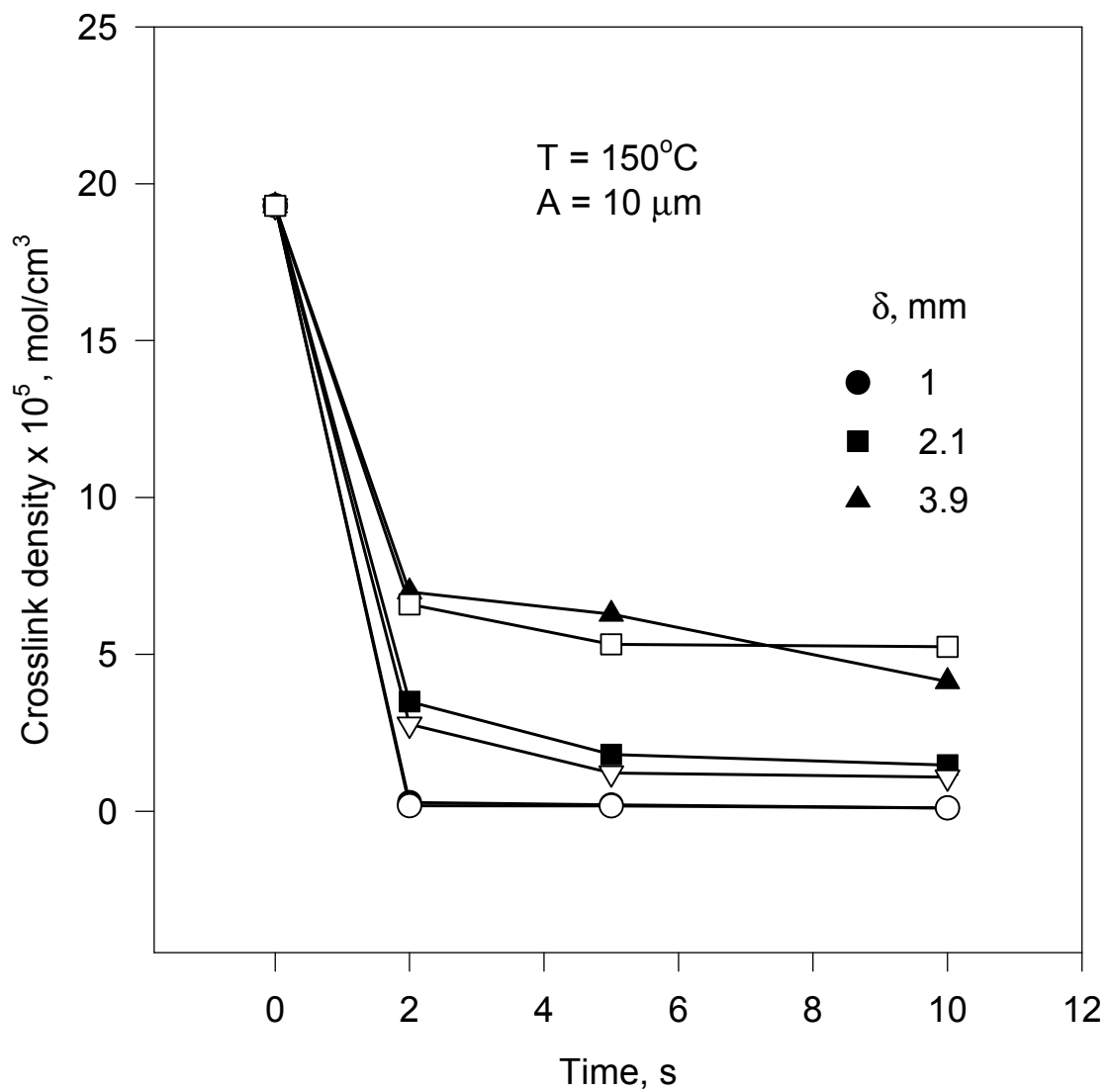


Figure 4.5 Crosslink density versus exposure time for different thickness samples. Samples are exposed to ultrasound at a temperature of 150°C , horn amplitude of $10 \mu\text{m}$ and pressures of 0.35 MPa (filled symbols) and 0.69 MPa (open symbols).

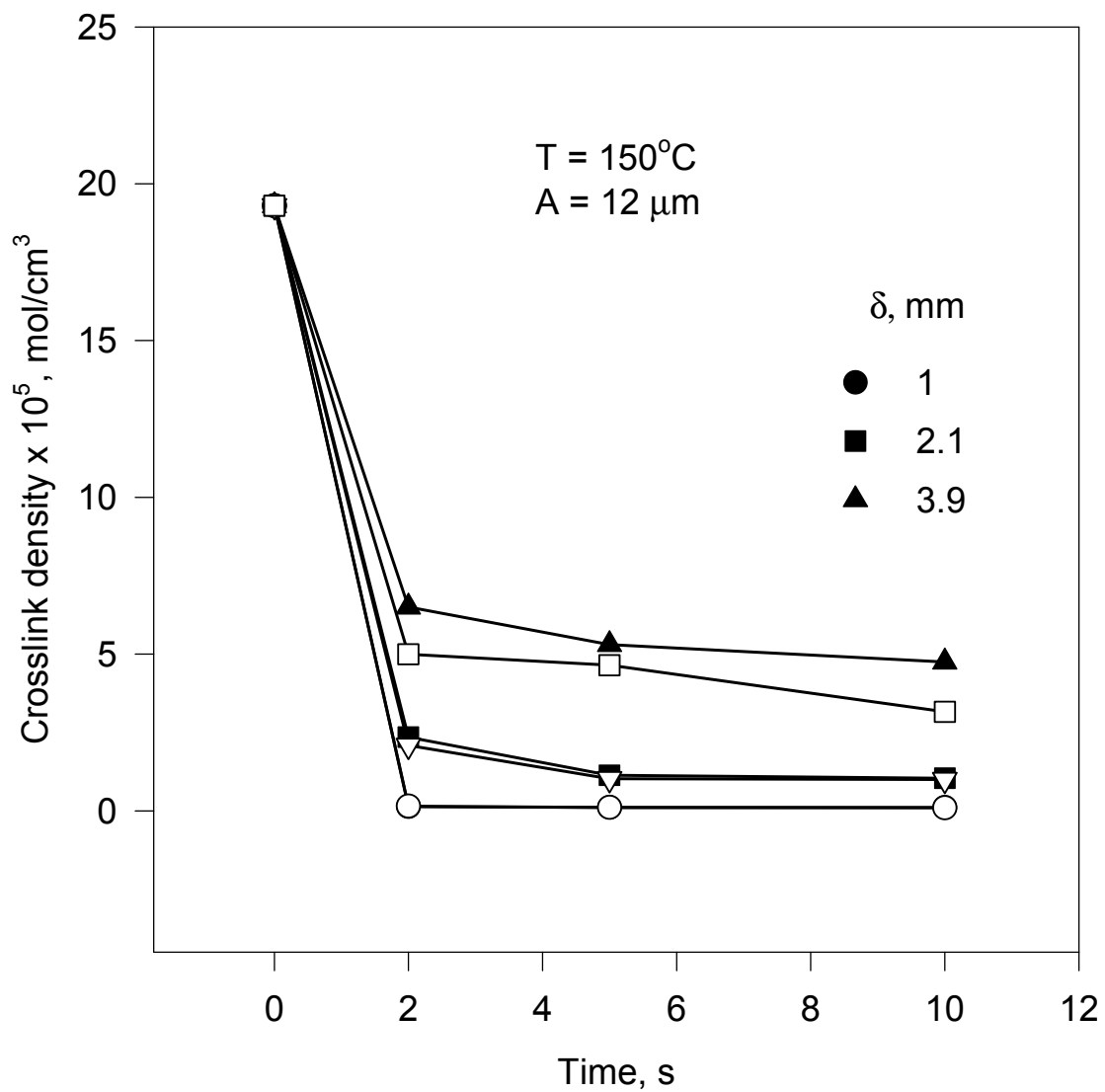


Figure 4.6 Crosslink density versus exposure time for different thickness samples. Samples are exposed to ultrasound at a temperature of 150°C, horn amplitude of 12 μm and pressures of 0.35 MPa (filled symbols) and 0.69 MPa (open symbols).

4.4 shows that at different pressures, the reaction to the treatment is essentially the same. The filled symbol specimens in Figure 4.4 are subjected to double the pressure of the open symbol specimens but still respond very similarly. The slopes in all of the figures are again very flat indicating that strain amplitude is more important than exposure time or pressure. Figure 4.5 shows specimens treated at higher amplitudes. The slopes of the curves are still flat indicating not much change with exposure time after 2 seconds. The resulting crosslink densities are slightly less than specimens treated at the lower amplitudes represented in Figure 4.4. Figure 4.6 shows specimens treated at the highest amplitude. These figures show a very flat curve with the response to specimen thickness being the overwhelming factor in treatment levels. Figures 4.7 through 4.9 are of crosslink density versus specimen thickness for different exposure intervals. The original crosslink density of the specimen before being exposed to the de-crosslinking process was $1.93 \times 10^{-4} \text{ mol/cm}^3$, an order of magnitude above the treated samples.

Figure 4.7 shows results for different pressures and exposure time, holding all other factors equal. As the thickness of the samples is increased, the process has a lessened decrosslinking effect on the materials. Figure 4.8 shows that the specimens subjected to higher ultrasound levels have lower resulting crosslink densities than their counterparts in Figure 4.7. In this case, an increase of pressure that the material is subjected to during the process decreases the sample crosslink density. As the amplitude of the ultrasonic horn is raised, as shown in Figure 4.8, pressure has a lessened affect and the results of each specimen and its counterpart are very similar. The same trend is noted in Figures 4.9. In Figures 4.8 and 4.9, again it is shown that when the amplitude is sufficient, increased exposure time to ultrasound is of little consequence after five seconds. The thickness of each specimen also inversely affects the response of the

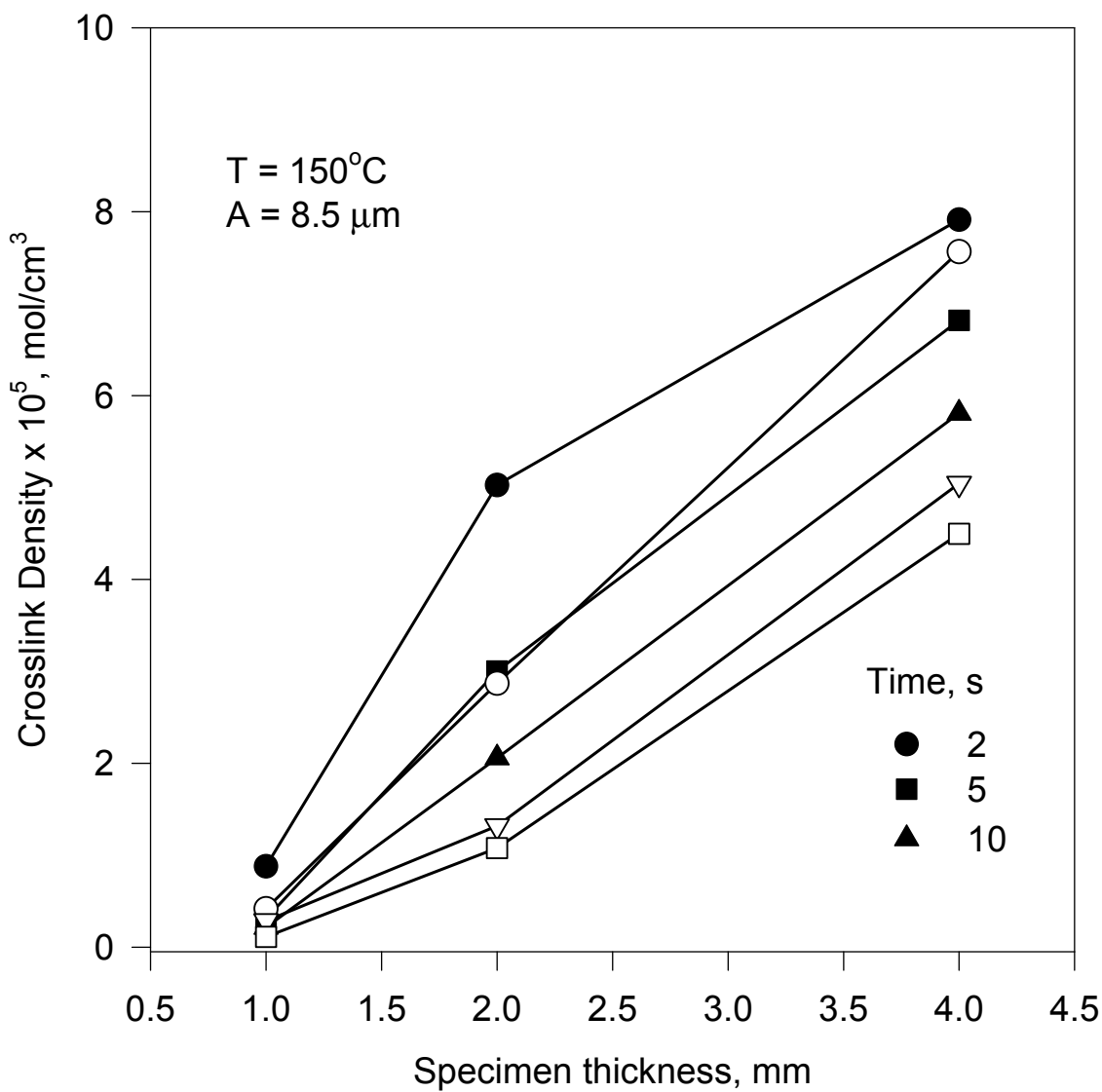


Figure 4.7 Crosslink density versus specimen thickness for different exposure times. Samples are exposed to ultrasound at 150°C, horn amplitude of 8.5 μm and pressures of 0.35 MPa (filled symbols) and 0.69 MPa (open symbols).

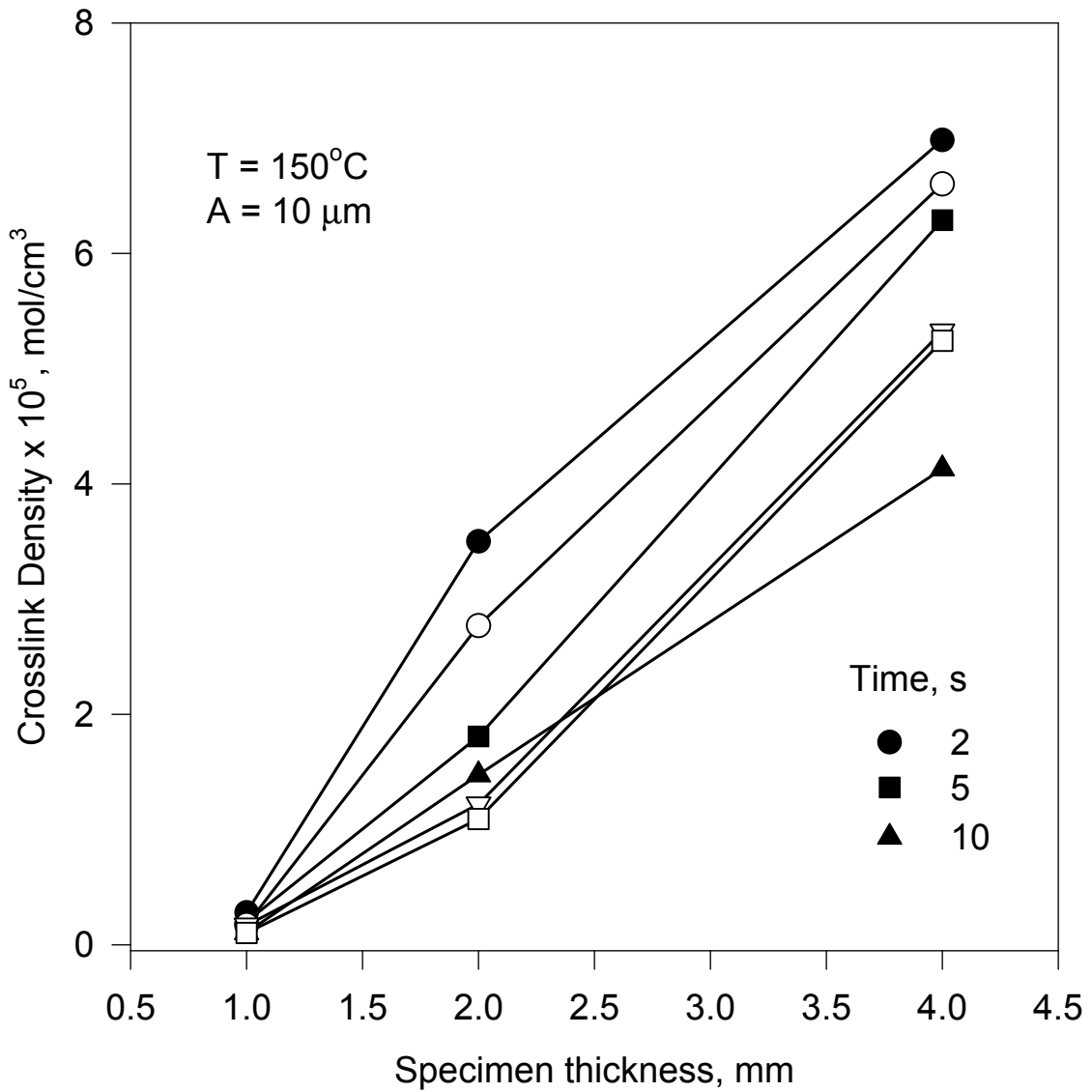


Figure 4.8 Crosslink density versus specimen thickness for different exposure times. Samples are exposed to ultrasound at 150°C, horn amplitude of 10 μm and pressures of 0.35 MPa (filled symbols) and 0.69 MPa (open symbols).

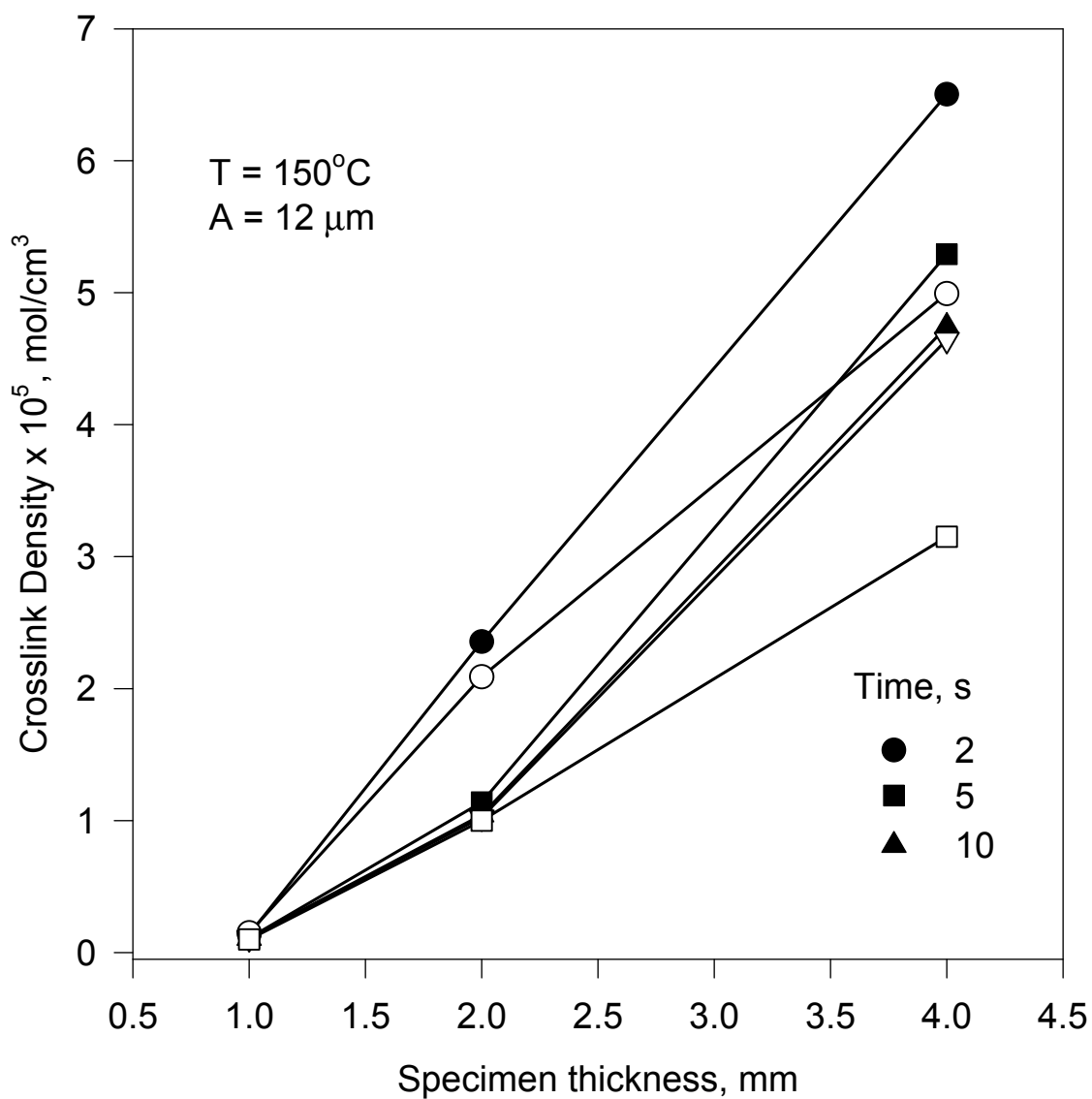


Figure 4.9 Crosslink density versus specimen thickness for different exposure times. Samples are exposed to ultrasound at 150°C, horn amplitude of 12 μm and pressures of 0.35 MPa (filled symbols) and 0.69 MPa (open symbols).

material to the treatment, i.e., the thicker specimens remained more highly crosslinked after the treatment.

Figures 4.10 through 4.12 show gel fraction versus crosslink density for different exposure time and sample thicknesses. Figures 4.10 and 4.11 are normalized gel fraction versus normalized crosslink density. In these figures it is apparent that specimen thickness lessens the overall response of the material to the process. This is another example of the strain amplitude effect. Another explanation is that the modulus of the specimen's surface is lowered enough that it no longer transports ultrasonic energy leaving the remaining portion of the sample untreated. In any case, the specimens are clearly grouped together by sample thickness with very little overlap. Figure 4.12 shows gel fraction versus crosslink density for all exposure times, thicknesses and both pressures. From this figure it can be concluded that there is no effect of the different pressures since all of the data falls near the same curve.

4.3 Continuous Extrusion Experiments

4.3.1 Gel Fraction and Crosslink Density

Continuous experiments were carried out and material properties were measured as they were in the static experiment. In this experiment we were able to obtain viscosity data using the RMS 800 along with tensile property data. This is because larger sample sizes were possible in the continuous experiment. Figures 4.13 through 4.74 show the data from these experiments. 36 specimens were run under different processing conditions and crosslink densities and gel fraction were measured. Independent variables were screw rpm (5, 10, 20 and 40 rpm with corresponding flow

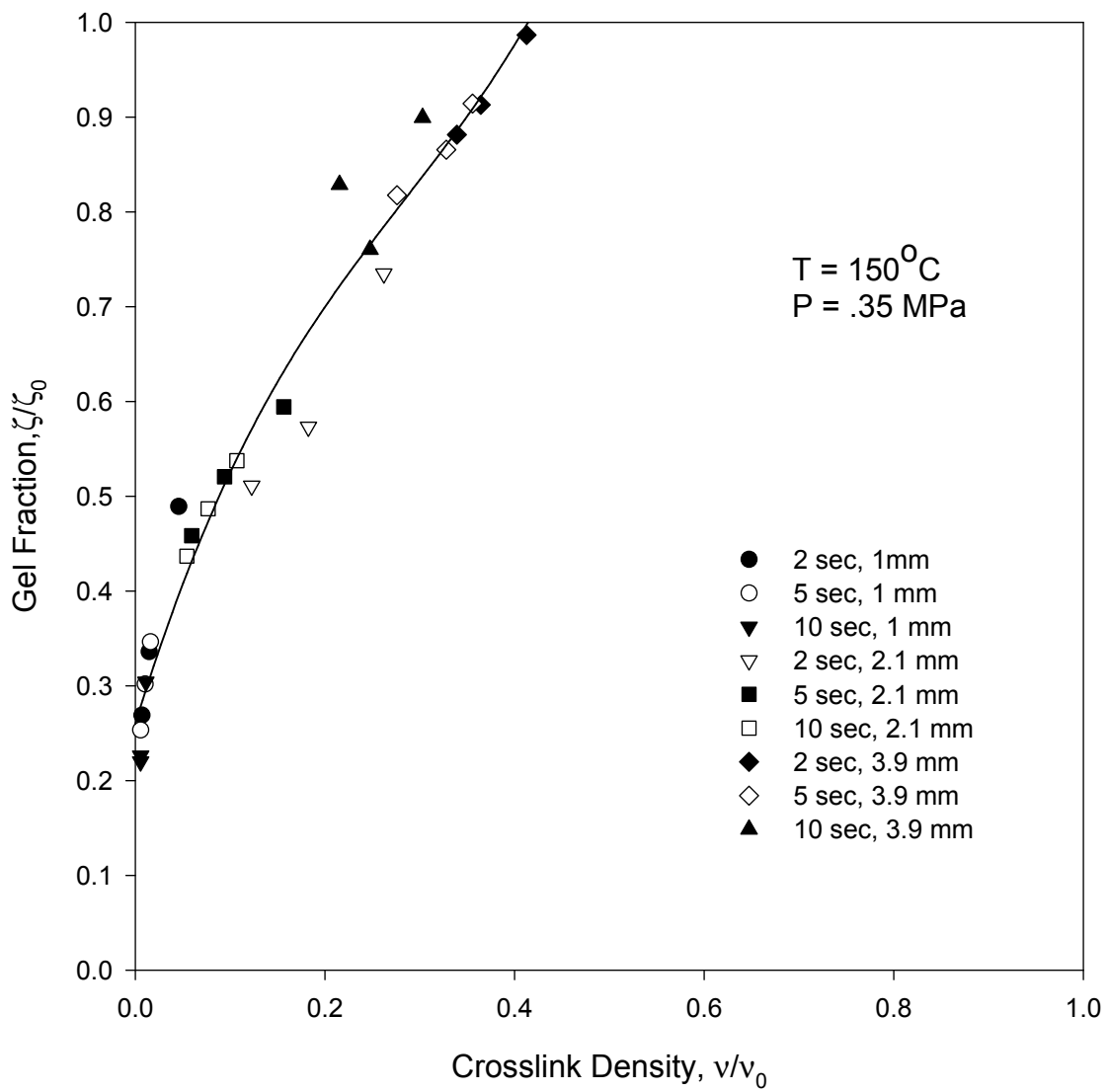


Figure 4.10 Gel fraction versus crosslink density for different exposure time and sample thicknesses. Samples are exposed to ultrasound at 150°C and pressure of .35 MPa.

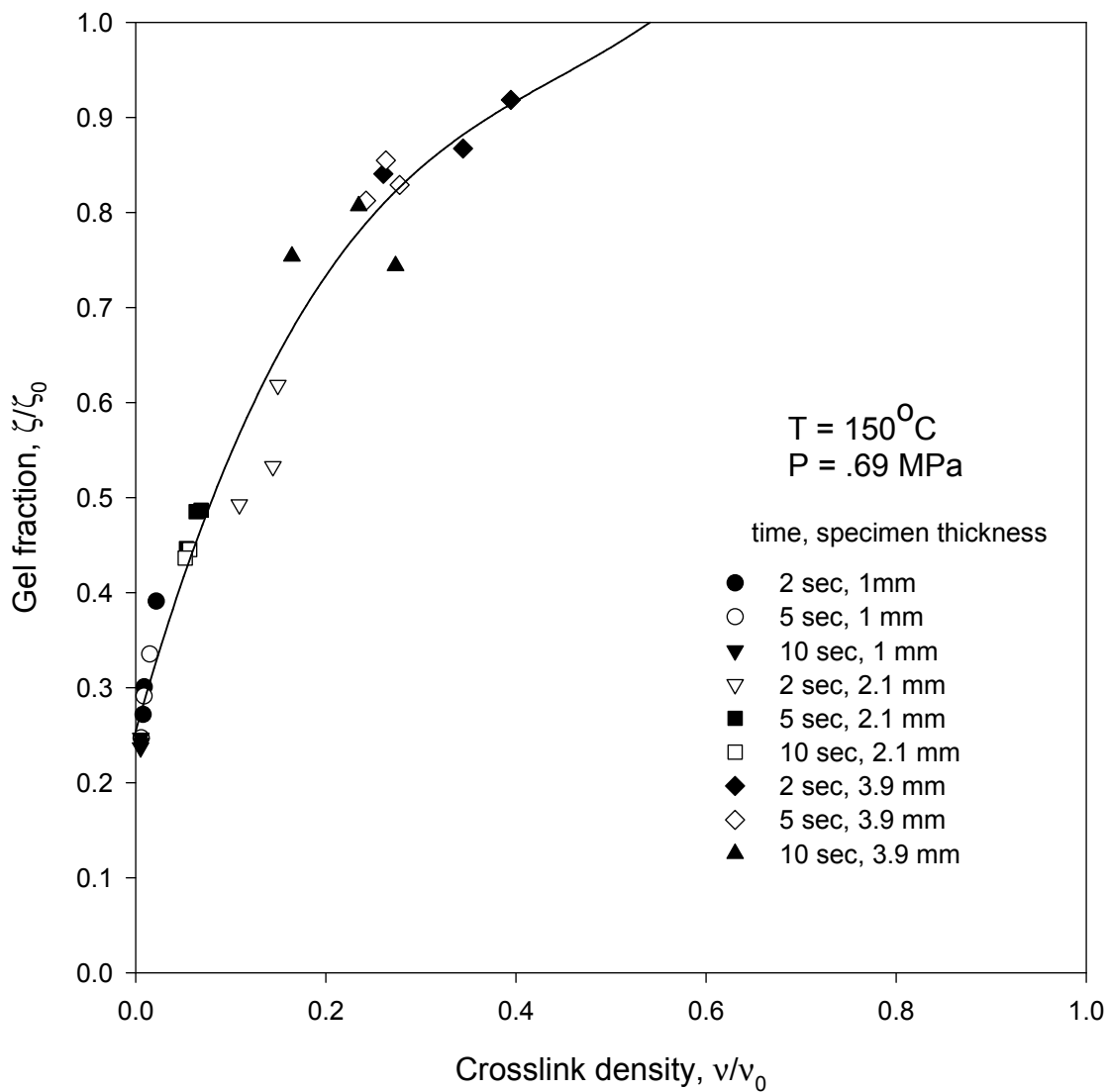


Figure 4.11 Gel fraction versus crosslink density for different exposure time and sample thicknesses. Samples are exposed to ultrasound at 150°C and pressure of .69 MPa.

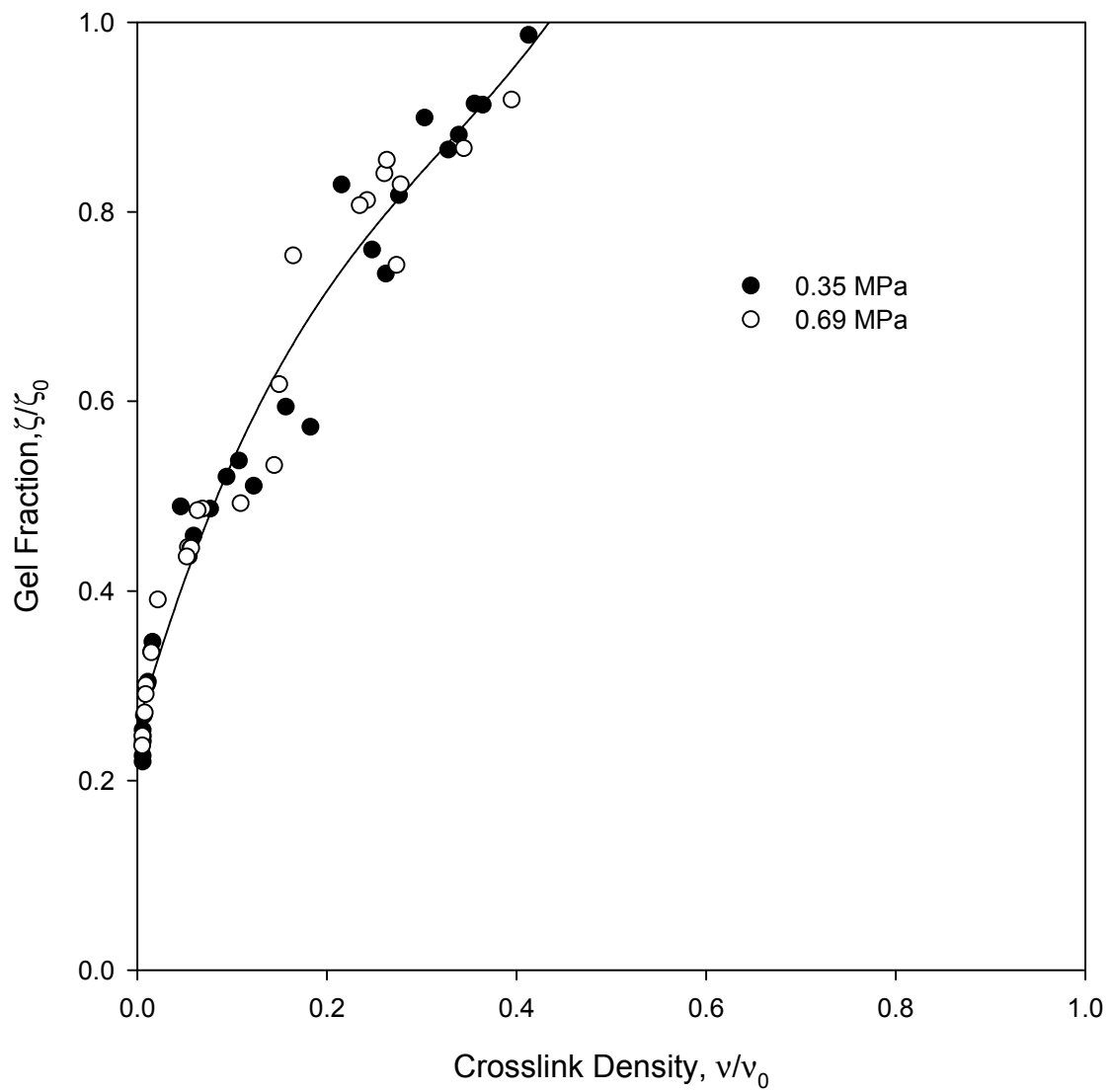


Figure 4.12 Gel fraction versus crosslink density for all exposure times and thicknesses. Samples are exposed to ultrasound at 150°C and pressures of .35 MPa and .69 MPa.

rates of 4.2, 8, 15.8, and 23.2 grams per minute). The three barrel zones were set at 150 °C. Using higher barrel temperatures produced a degraded product. The screw was flood fed. The gap between die outlet and the ultrasonic horn was set at 1, 2, and 4 mm. Different amplitudes were experimented with. The different amplitudes were achieved by varying the power output at 60, 80, and 100 %. Amplitudes were measured without load on the horn. They should however be comparable on relative basis. The actual amplitude measurements are 16.5, 20 and 25 micrometers, without load.

Figures 4.13 through 4.15 show the effect of flow rate on crosslink density as the ultrasonic energy and gap size. All three figures show the same primary trend that is materials run were barely affected by the process except at the lowest flow rate. Materials run at the 1 and 2 mm gap were affected to almost the same degrees with amplitude only being a factor in the materials run with the lowest flow rate. Materials run at the 4mm gap are even more clearly separated in the figure by flow rate.

In Figure 4.15, the material obtained with the 4 mm gap run at 4.2 g/min was affected to a greater degree than the others. Materials processed with a gap of 1 and 2 mm were affected to nearly the same degree at all throughput rates and gap sizes but still clearly more affected at the lower throughput rate. As shown in static experiments, the thicker samples strain amplitude is too low to affect the material. In this case, the gap of 4 mm is too large for enough energy to be transmitted through the sample as it passes the ultrasonic treatment area and is therefore unaffected or very slightly affected. As the gap size is reduced, the strain amplitude is increased and the material begins to be affected by the process. As the strain amplitude reaches the point that it is able to break crosslinks, the crosslink density is reduced. Higher energy levels introduce higher strain amplitude to the material and can reach the point of degradation. Additionally, as the crosslinks are broken, the material transmits energy less efficiently. When the energy is

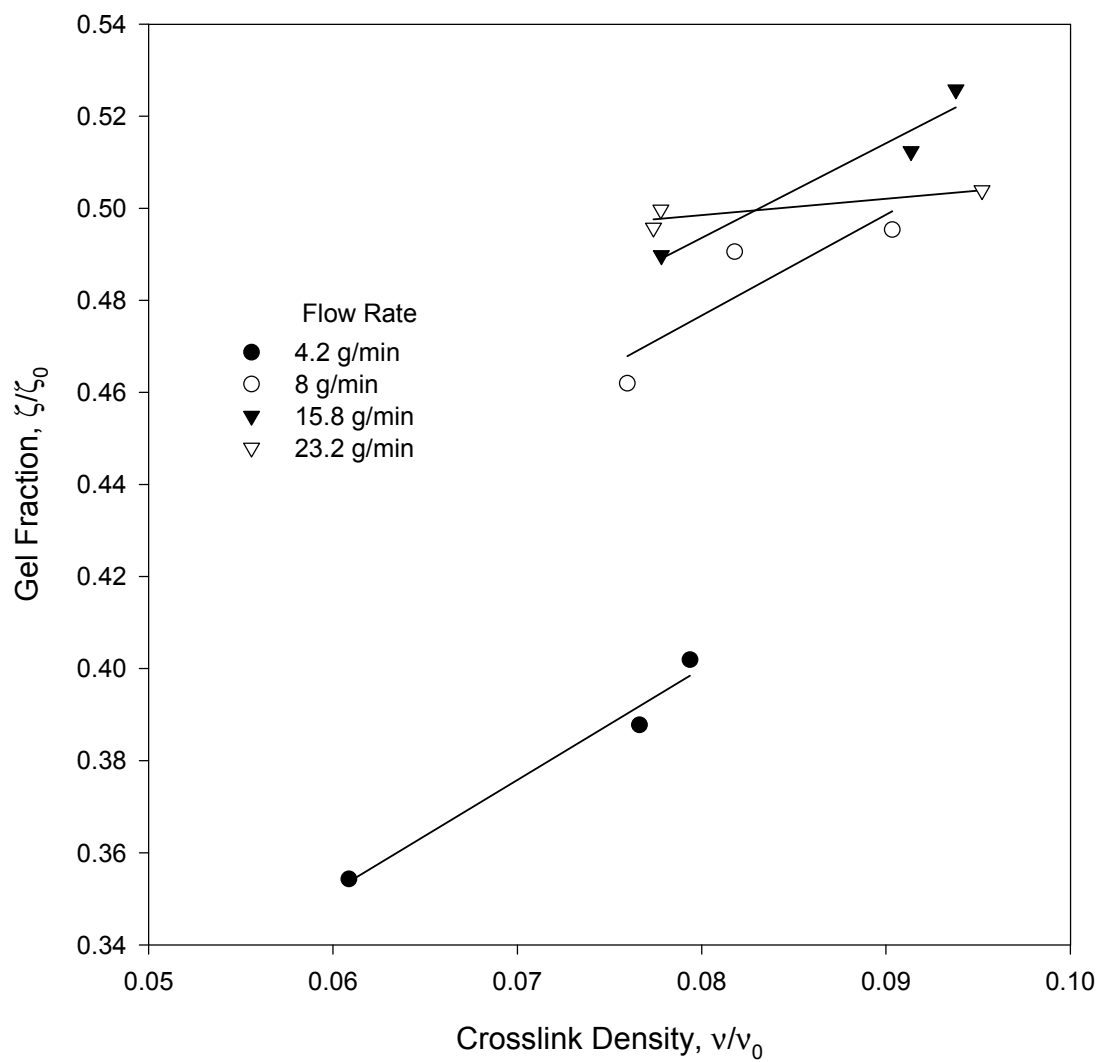


Figure 4.13 Gel fraction versus crosslink density for different flow rates and 1 mm gap in continuous decrosslinking.

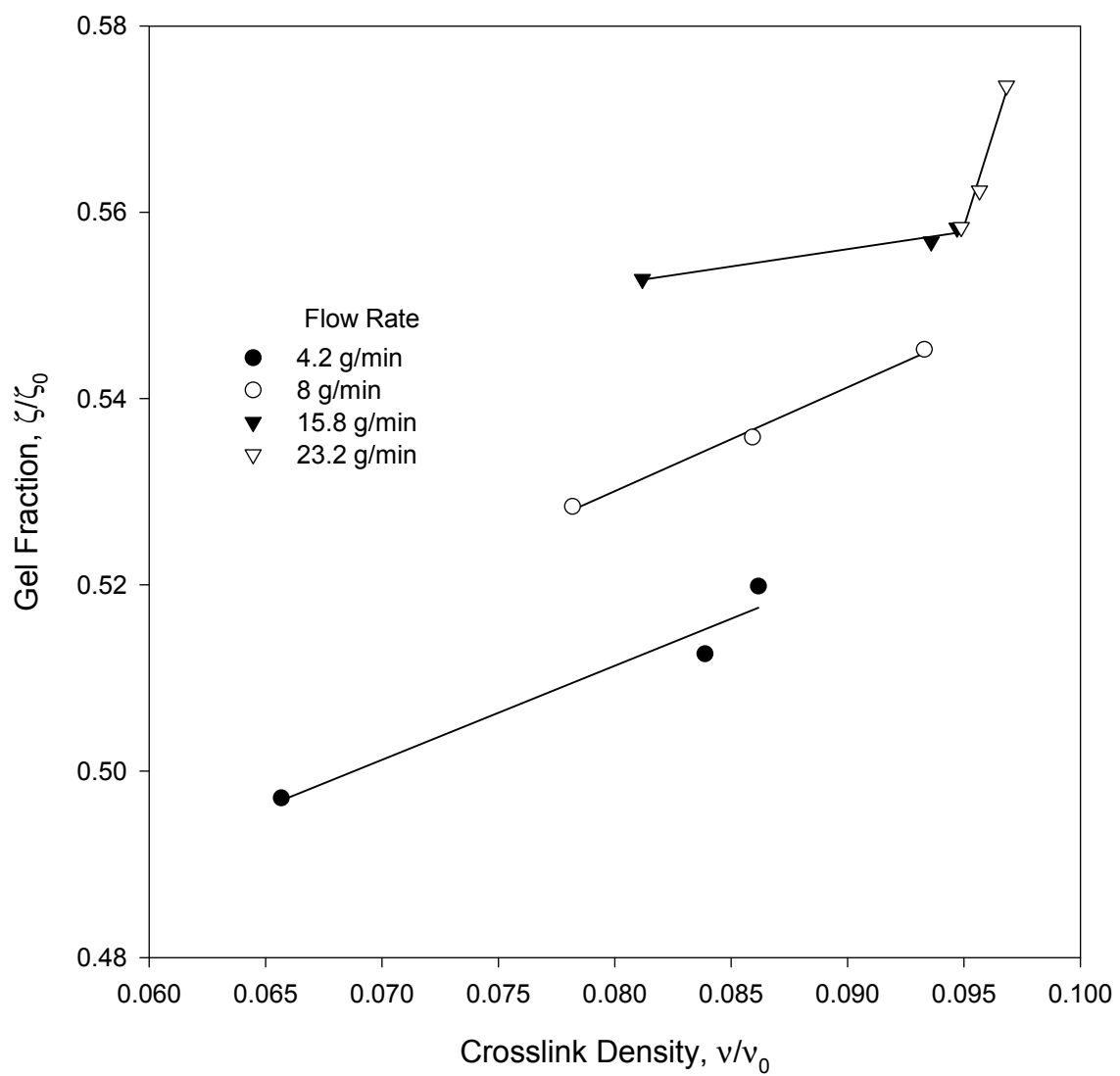


Figure 4.14 Gel fraction versus crosslink density for different flow rates and 2 mm gap in continuous decrosslinking.

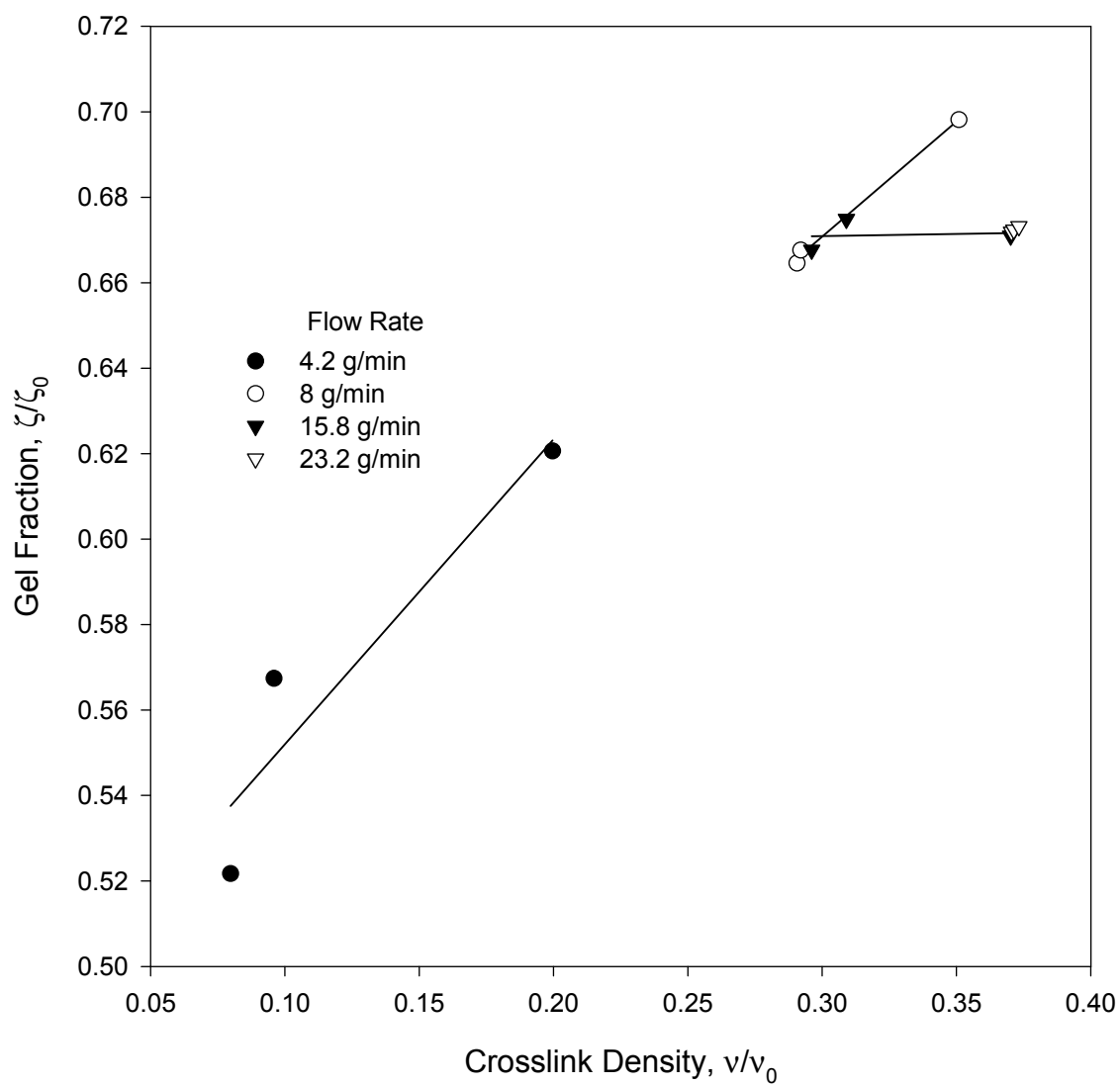


Figure 4.15 Gel fraction versus crosslink density for different flow rates and 4 mm gap in continuous decrosslinking.

high enough to break crosslinks they are all broken to the degree apparent from the graphs and are not broken any further until the strain amplitude is high enough to cause degradation. This concept becomes more evident as the remaining figures are analyzed.

Figure 4.16 shows gel fraction versus crosslink density for all gaps. The samples treated with 4 mm gap have less extractables and more gel therefore they differ from samples treated with 1 mm and 2 mm. We can conclude that the 4mm gap was too large for the specimens to be sufficiently treated. Since the amplitude that the thicker samples is subjected to from the movement of the ultrasonic horn is the same amplitude that the thinner samples are subjected to, its effect on the entire network is diminished. Additionally, if the crosslinks are broken on the surface of the specimen and the viscosity is reduced such that the material network is no longer rigid enough to transport ultrasound, then it is reasonable to say that the material below this decrosslinked region remains unaffected by the process. Figure 4.17 combines the results for static and continuous decrosslinking. The same specimens from Figure 4.16 that showed up outside of the expected range are seen again. Excluding those samples, a very consistent and predictable result is shown from the treatment indicating that the mechanism of decrosslinking in the static and continuous experiments is the same.

Figures 4.18 through 4.21 show the effect of flow rate on crosslink density as the gap size and ultrasonic horn amplitude is changed. All of the graphs show the same primary trend that is materials run with a gap of 4 mm and flow rates of 4.2, 8.0, 15.8, and 23.2 grams per minute were barely affected by the process than that of other gaps. Materials run at the 1 and 2 mm gap were affected to almost the same degrees with amplitude only being a factor in the materials run with the lowest flow rate.

Figures 4.22 through 4.24 show the crosslink density versus gap size. In each graph the amplitude is held constant while the throughput and gap sizes change.

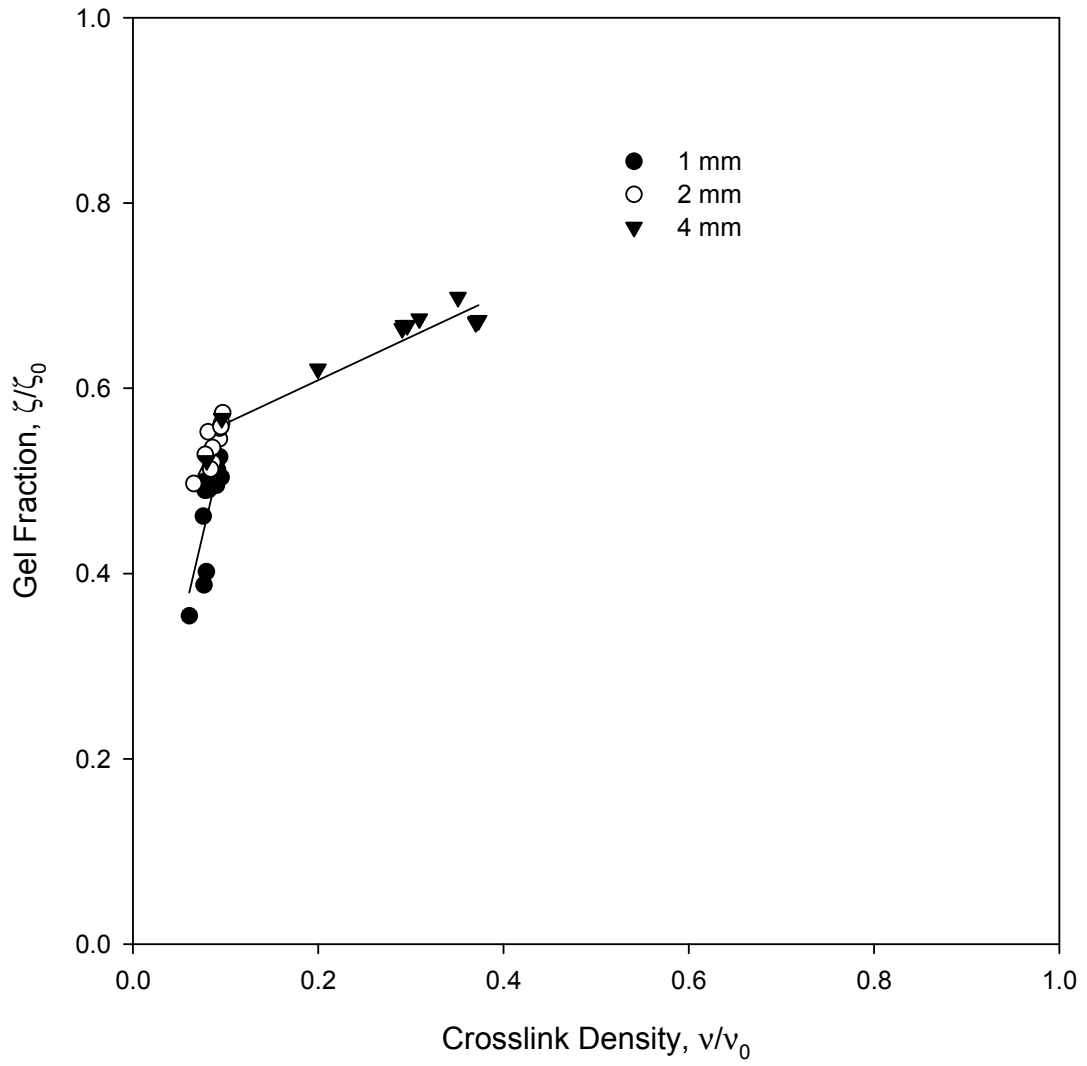


Figure 4.16 Gel fraction versus crosslink density for all gaps in continuous decrosslinking.

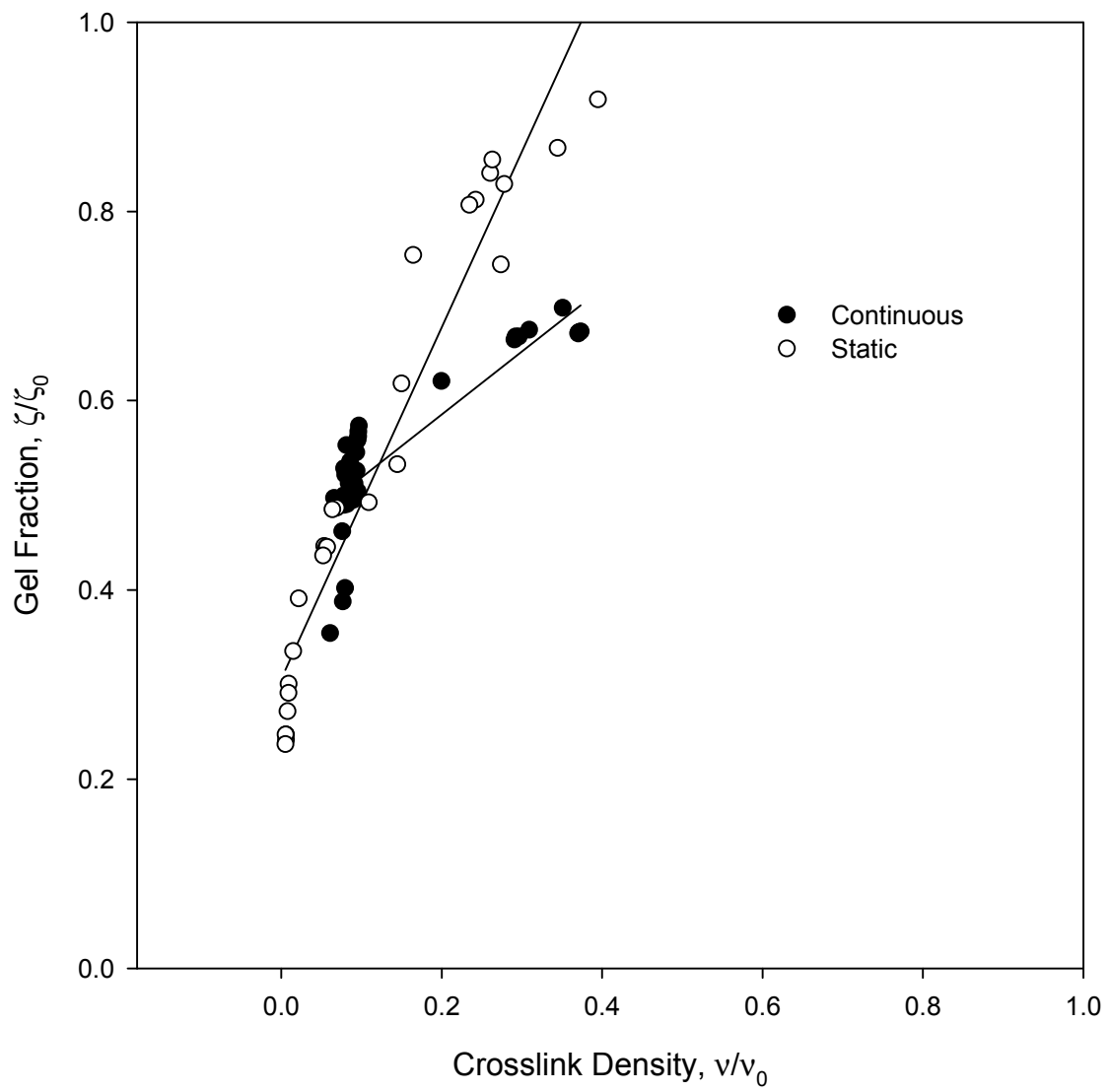


Figure 4.17 Gel fraction versus crosslink density for all samples.

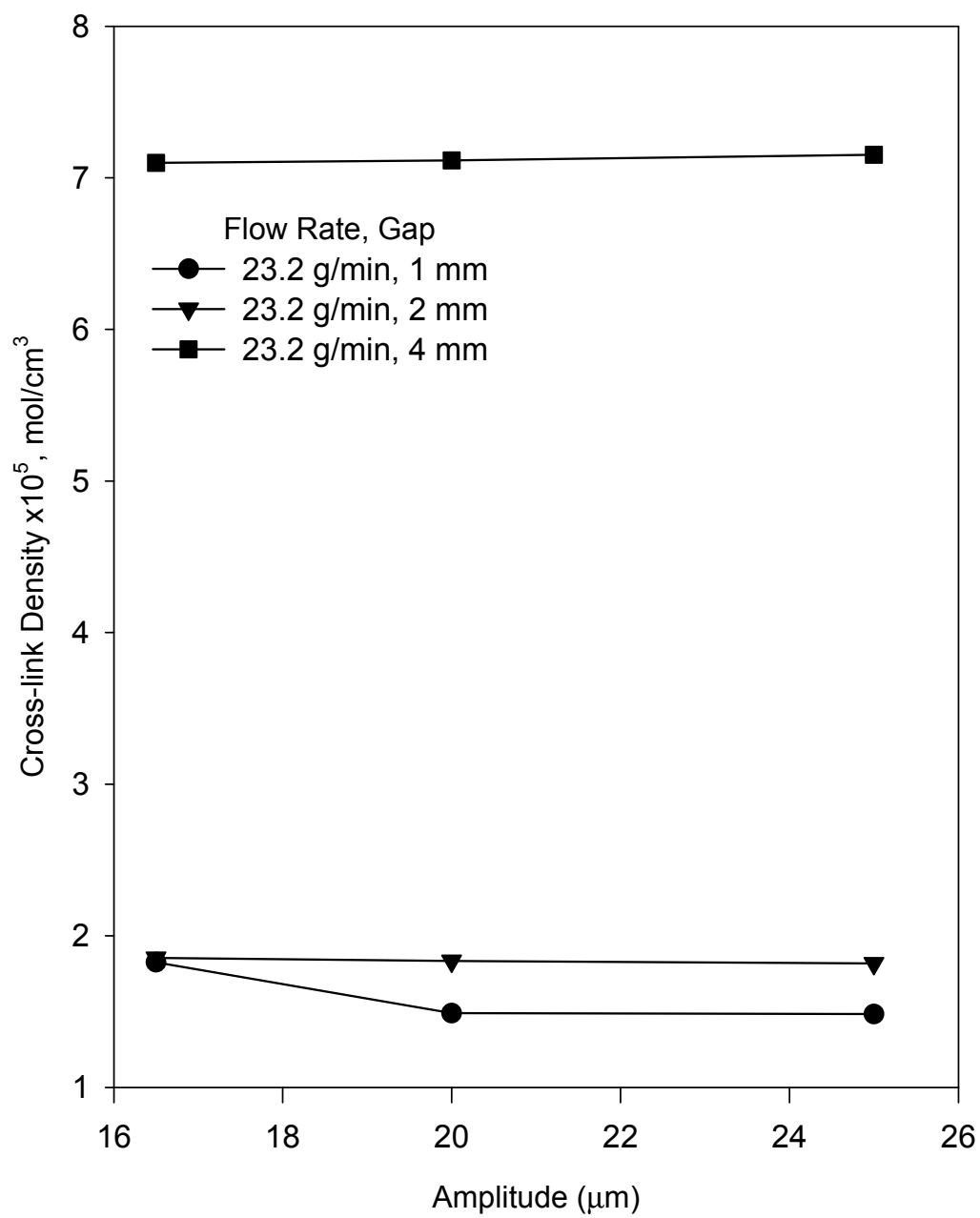


Figure 4.18 Crosslink density as a function of amplitude at various gaps and a flow rate of 23.2 g/min.

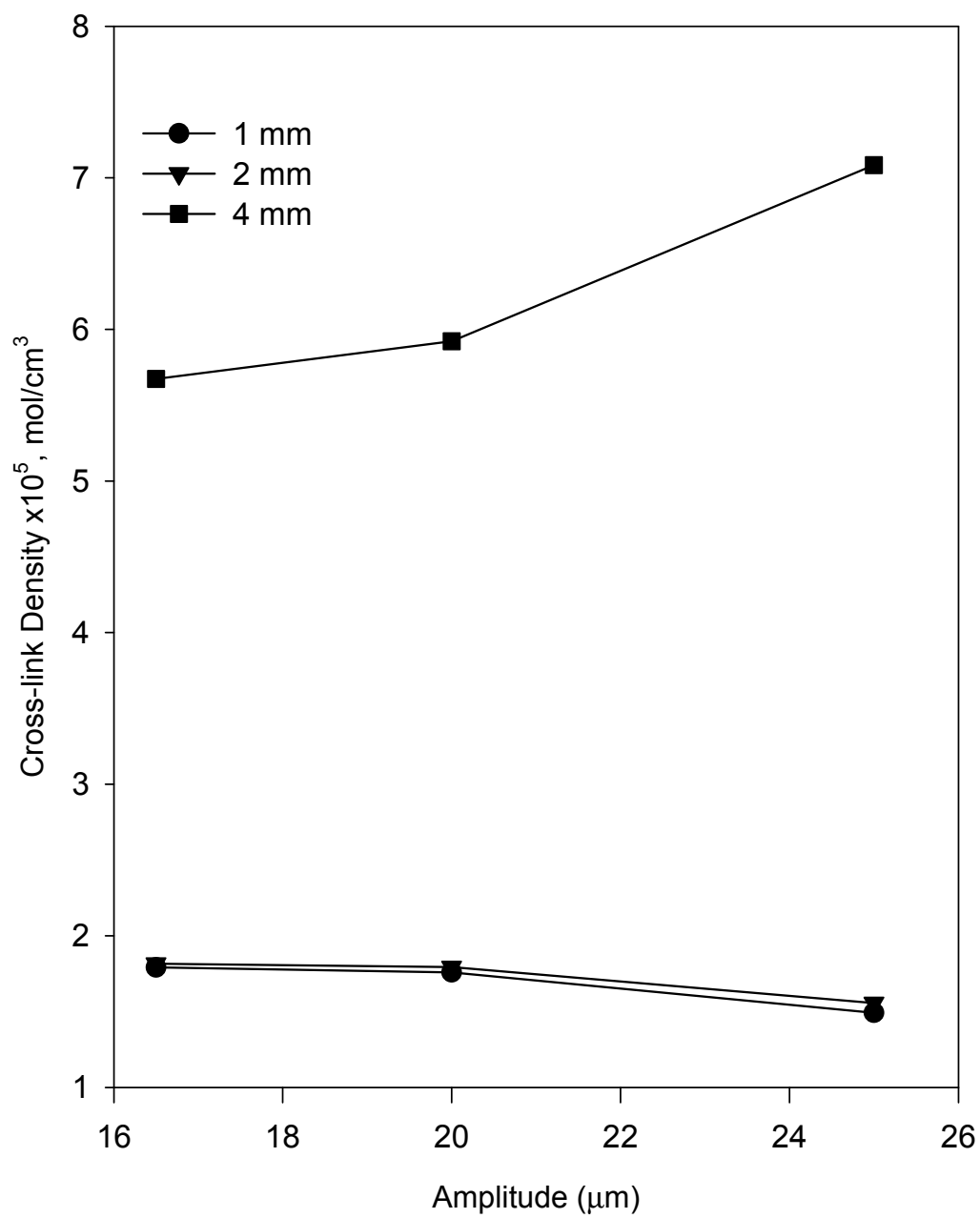


Figure 4.19 Crosslink density as a function of amplitude at various gaps and a flow rate of 15.8 g/min.

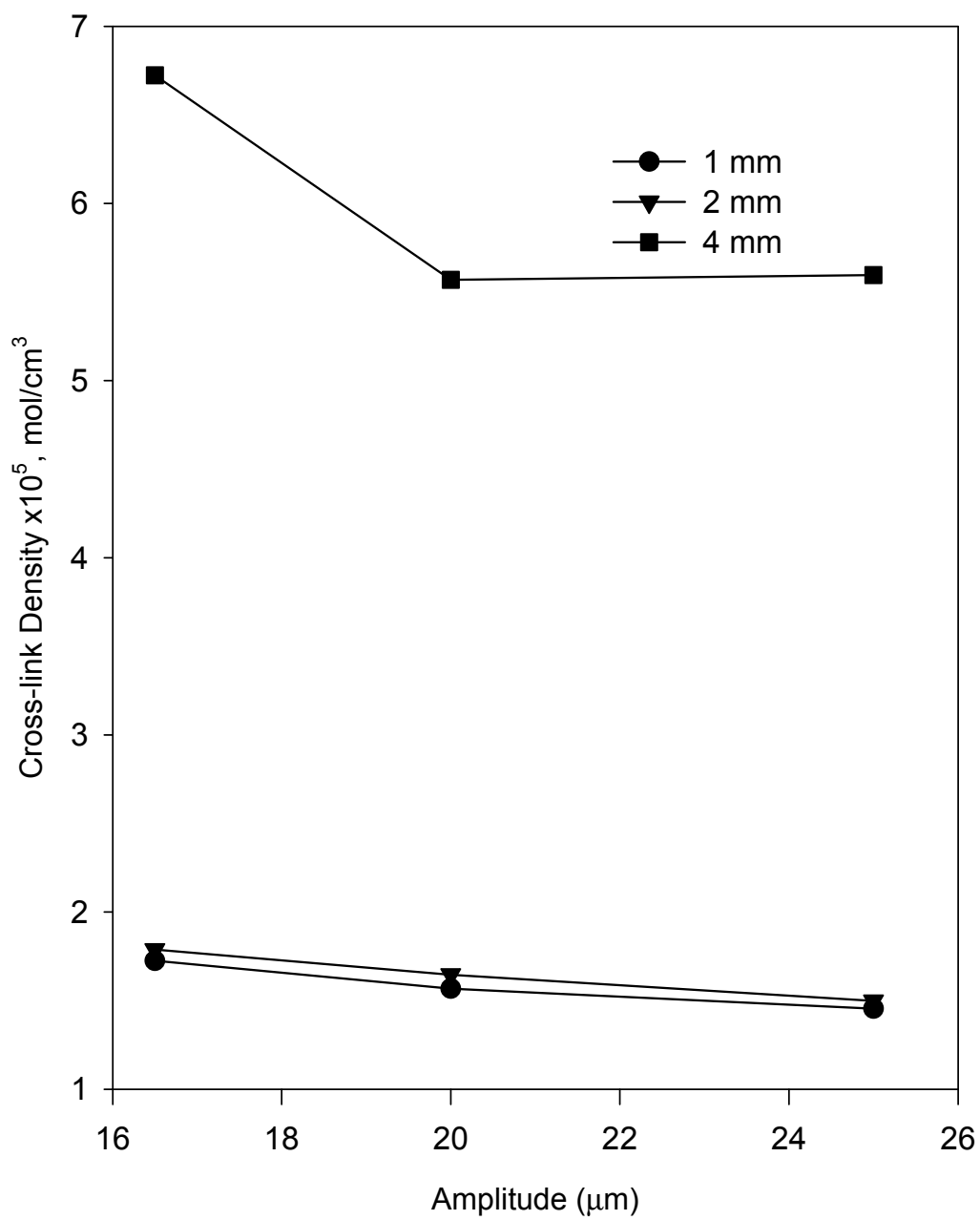


Figure 4.20 Crosslink density as a function of amplitude at various gaps and a flow rate of 8 g/min.

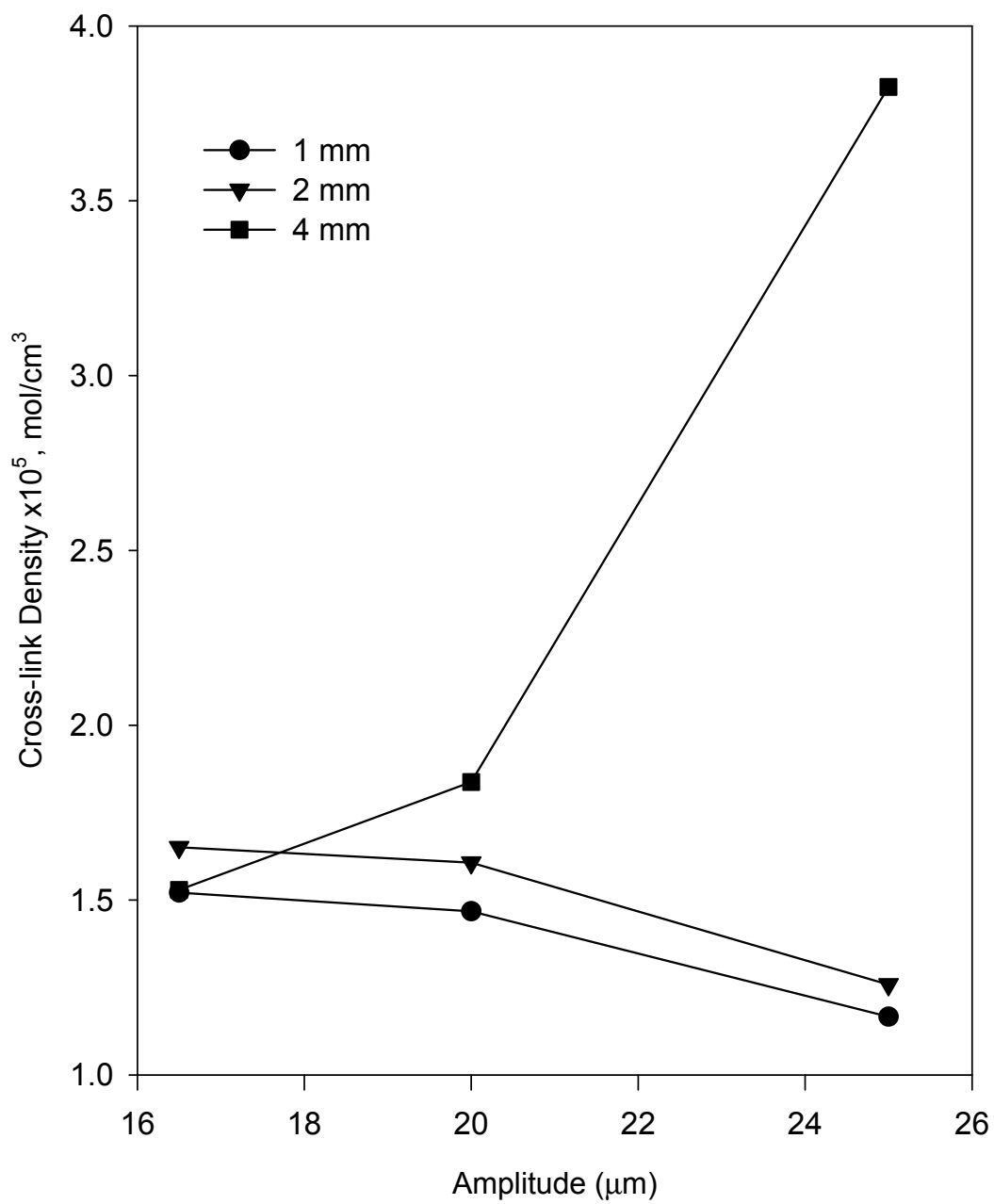


Figure 4.21 Crosslink density as a function of amplitude at various gaps and a flow rate of 4.2 g/min.

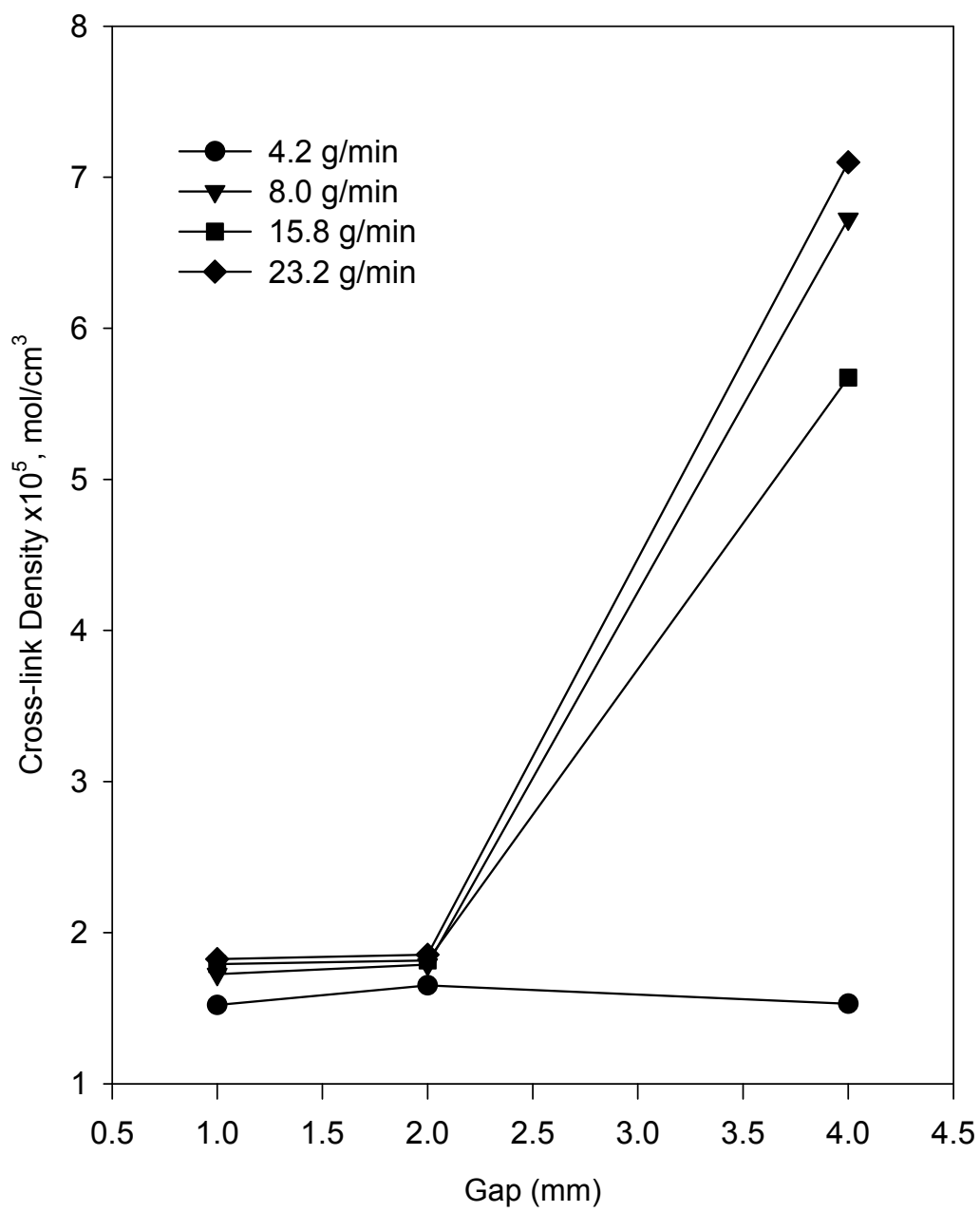


Figure 4.22 Crosslink density as a function of gap at various throughput rates and at amplitude of 16.5 μm .

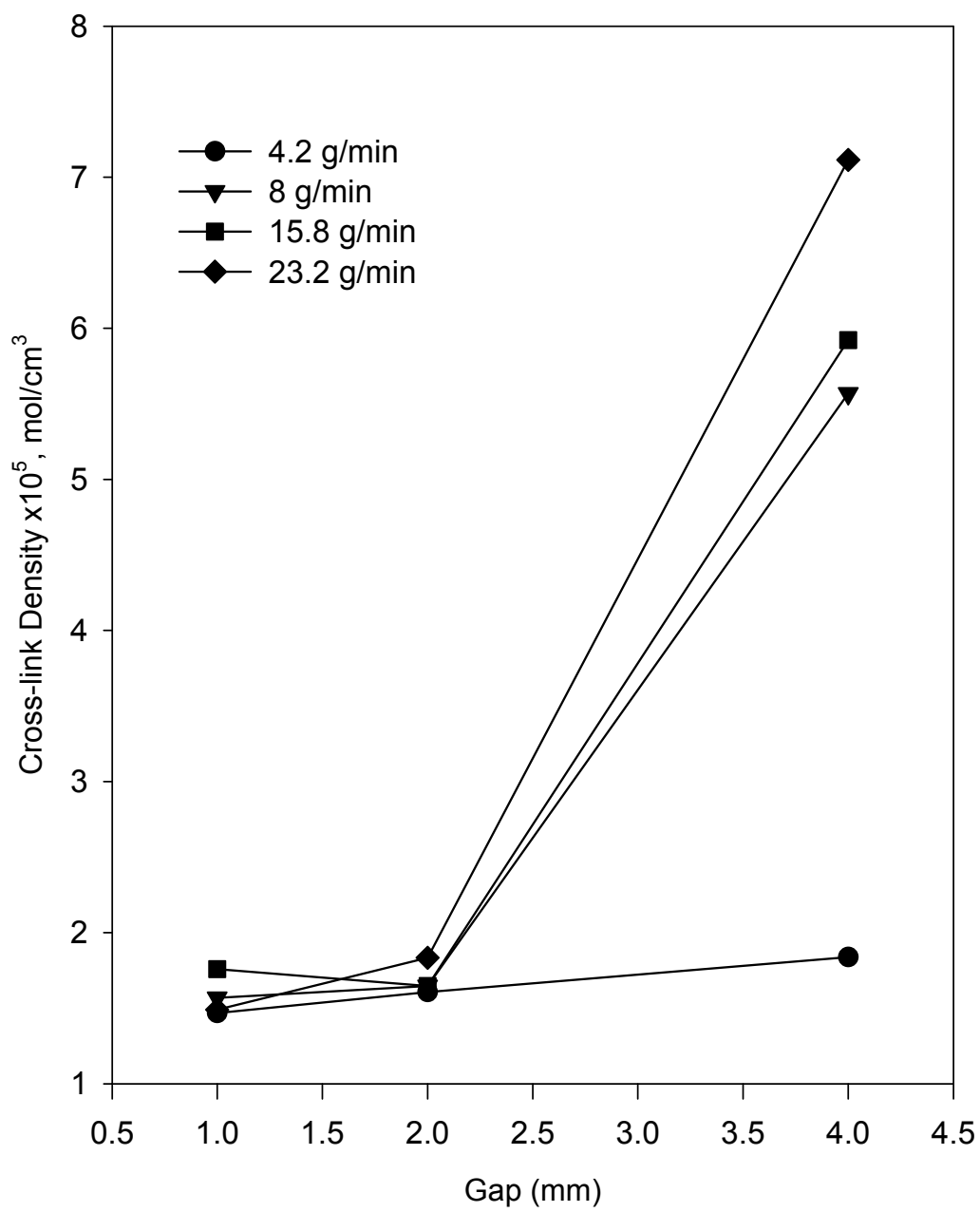


Figure 4.23 Crosslink density as a function of gap at various throughput rates and at amplitude of 20 μ m.

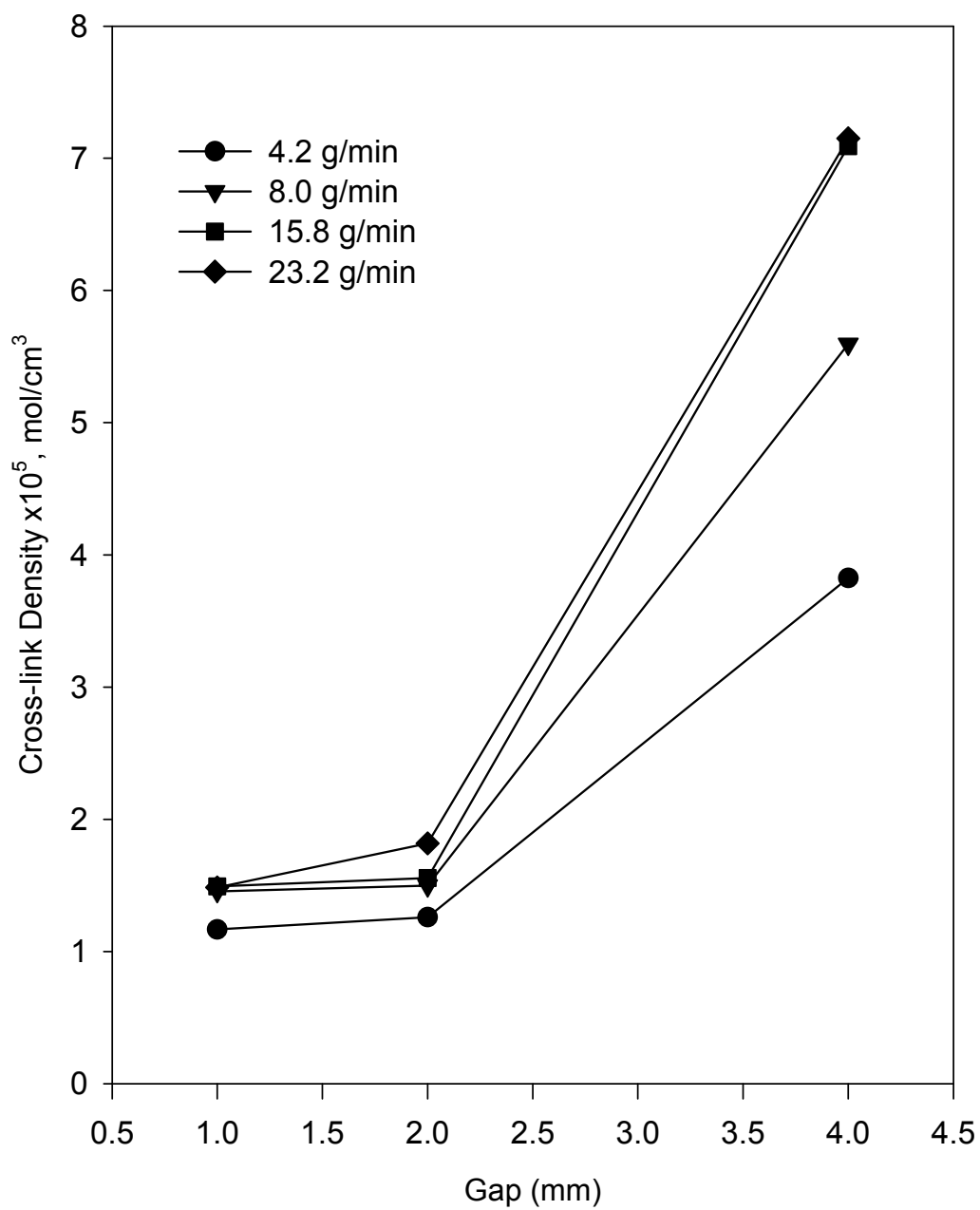


Figure 4.24 Crosslink density as a function of gap at various throughput rates and at amplitude of 25 μm .

This set of graphs shows even more clearly that the materials run at 1 and 2 mm gap end up with relatively the same crosslink density while the materials run at the higher 4 mm gap are affected to different degrees by the treatment, largely dependant on flow rate. The data taken from material run at the 4 mm gap shows decrosslinking that corresponds to throughput. As throughput increases and treatment exposure time is reduced, the decrosslinking effect is reduced. In Figure 4.22, materials run at a 4 mm gap, 23.2 grams per minute, and ultrasound amplitude of 16.5 μm are barely affected. As the throughput is reduced and exposure time is increased, the treatment has greater affect on the material. The same trend is observed in Figures 4.23 and 4.24. The figures represent a clear demonstration of how exposure time to the process affects treatment level.

Figure 4.25 through 4.27 show crosslink density versus flow rate. The amplitudes were varied while gap remained the same for individual figures. The same conclusion is reached for each figure and is dramatically displayed in Figure 4.27. The materials run at low throughput speeds and therefore higher specific energies were most affected by the ultrasonic treatment and materials ran at high throughputs were less affected by the treatment. Figure 4.25 initially appears to show a trend that is the reverse of this but a quick check of the scale for crosslink density shows that these numbers are first of all significantly lower than the original crosslink density and secondly all roughly the same, indicating that all of the material was affected by the process because of the small gap and therefore higher strain amplitude. Figure 4.26 also shows similar results for each sample after treatment. Figure 4.27 displays the materials run at the lower flow rate have a lowered crosslink density, but as the flow rate is increased and exposure time is reduced, the treatment becomes less effective at even the highest amplitude.

Figures 4.28 through 4.31 show the effect of flow rate on gel fraction as the gap size and ultrasonic horn amplitude is changed. The gel fraction of the original

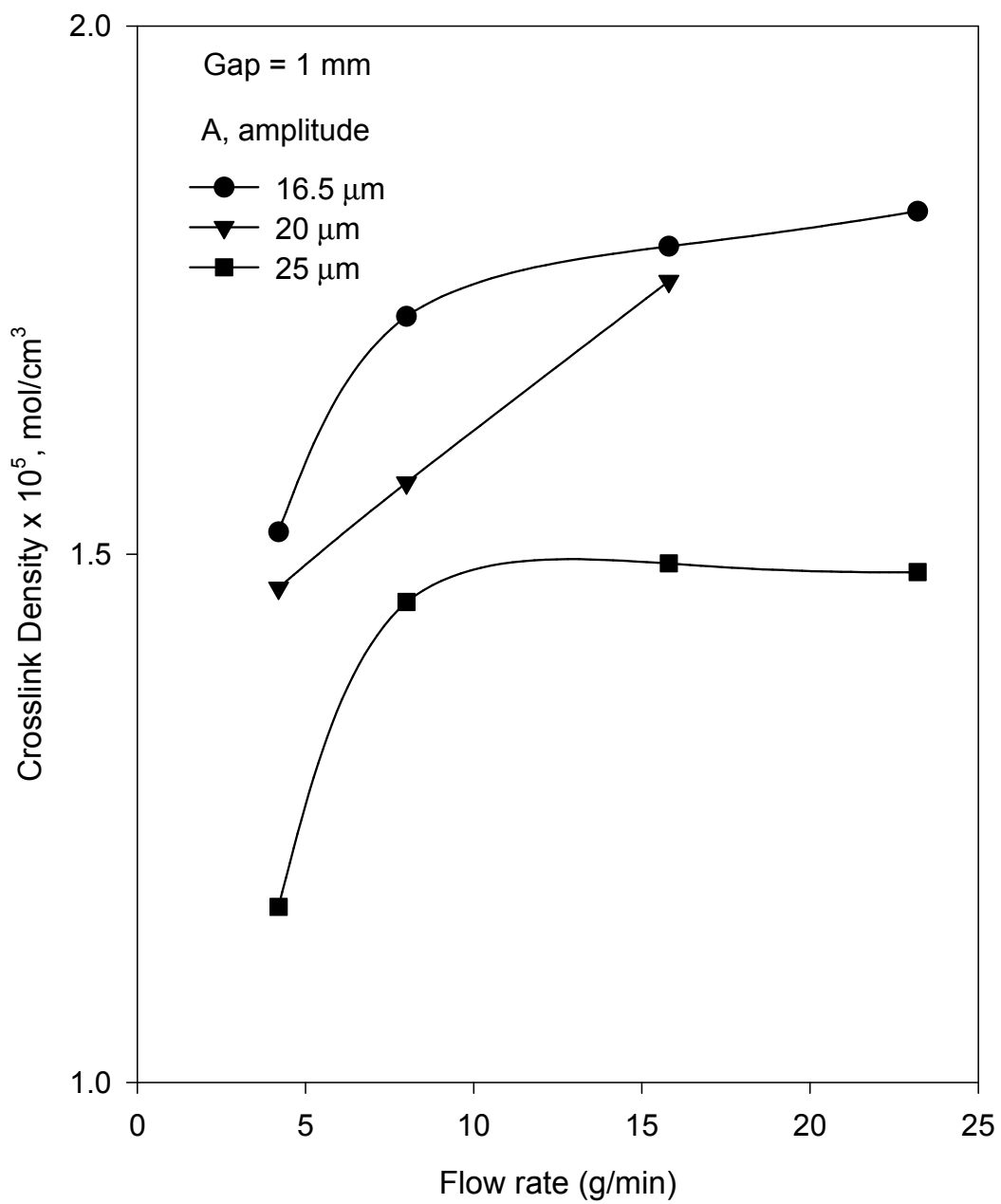


Figure 4.25 Crosslink density as a function of flow rate at various amplitudes and at a sample thickness of 1 mm.

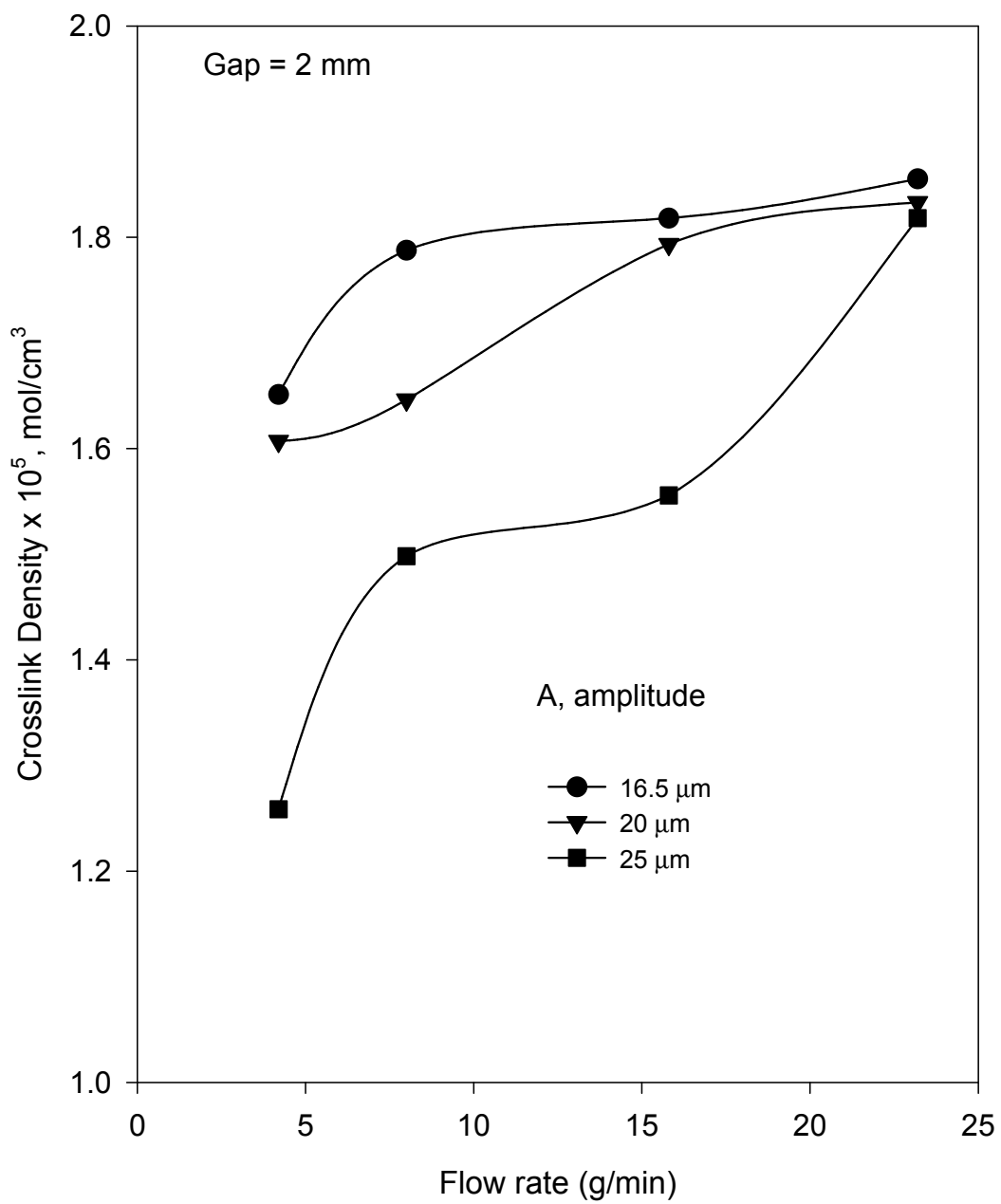


Figure 4.26 Crosslink density as a function of flow rate at various amplitudes and at a sample thickness of 2 mm.

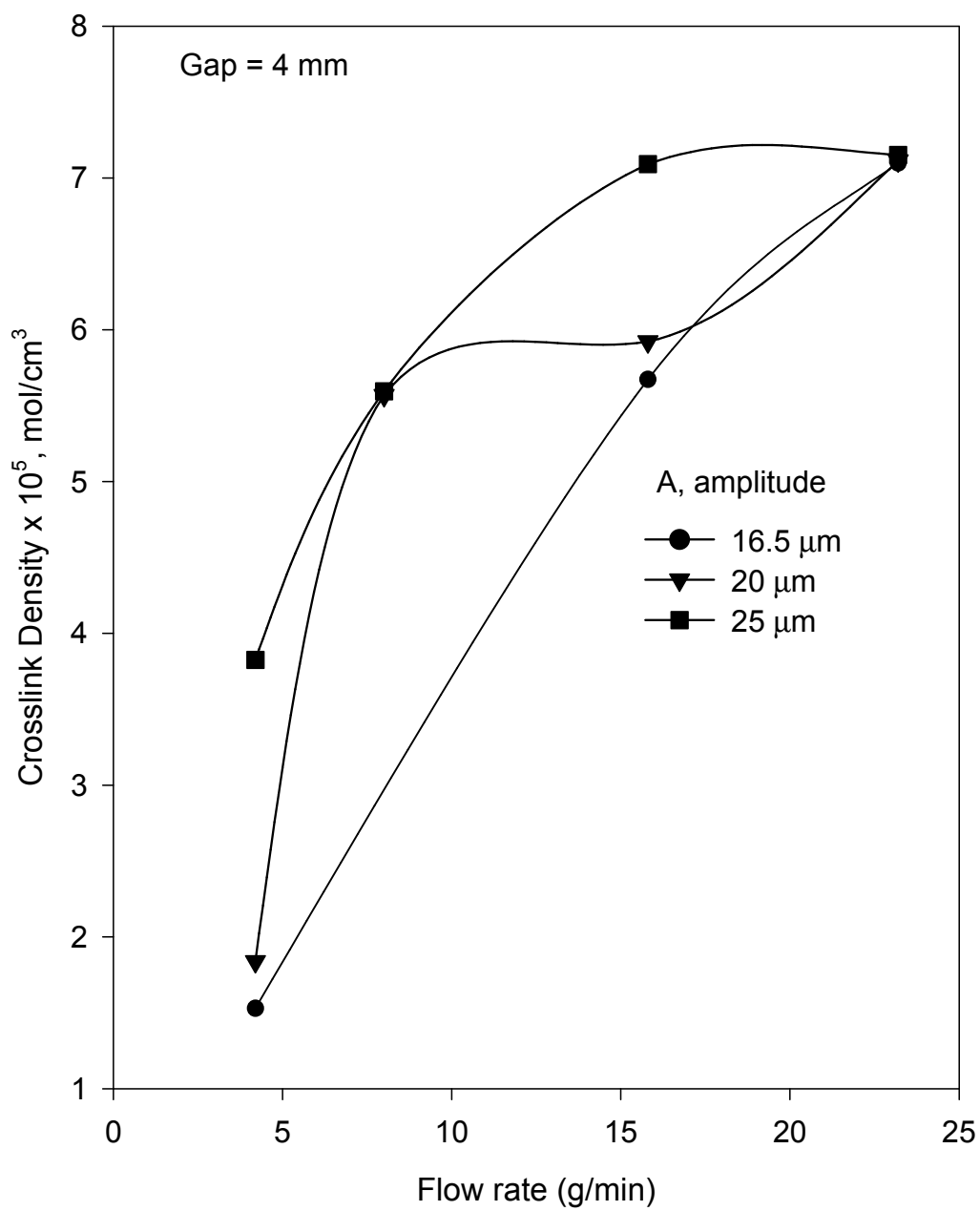


Figure 4.27 Crosslink density as a function of flow rate at various amplitudes and at a sample thickness of 4 mm.

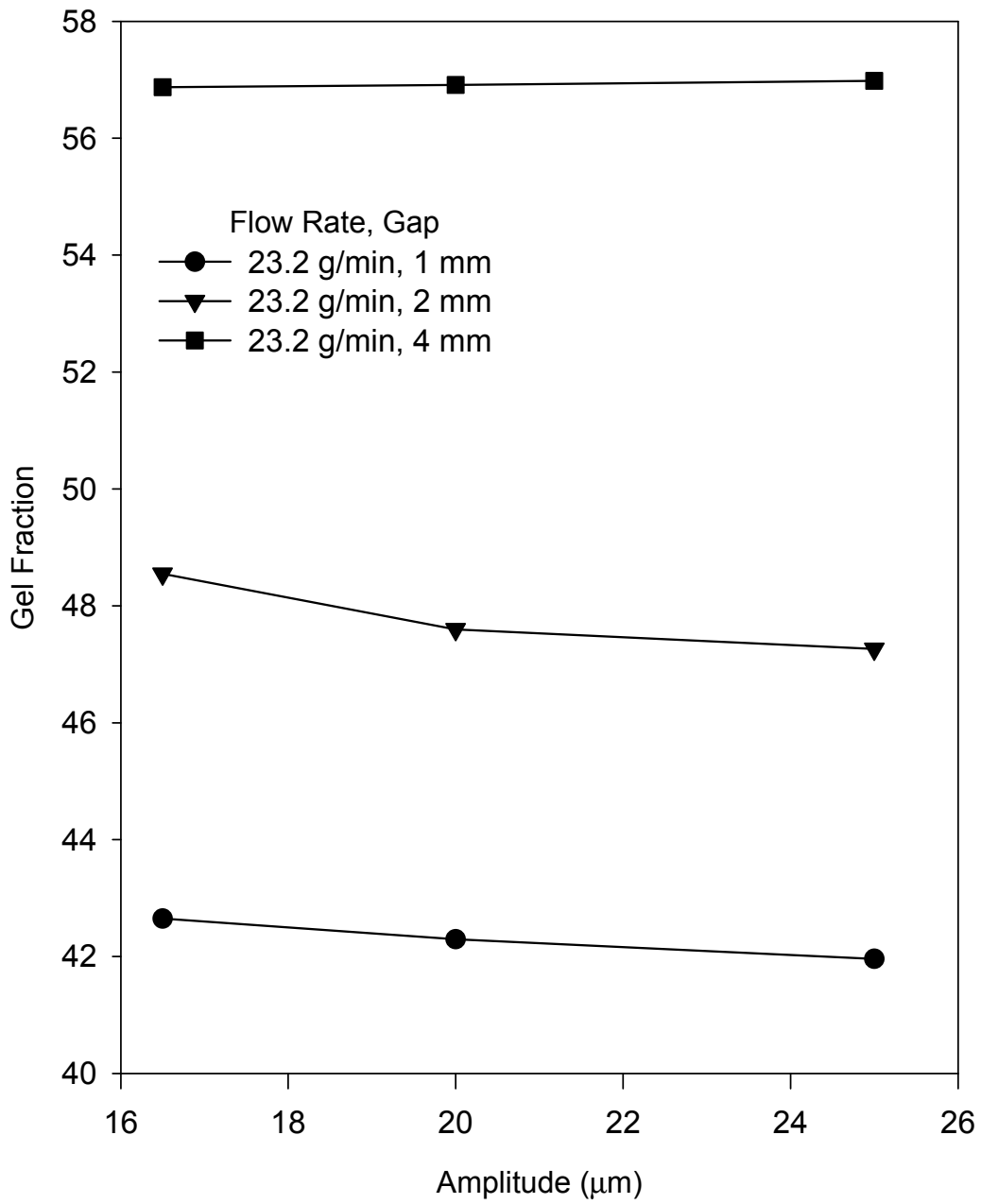


Figure 4.28 Gel Fraction as a function of amplitude at various gaps and at a flow rate of 23.2 g/min.

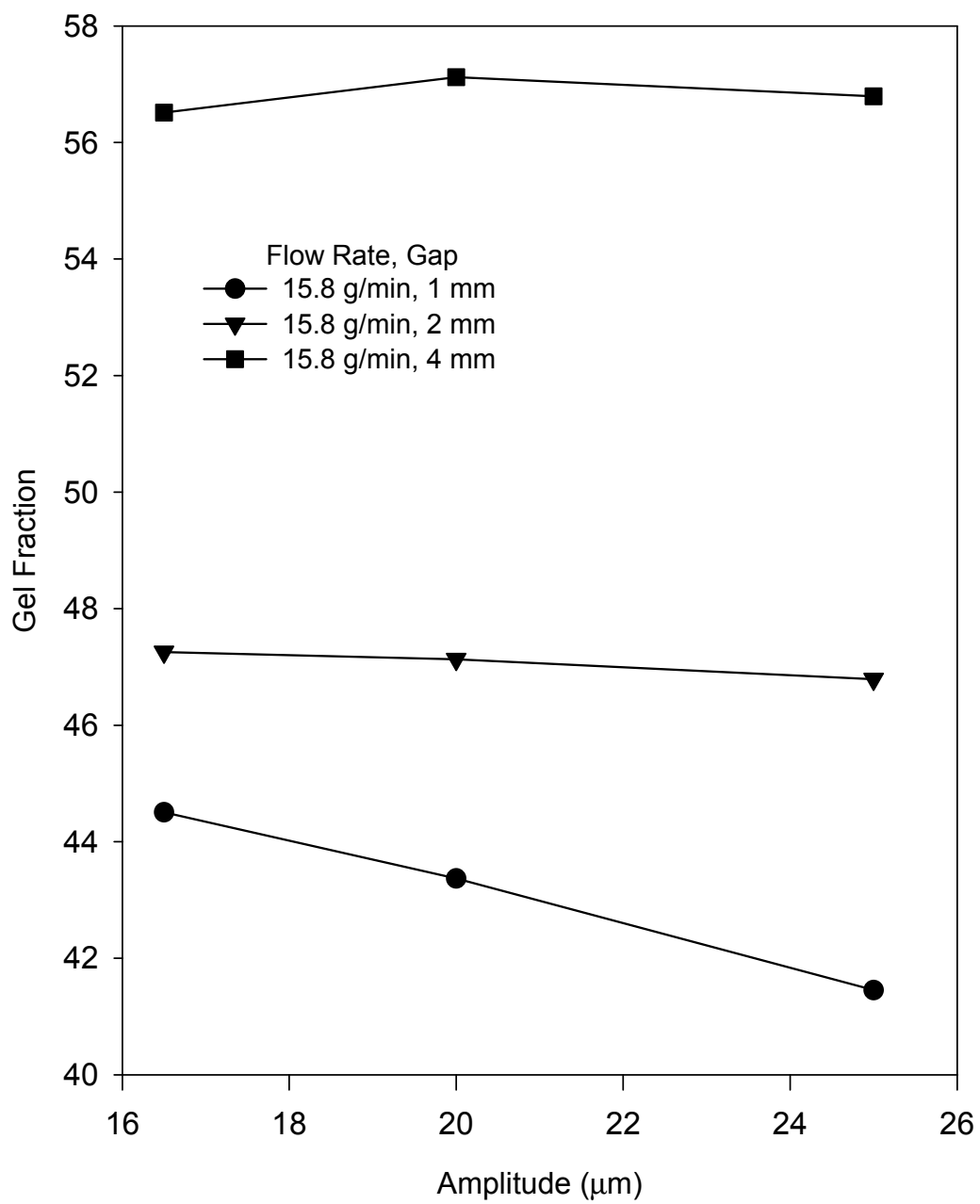


Figure 4.29 Gel Fraction as a function of amplitude at various gaps and at a flow rate of 15.8 g/min.

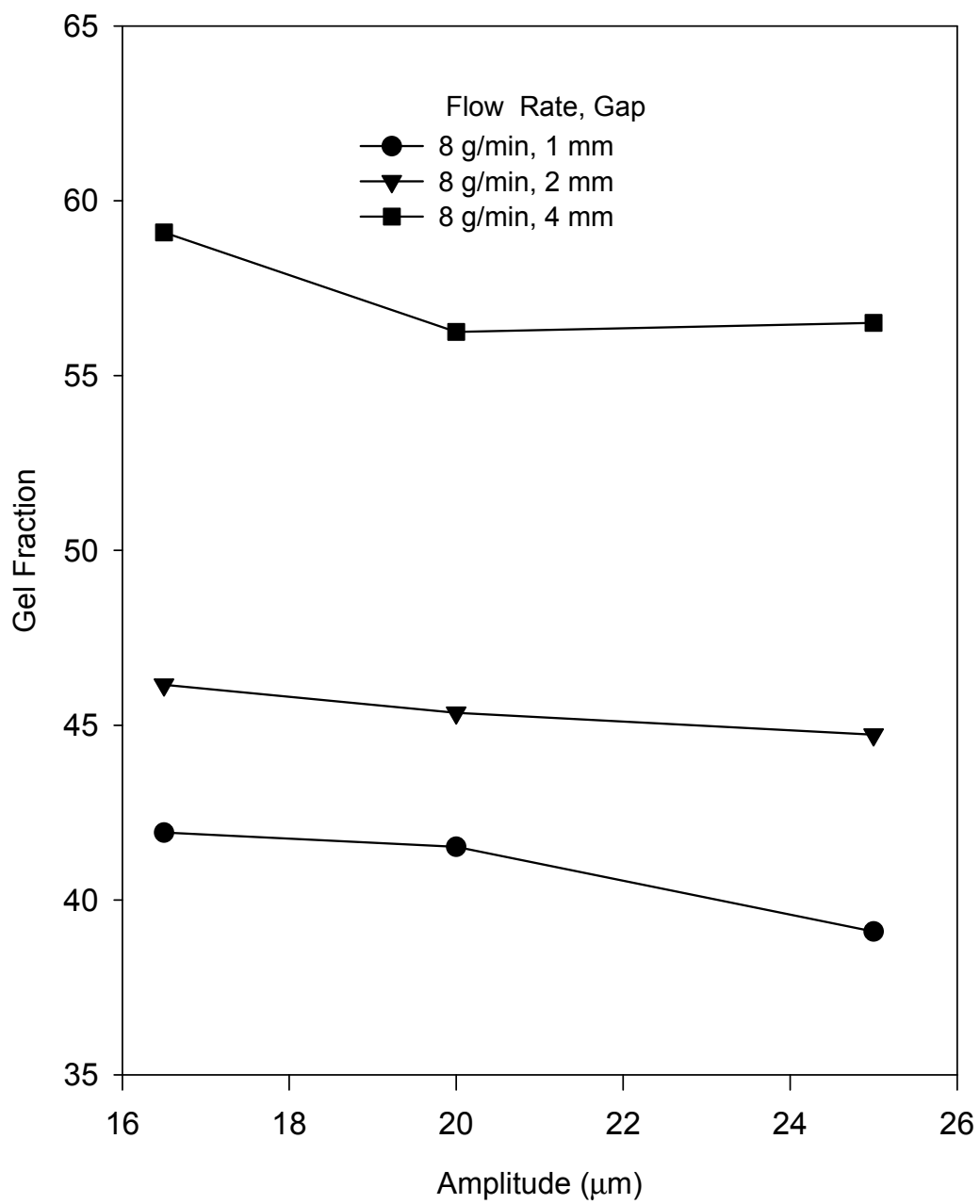


Figure 4.30 Gel Fraction as a function of amplitude at various gaps and at a flow rate of 8 g/min.

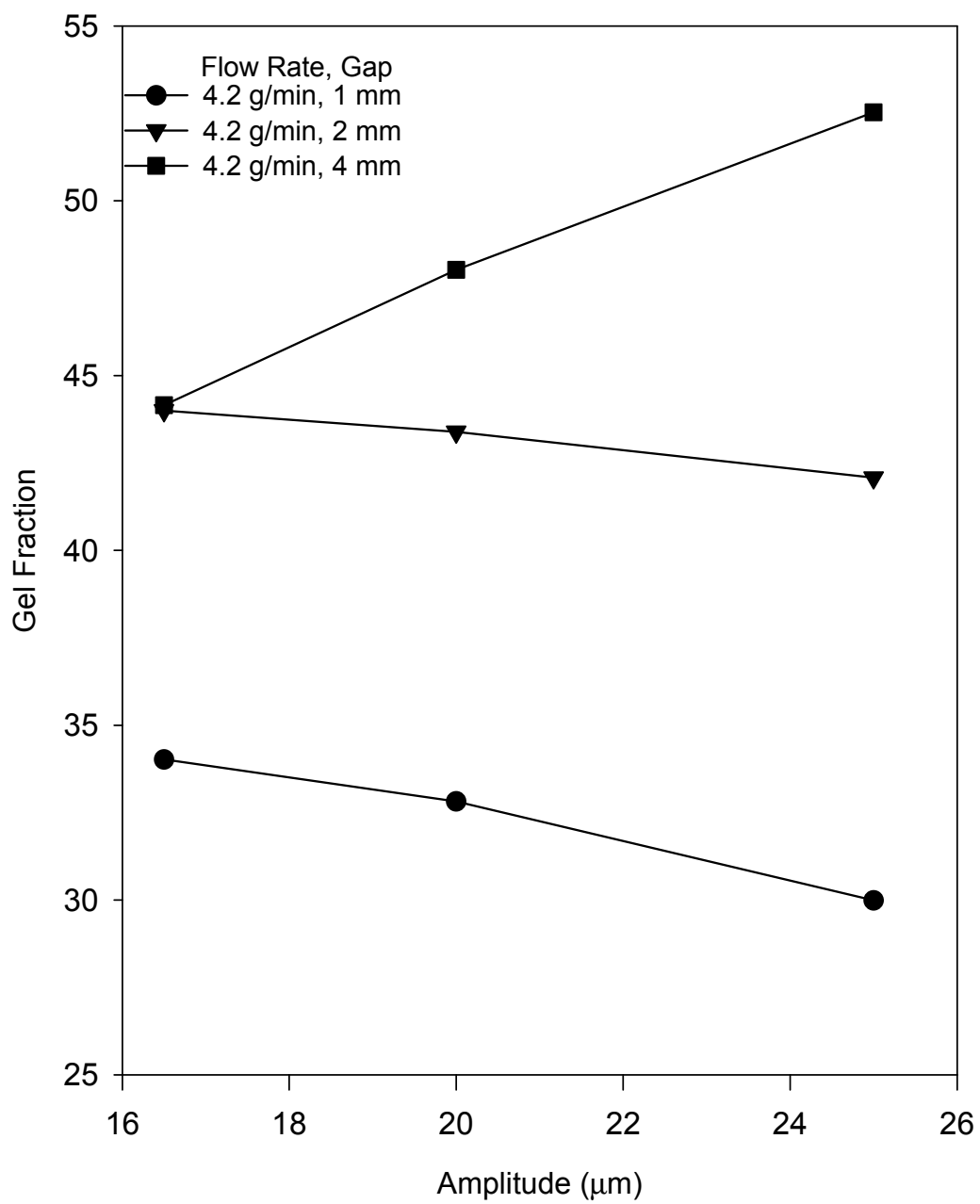


Figure 4.31 Gel Fraction as a function of amplitude at various gaps and at a flow rate of 4.2 g/min.

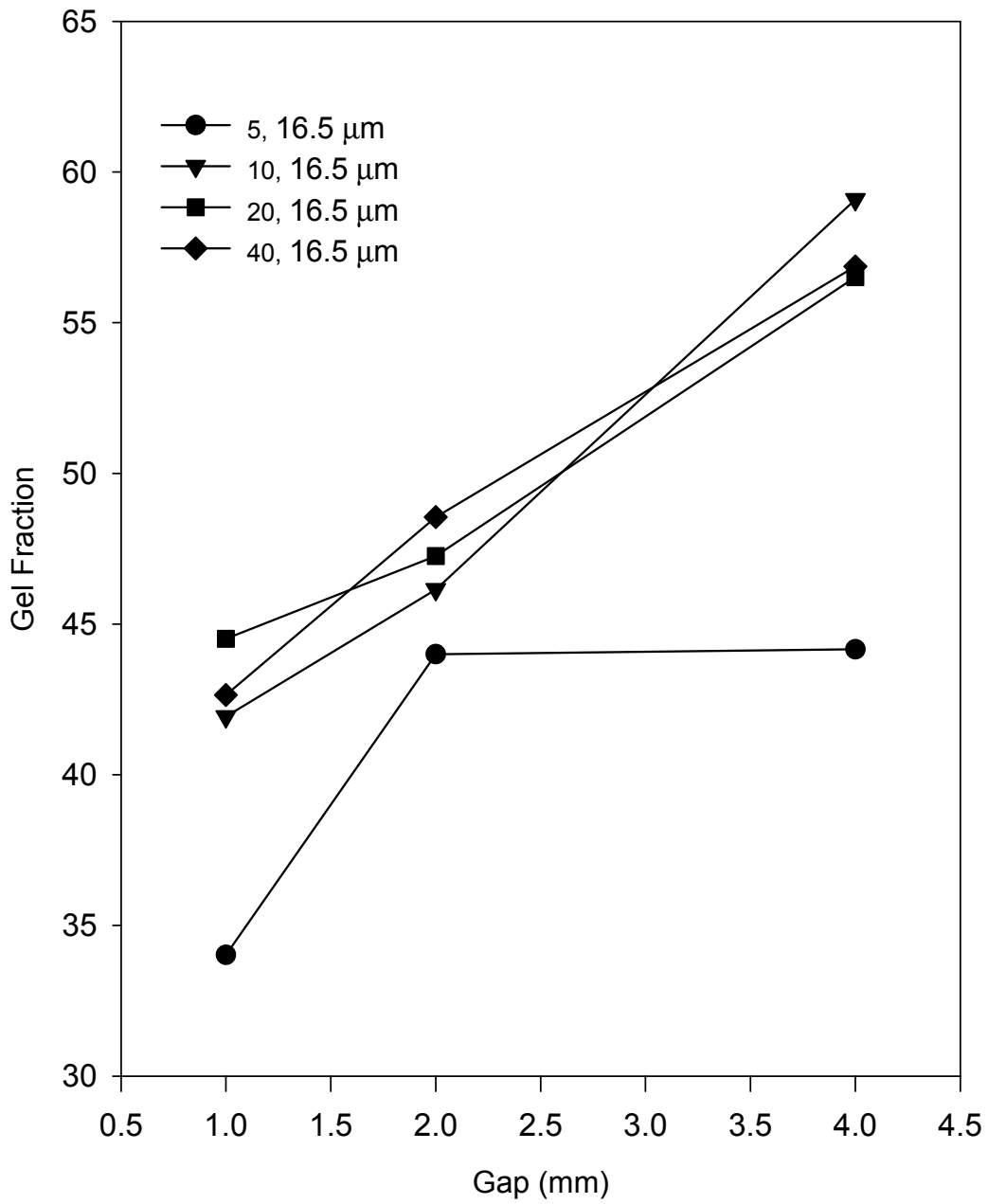


Figure 4.32 Gel Fraction as a function of gap at various flow rates and at an amplitude of 16.5 μm

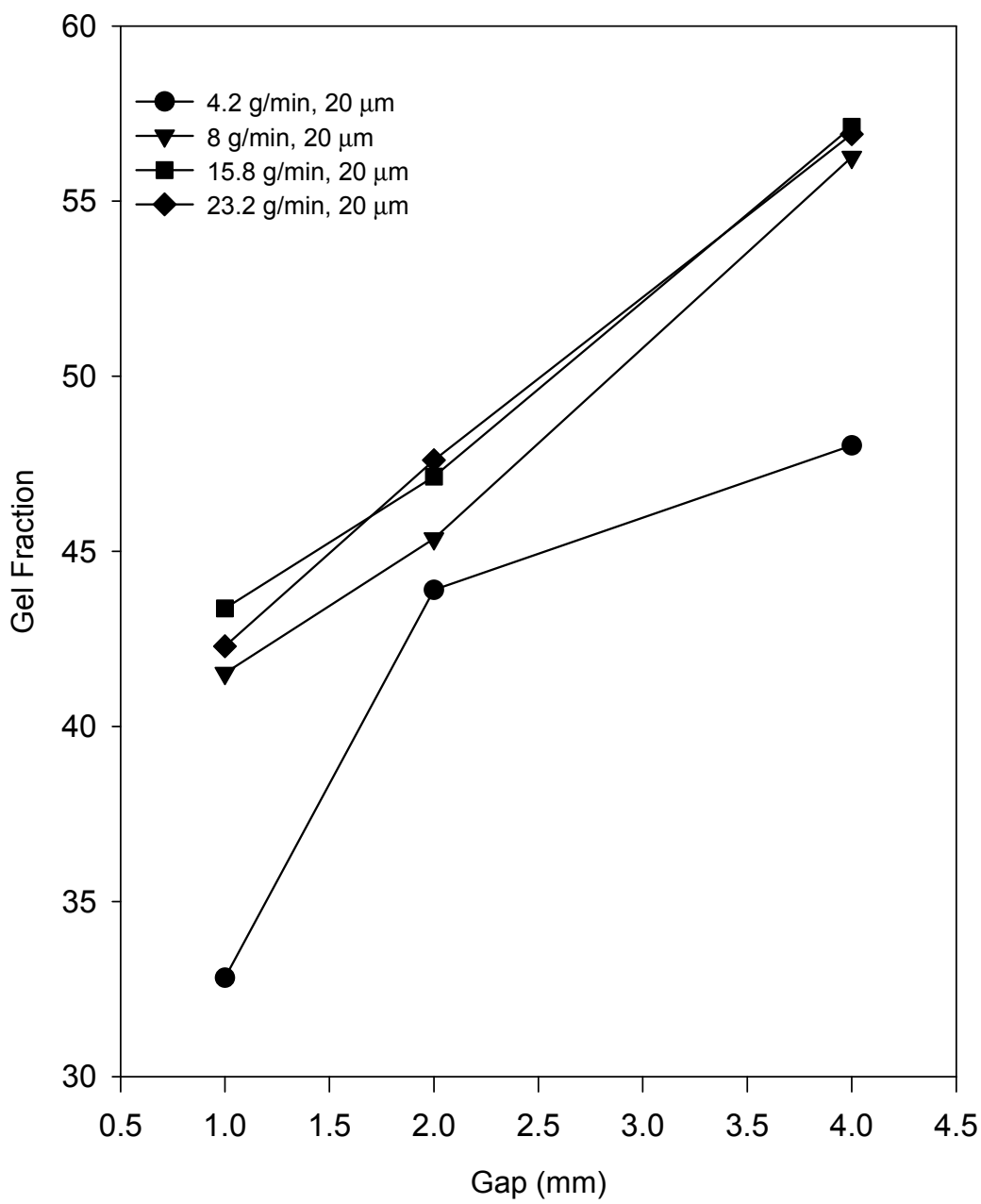


Figure 4.33 Gel Fraction as a function of gap at various flow rates and at an amplitude of 20 mm

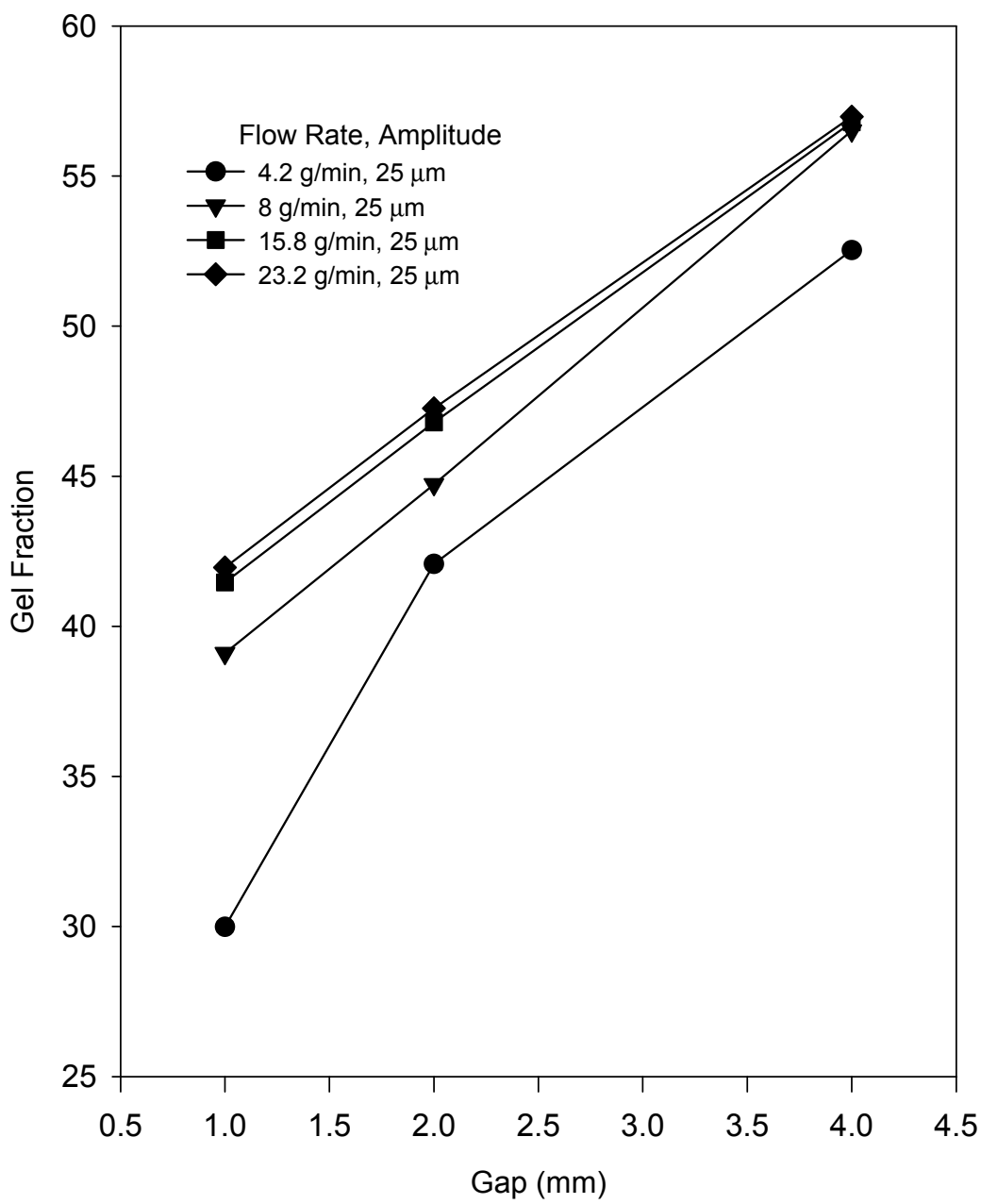


Figure 4.34 Gel Fraction as a function of gap at various flow rates and at an amplitude of 25 mm.

material was 84.64 %. In each figure the same primary trend is shown that is gap size was critical in determining the degree to which the materials gel fraction. Figures 4.28, 4.29, and 4.30 while not identical, are very similar in value and trends. Figure 4.31 has the lowest flow rate and shows the same trend, but the gel fraction values are at a significantly lower level than the higher flow rate figures show.

Figures 4.32 through 4.34 show the gel fraction versus gap size. In each graph the amplitude is held constant while the throughput and gap sizes change. This set of graphs shows that gel fraction increases as gap size increases in every case. These figures all show that material run at the lowest flow rate of 4.2 g/min is more affected by the process than materials run at higher flow rates. In each graph, the materials run at the higher flow rates showed very similar results at each gap size, regardless of amplitude. The materials run at the lowest flow rate are differentiated from the others by the fact that their exposure time to the treatment was longer. The higher flow rates may have allowed the surface of the materials to be treated without treating the rest of the material

Figures 4.35 through 4.37 show gel fraction versus flow rate. The amplitudes were varied while gap remained the same for individual figures. The same conclusion is reached for each figure. Figure 4.35 shows very clearly that the materials run at low throughput speeds and therefore higher specific energies were most affected by the ultrasonic treatment and materials ran at high throughputs were less affected by the treatment. Figure 4.36 also shows similar results for each sample after treatment. Figure 4.37 displays the materials run at the lower flow rate have a lowered gel fraction, but as the flow rate is increased and exposure time is reduced, the affect of flow rate on the treatment becomes less important at even the highest amplitude.

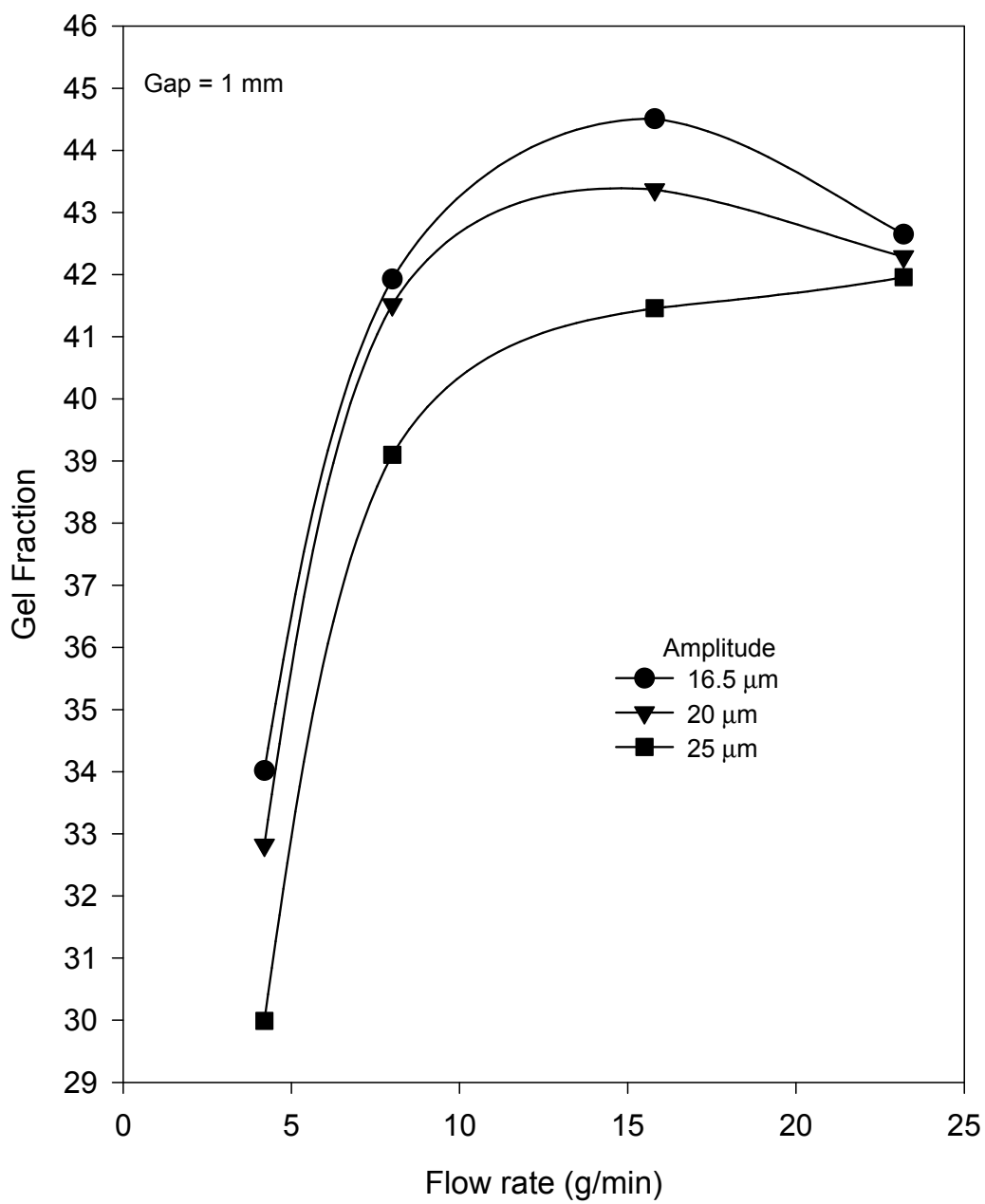


Figure 4.35 Gel fraction as a function of flow rate at various amplitudes and at a constant gap of 1 mm.

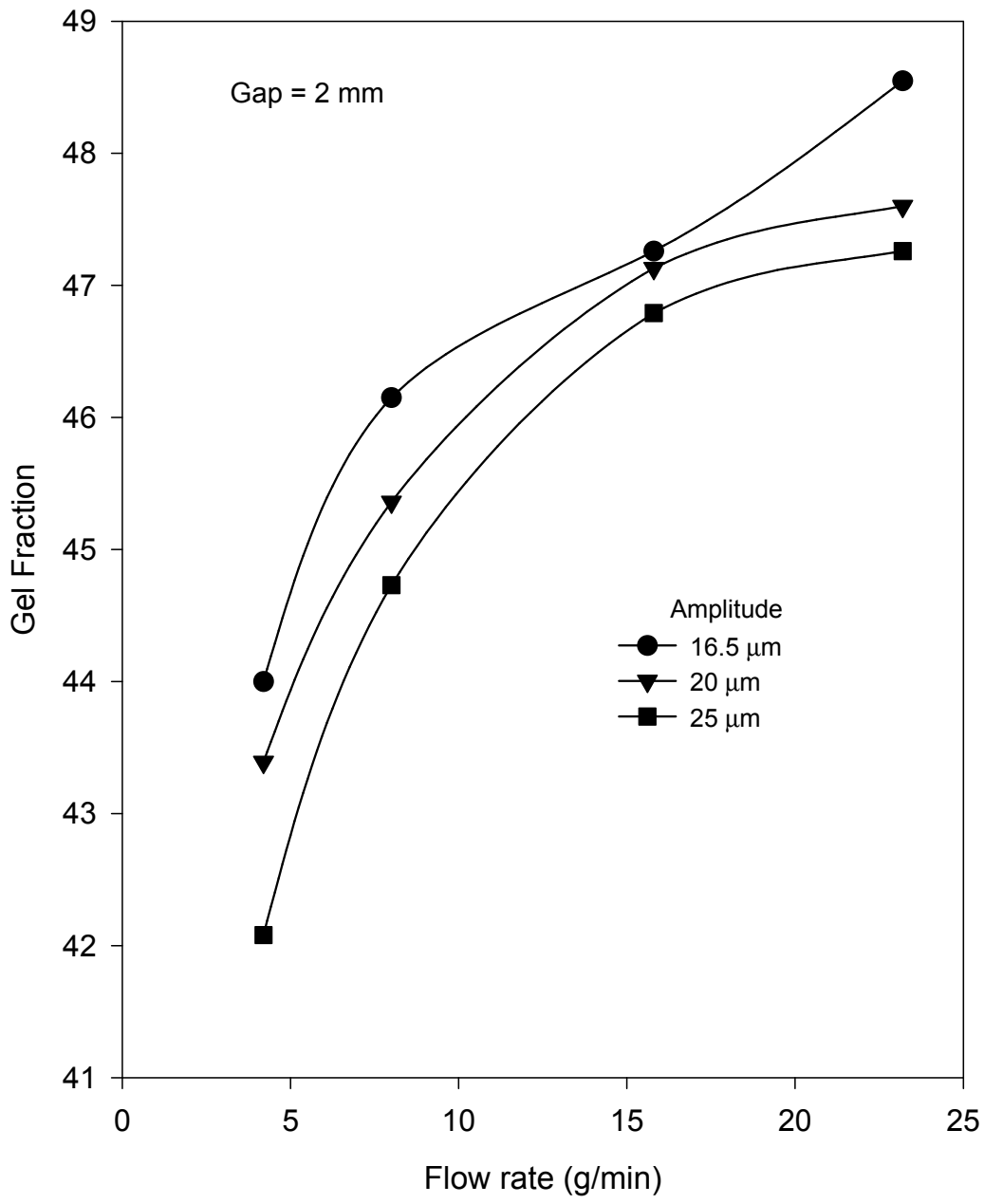


Figure 4.36 Gel fraction as a function of flow rate at various amplitudes and at a constant gap of 2 mm.

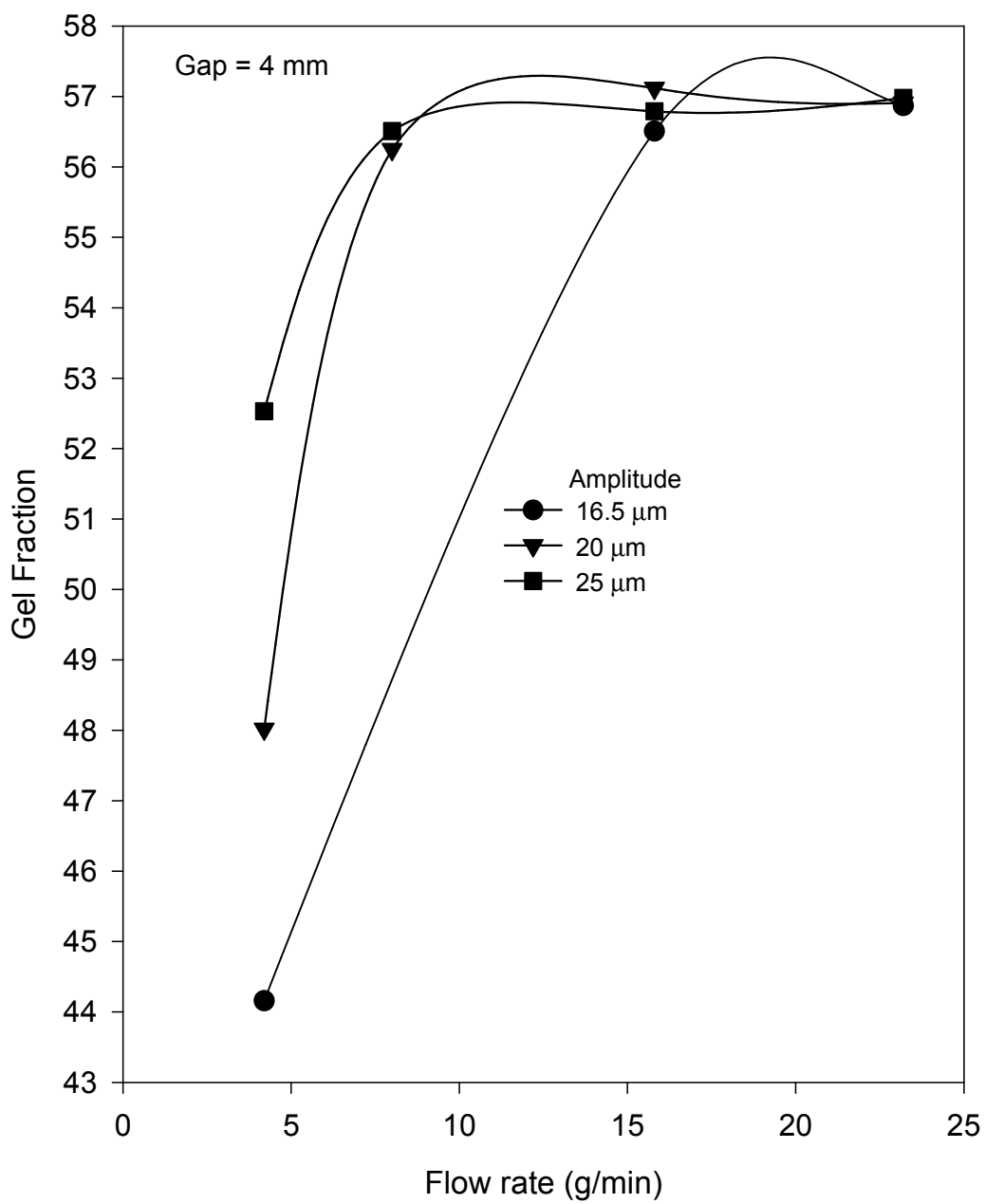


Figure 4.37 Gel fraction as a function of flow rate at various amplitudes and at a constant gap of 4 mm.

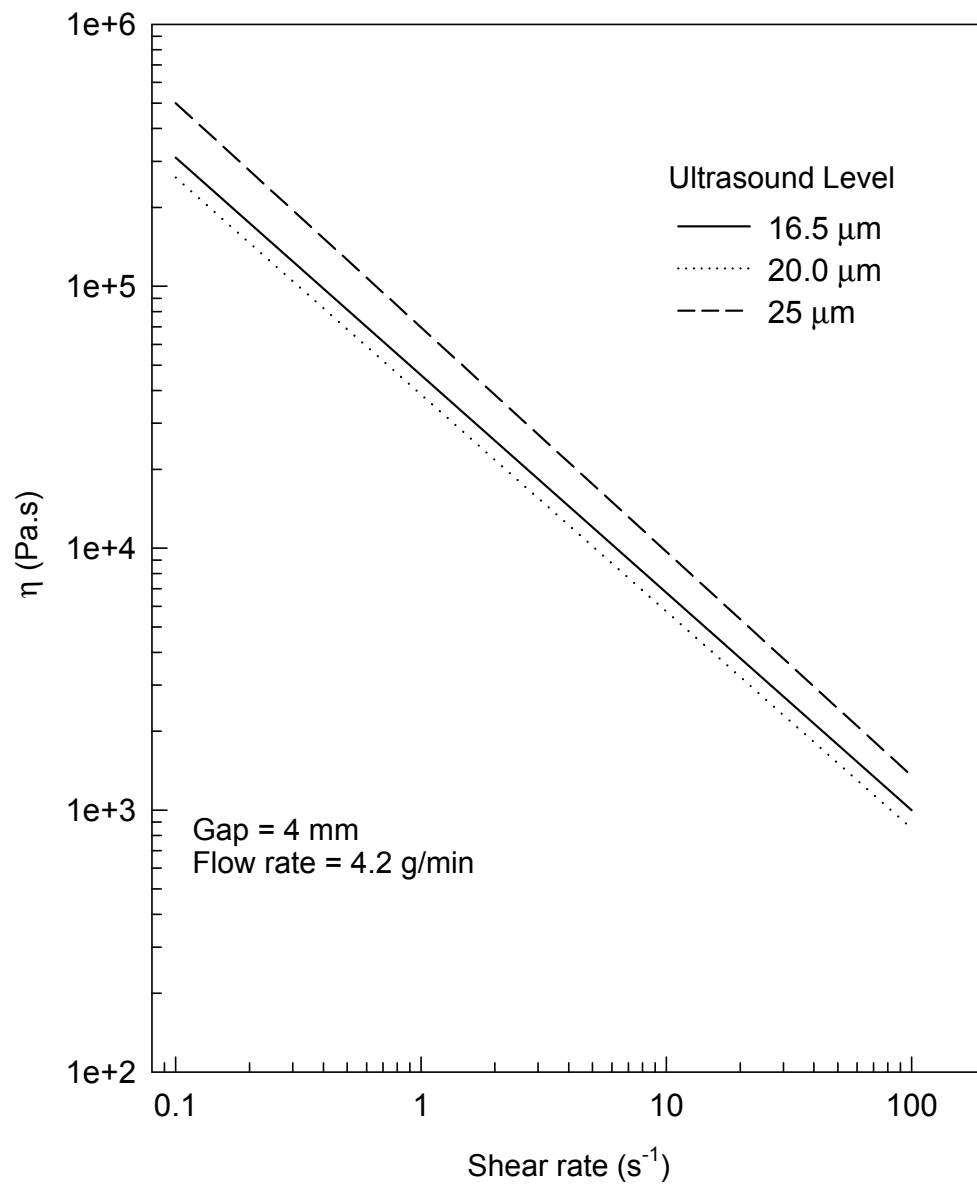


Figure 4.38 Viscosity versus shear rate for samples treated at various amplitudes. Gap is 4 mm and flow rate is 4.2 g/min.

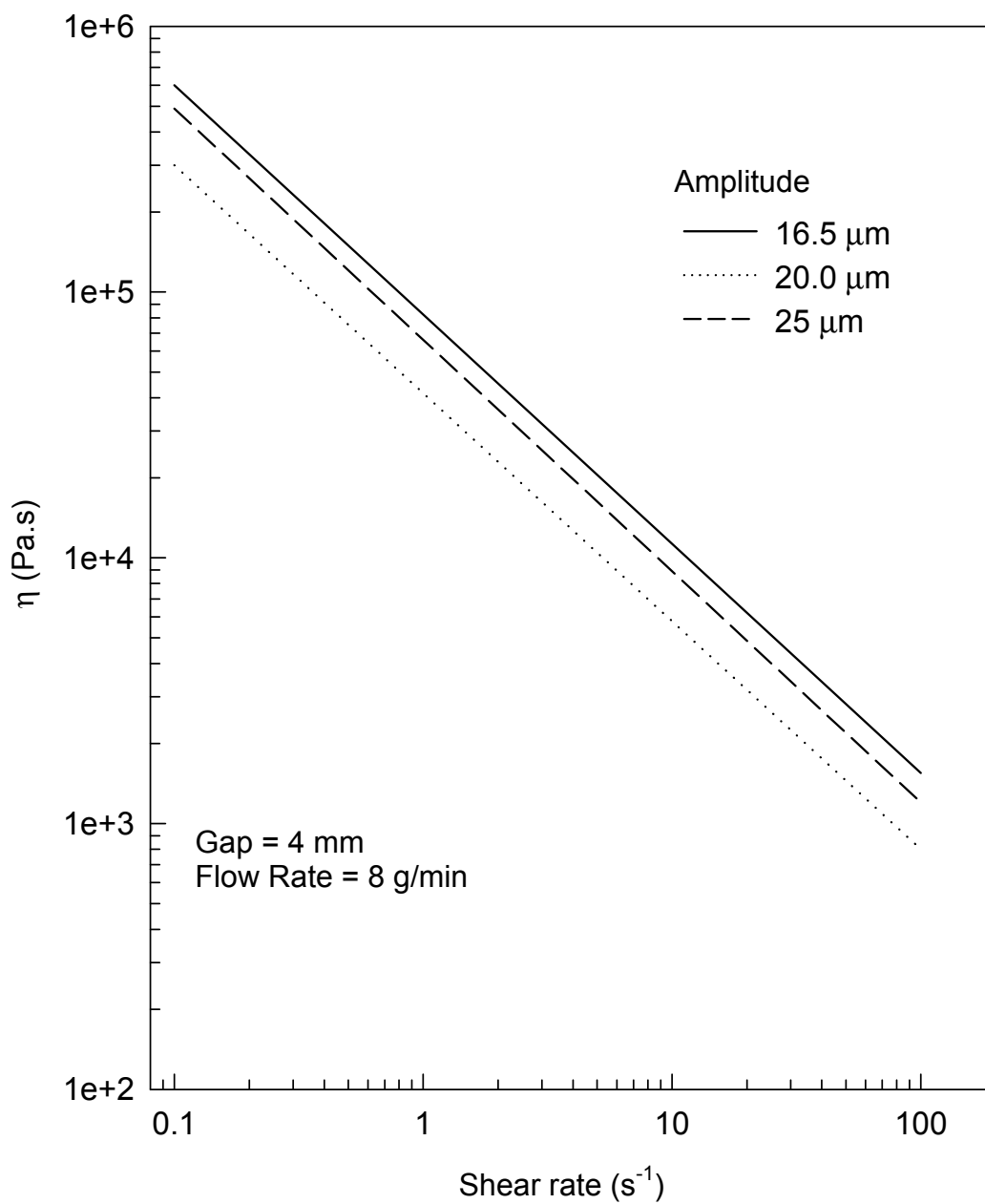


Figure 4.39 Viscosity versus shear rate for samples treated at various amplitudes. Gap is 4 mm and flow rate is 8 g/min.

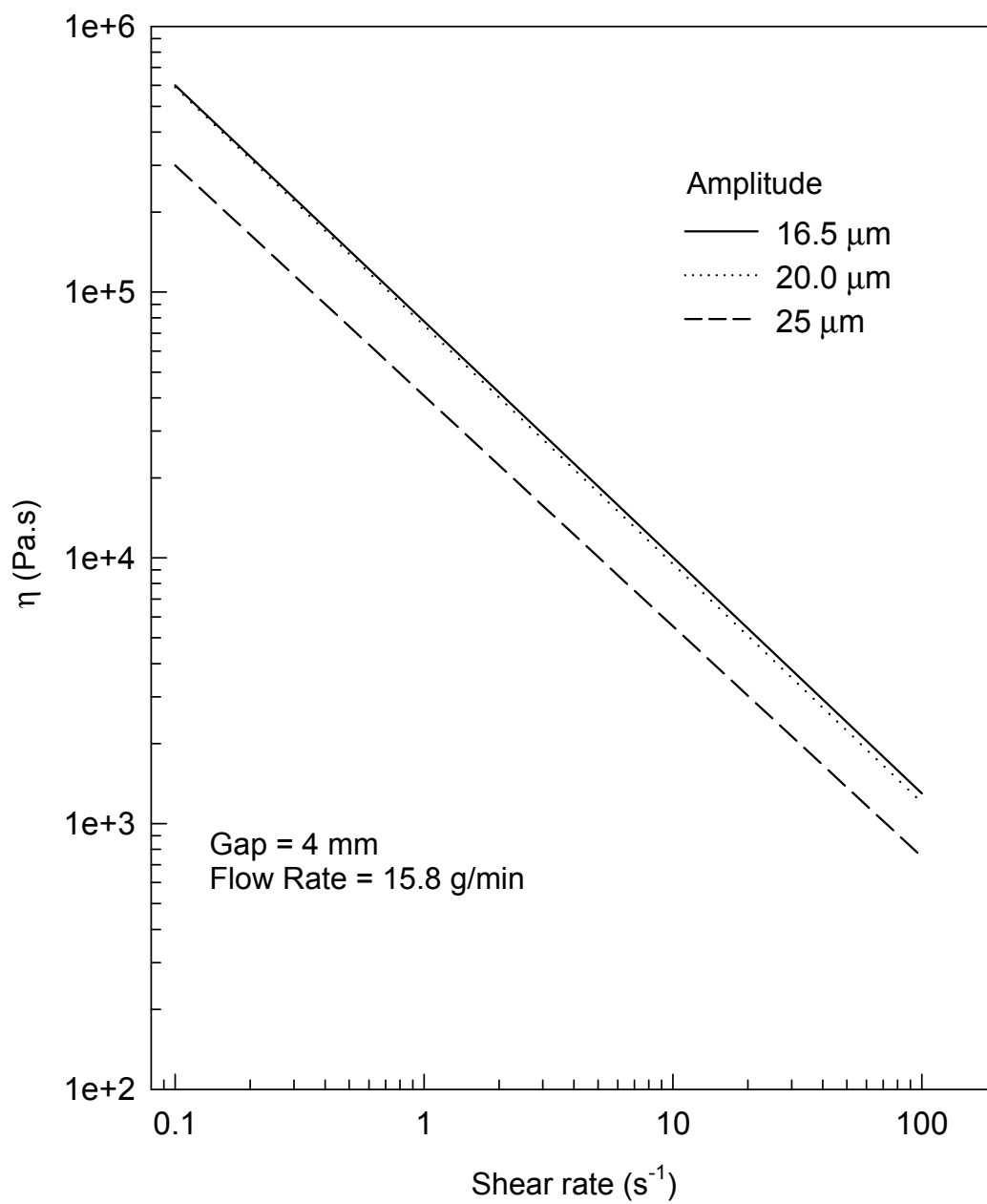


Figure 4.40 Viscosity versus shear rate for samples treated at various amplitudes. Gap is 4 mm and flow rate is 15.8 g/min.

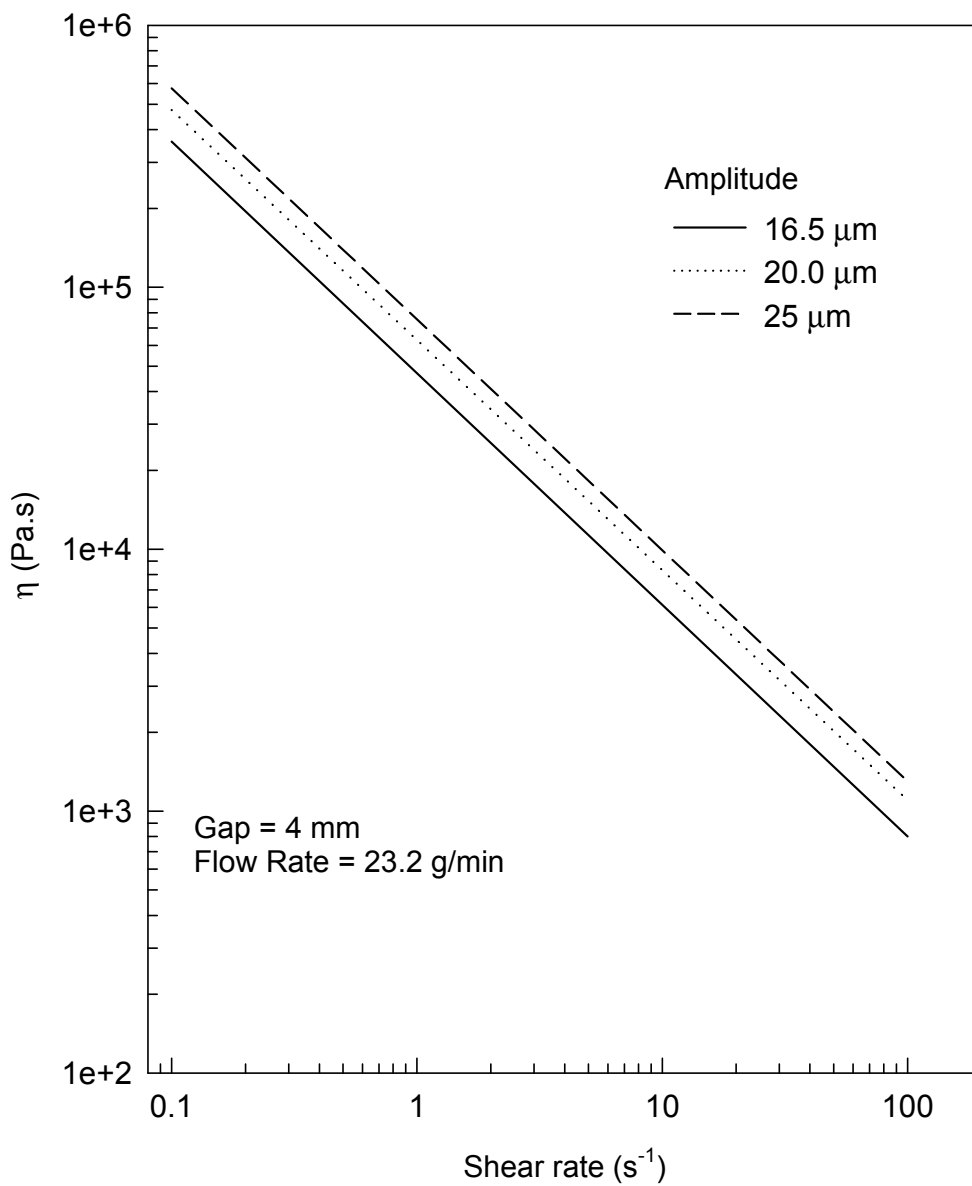


Figure 4.41 Viscosity versus shear rate for samples treated at various amplitudes. Gap is 4 mm and flow rate is 23.2 g/min.

4.4 Rheological Behavior

Figures 4.38 through 4.70 compare viscosity data from the 36 continuously processed materials as described in Section 3.2. These results are best explained in groups of figures rather than individually.

The first group of figures, Figures 4.38 through 4.49, represents materials processed using all three gaps run at four throughput rates. The general observation from these figures is that the behavior of the viscosity function is according to that of a power law model. Figures 4.38 through 4.41 show materials run with the largest gap (4 mm) and different throughput rates respectively. These figures do not show a regular trend with viscosity relative to ultrasound energy exposure. Since the gap is large, it is possible that the material undergoes different amounts of treatment as it passes through the opening and erratic results are obtained. Some material in the 4 mm gap is allowed to pass the treatment point unaffected because energy is absorbed in the depth of the first one or two mm. This would explain the random results of the viscosity testing. This phenomenon shows itself in the groups of figures that show materials processed using the larger gap.

Figures 4.42 through 4.45 show the same type of data taken from samples that were processed with a 2 mm gap. The results in Figures 4.42 and 4.43 show almost identical viscosities for the materials and are too similar to differentiate. Both figures show data taken at the lowered throughput rates and therefore higher exposure time in the process. This is an indication that there is a limit to the amount of decrosslinking the treatment will impose on the samples. These results begin to make more sense. Figures 4.44 and 4.45 show individually that as the amplitude is increased, the viscosity is reduced to different degrees depending on the level of ultrasonic exposure. Together they

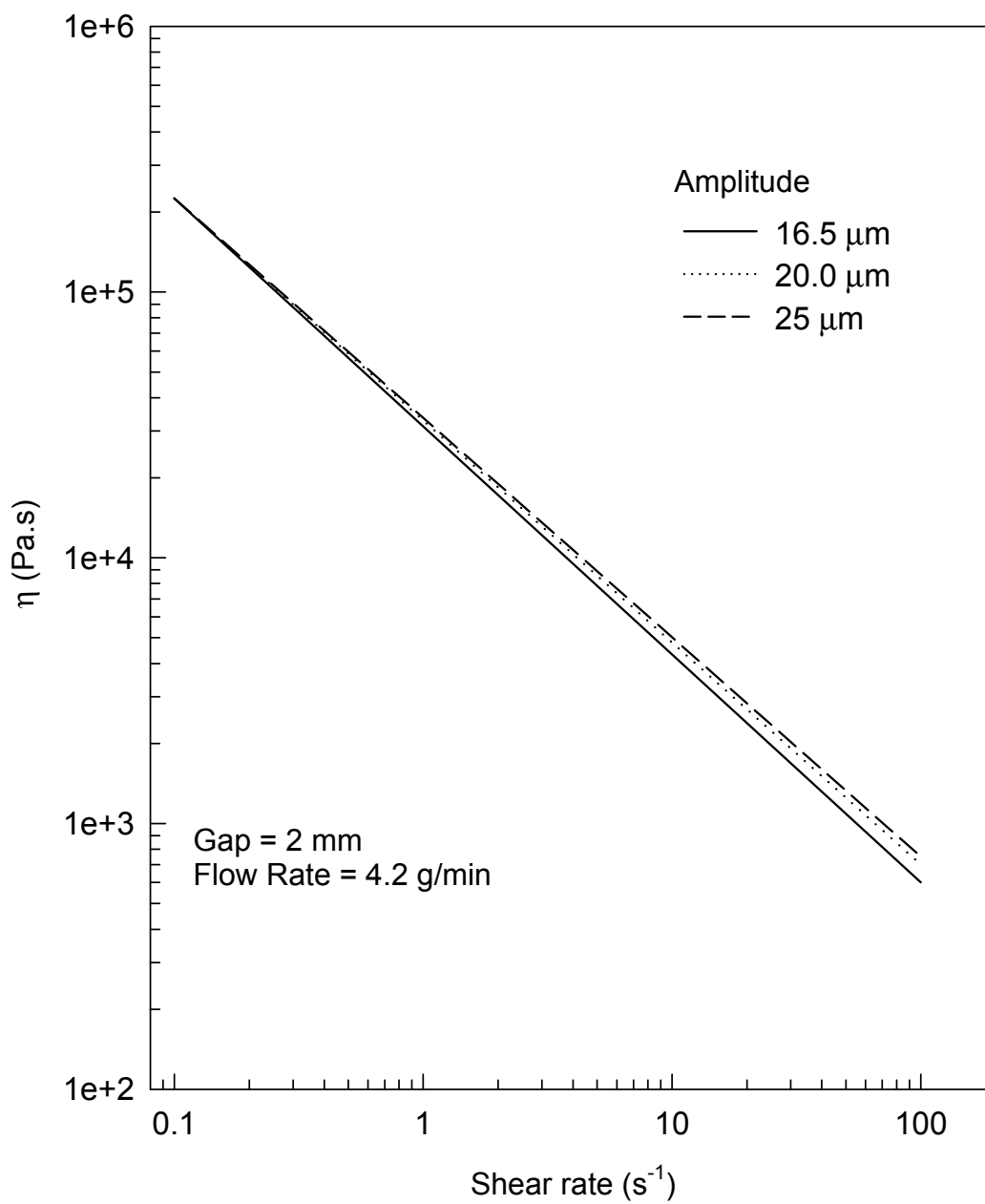


Figure 4.42 Viscosity versus shear rate for samples treated at various amplitudes. Gap is 2 mm and flow rate is 4.2 g/min.

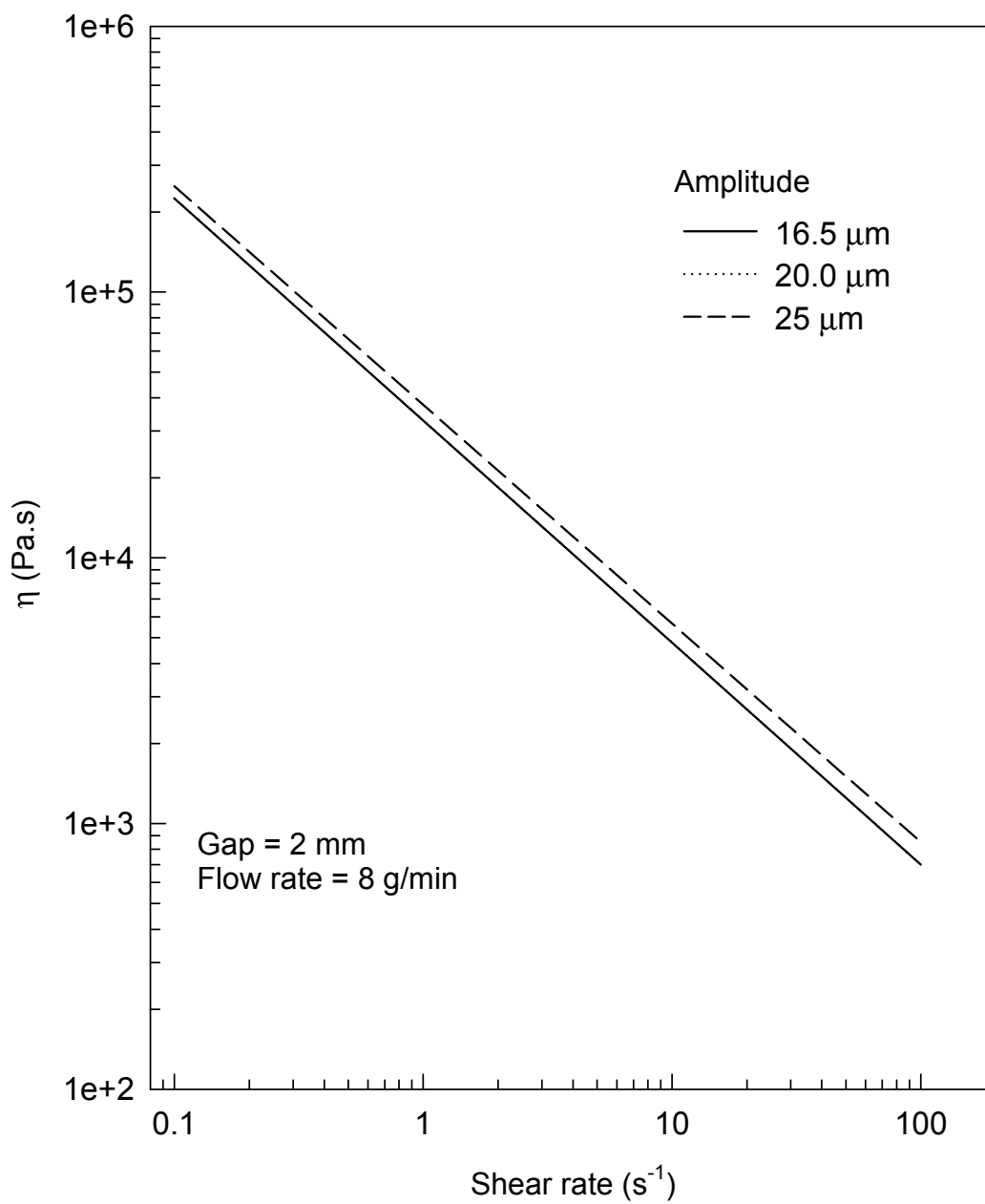


Figure 4.43 Viscosity versus shear rate for samples treated at various amplitudes. Gap is 2 mm and flow rate is 8 g/min.

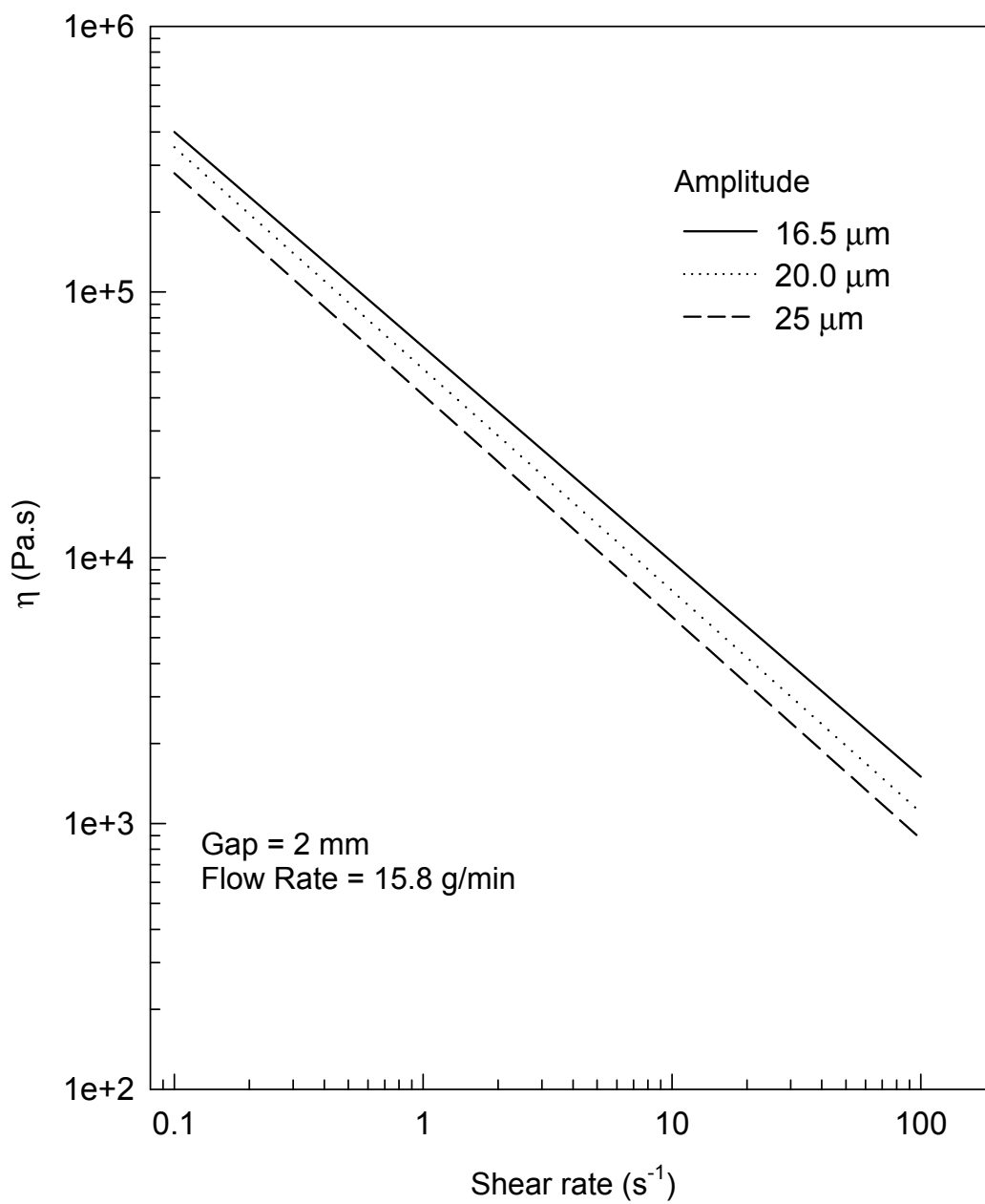


Figure 4.44 Viscosity versus shear rate for samples treated at various amplitudes. Gap is 2 mm and flow rate is 15.8 g/min.

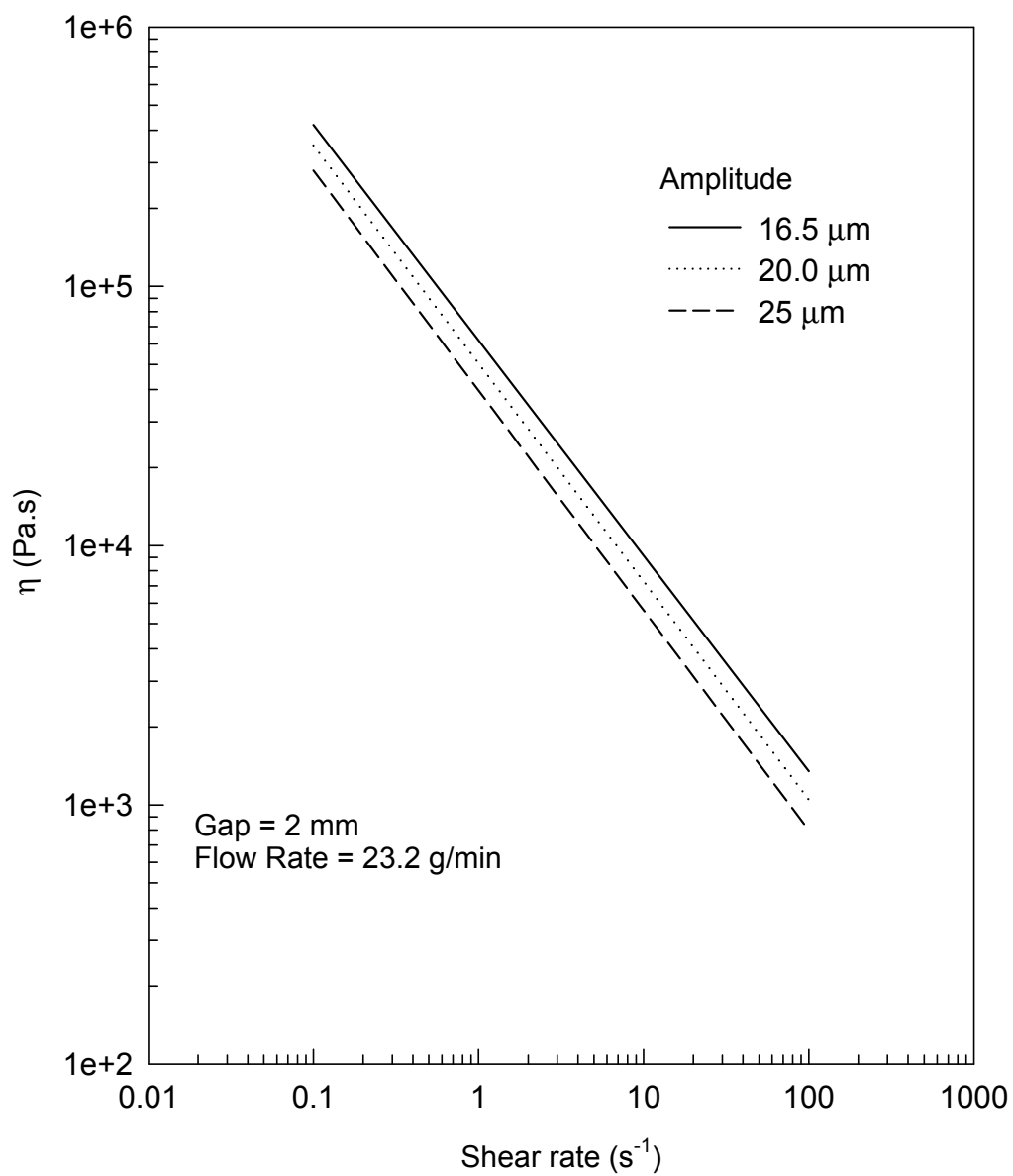


Figure 4.45 Viscosity versus shear rate for samples treated at various amplitudes. Gap is 2 mm and flow rate is 23.2 g/min.

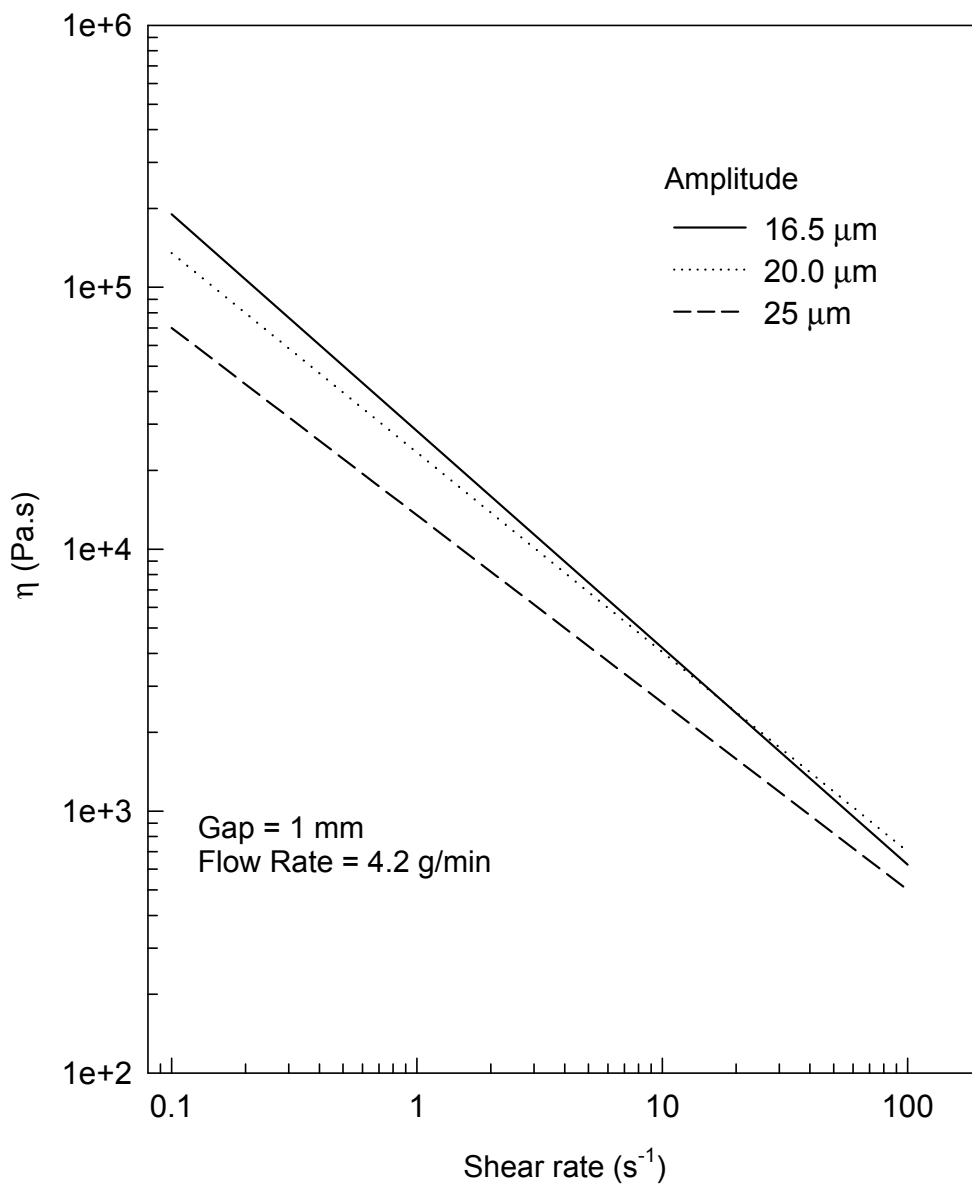


Figure 4.46 Viscosity versus shear rate for samples treated at various amplitudes. Gap is 1 mm and flow rate is 4.2 g/min.

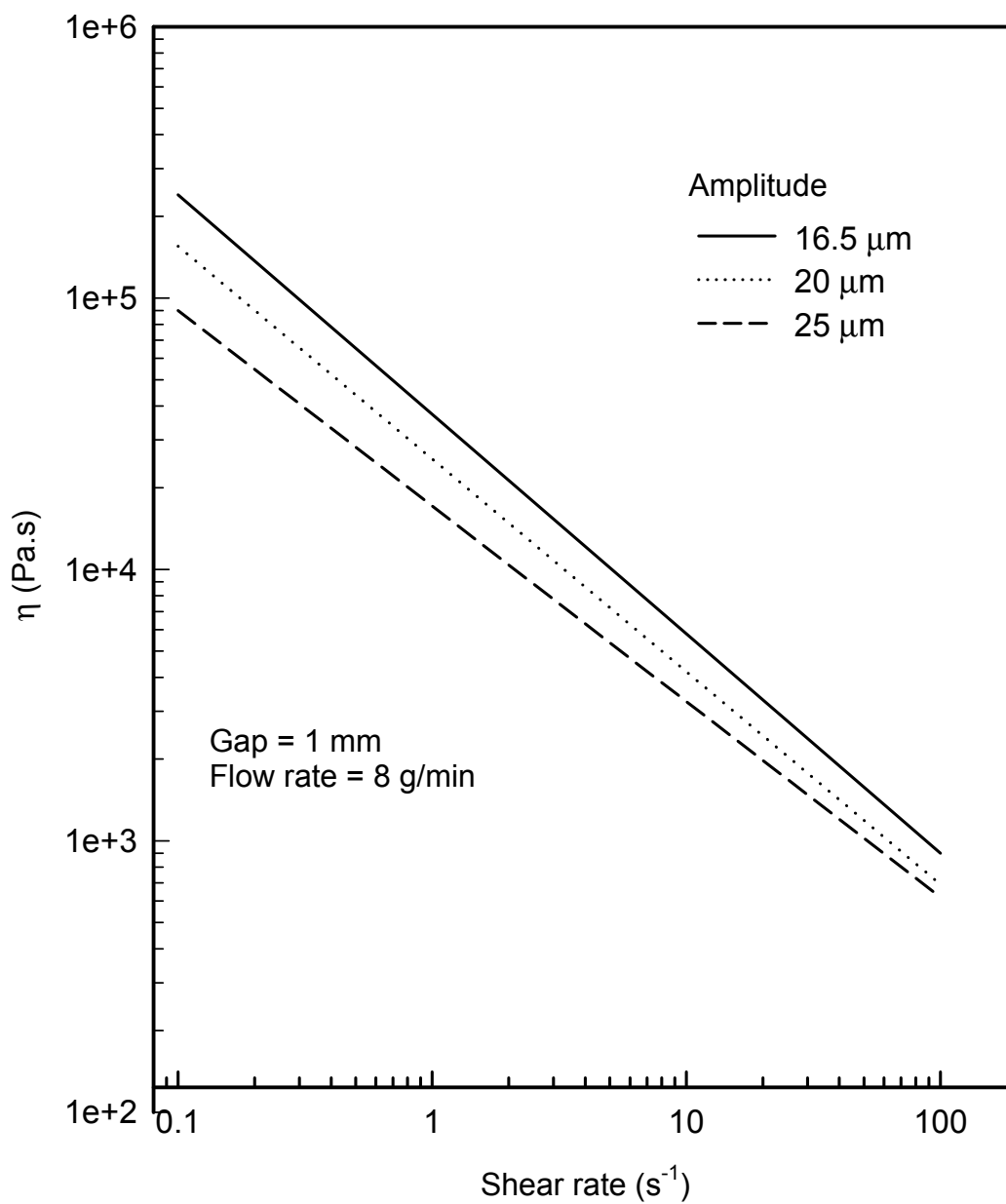


Figure 4.47 Viscosity versus shear rate for samples treated at various amplitudes. Gap is 1 mm and flow rate is 8 g/min.

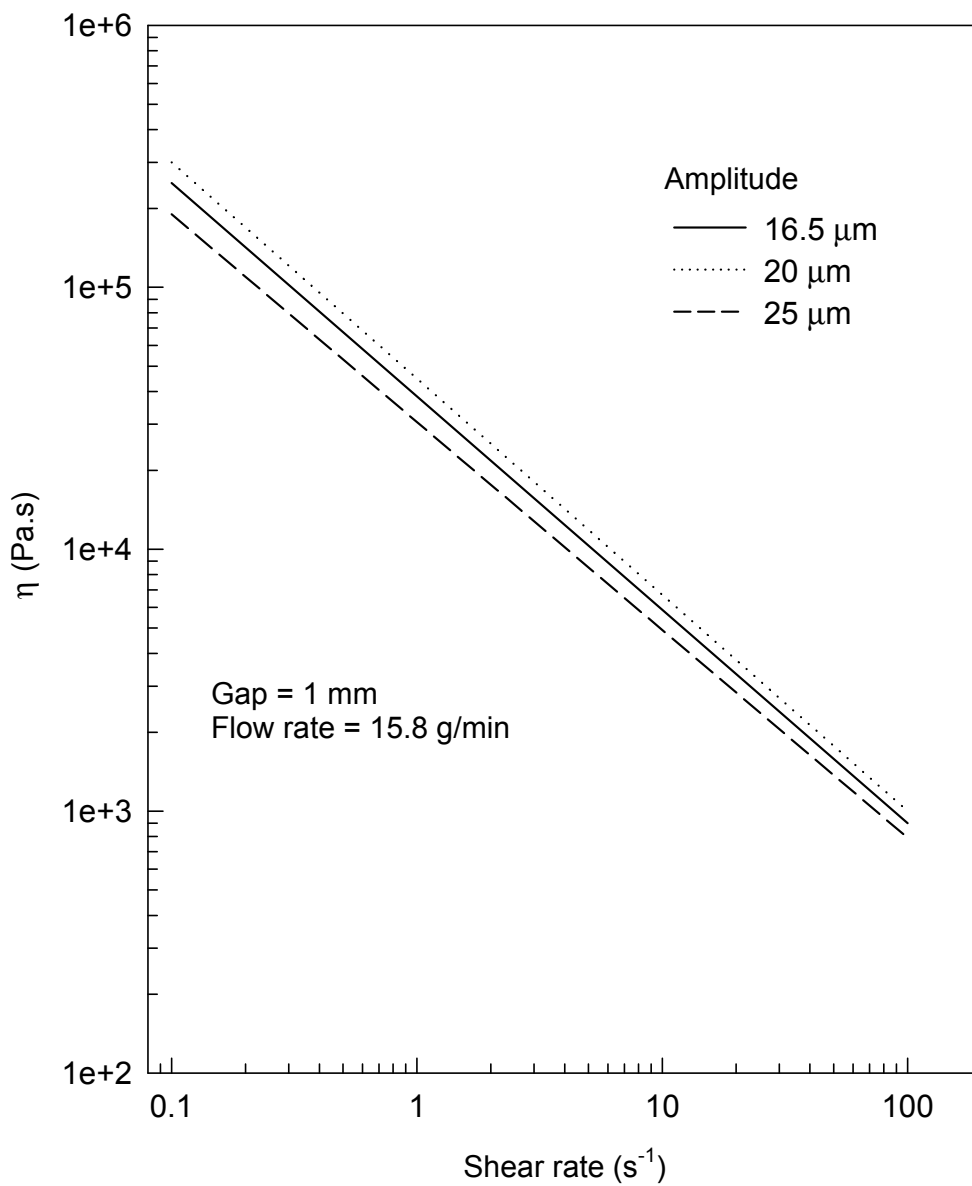


Figure 4.48 Viscosity versus shear rate for samples treated at various amplitudes. Gap is 1 mm and flow rate is 15.8 g/min.

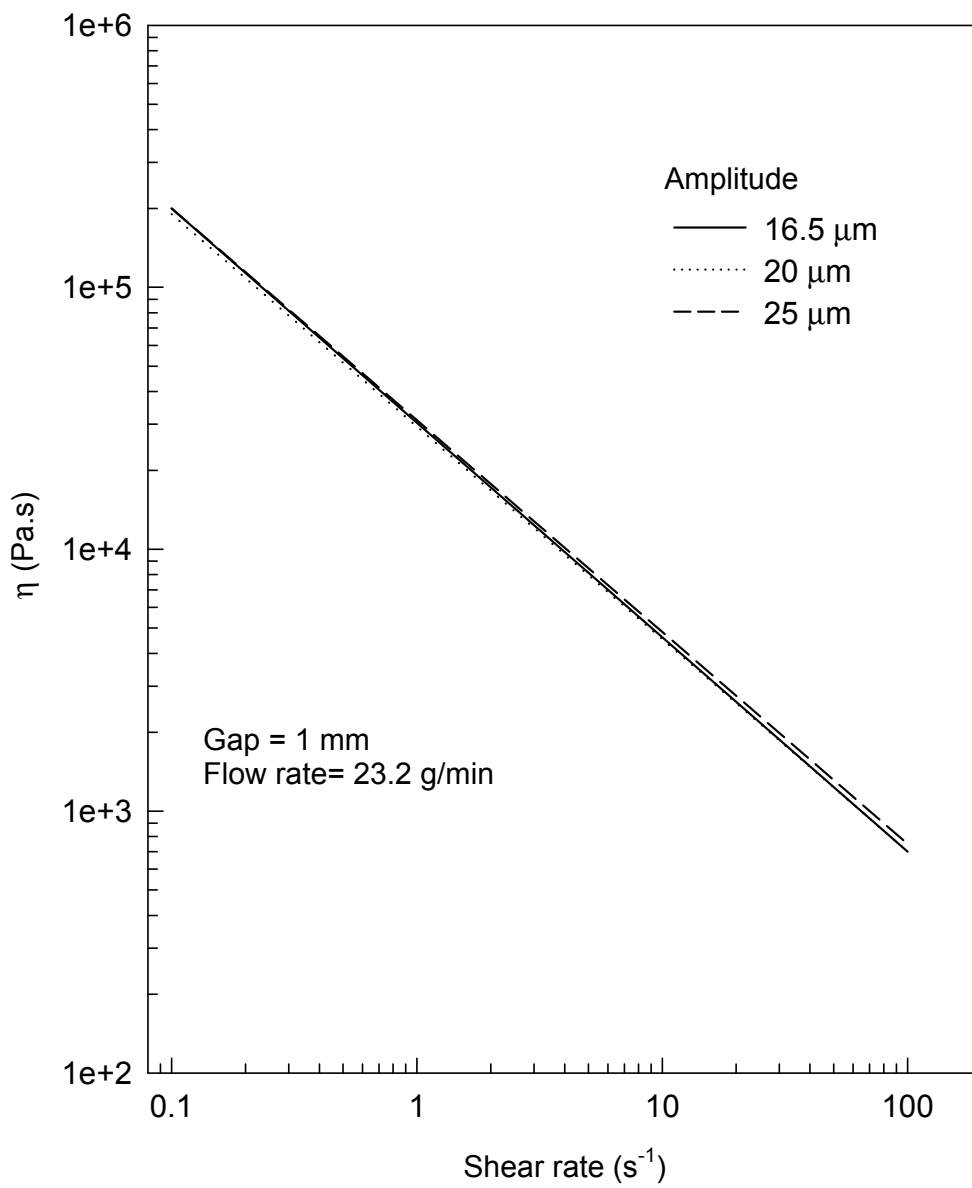


Figure 4.49 Viscosity versus shear rate for samples treated at various amplitudes. Gap is 1 mm and flow rate is 23.2 g/min.

show that as the amplitude is increased, the difference in the affect of energy on the material is more pronounced. The first two graphs show that the materials have very similar viscosities at any energy level. The low throughput rate allows the materials to be thoroughly treated. Figures 4.44 and 4.43 show clearly that different exposure time in the process produces specimens of different viscosity.

The final set of figures in this group, Figures 4.46 through 4.49, displays very clearly that the materials viscosities are reduced according to exposure to ultrasound. The 1 mm gap allows the differences in exposure to clearly be seen in all four graphs with the curves of various amplitudes closer to each other as the throughput is increased. It is important to note that while the first conclusion that can be reached is that material viscosities are reduced according to exposure to ultrasound, the gap that the materials are run at have an important affect on the results.

The next group of figures, Figures 4.50 through 4.78 is composed of three sets of figures, with data obtained from material run at different gaps between the ultrasonic horn and the extruder die exit. Each set of three figures shows data for materials run at different ultrasonic treatment levels (16.5, 20, and 25 μ m). The figures of materials run with the largest gap of 4 mm, Figures 4.50 through 4.52, again show erratic results reinforcing the idea that the gap size is too large for this material to be consistently treated.

Figures 4.53 through 4.55 begin to show more anticipated behaviors. These materials were run with a 2 mm gap. The figures all show that the viscosity of the treated materials has a direct relationship to throughput rate. This is most clearly shown in Figures 4.53. As the throughput is increased and exposure time to the treatment is reduced, the effect of the treatment on the material is reduced and the viscosity of the specimen increases.

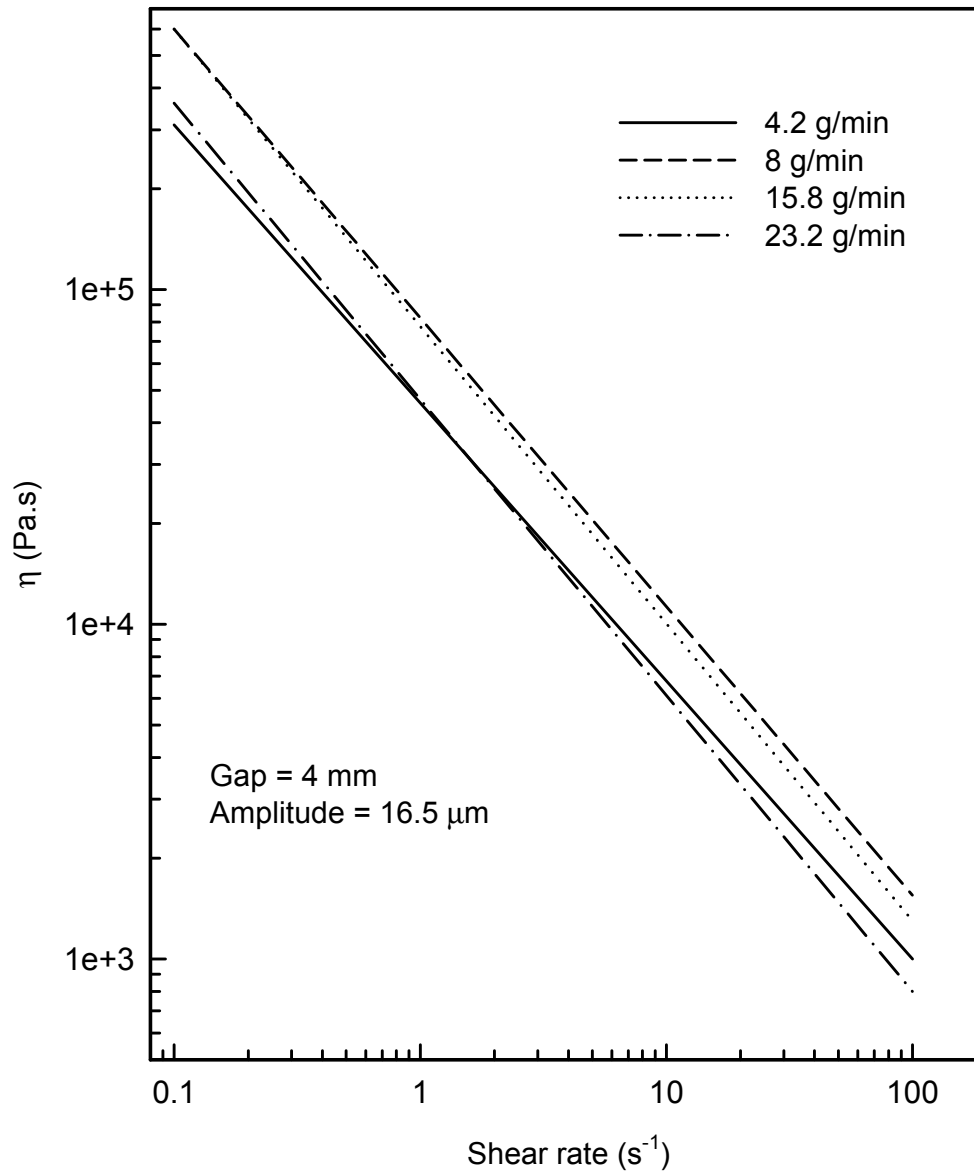


Figure 4.50 Viscosity versus shear rate for samples obtained at various throughput rates. Gap is 4 mm and amplitude is 16.5 μm .

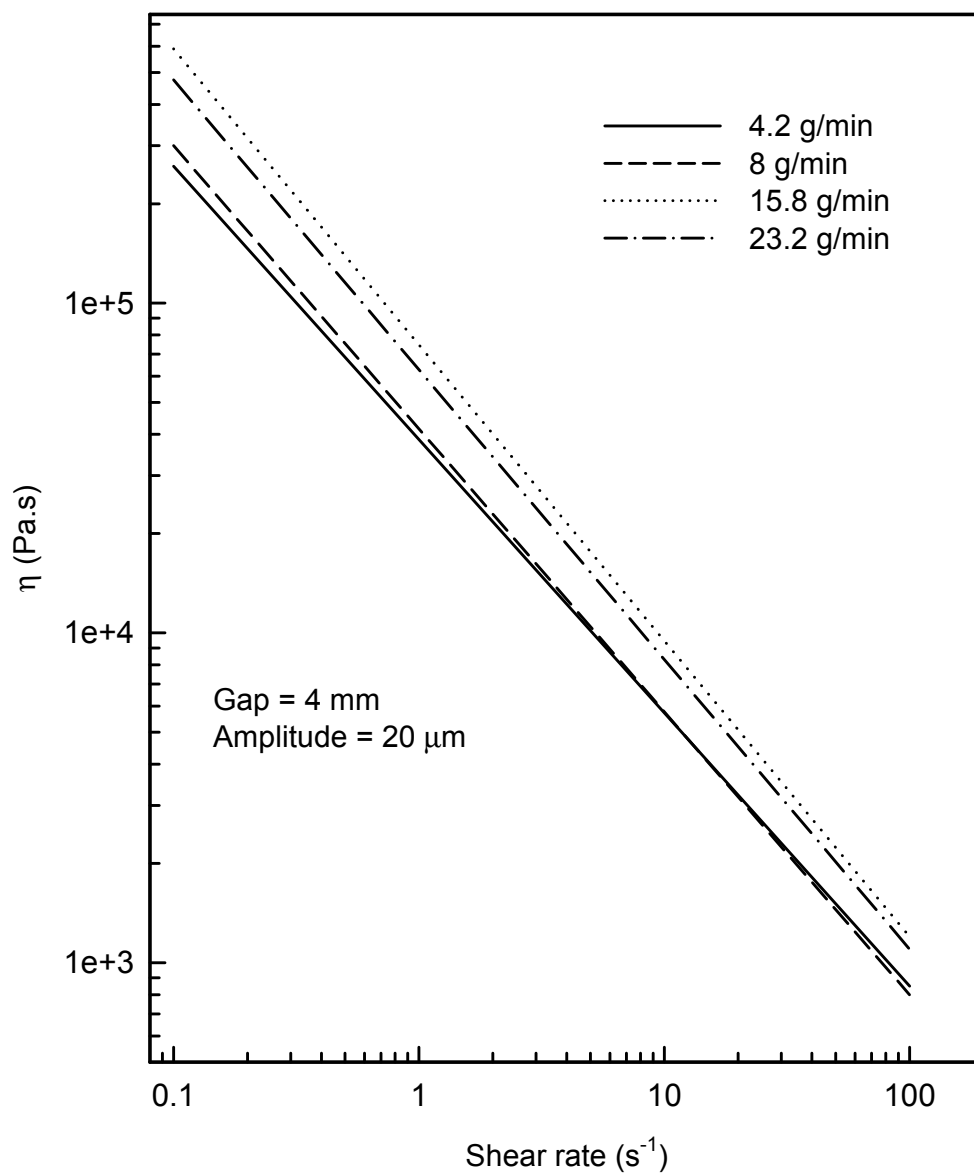


Figure 4.51 Viscosity versus shear for samples obtained rate at various flow rates. Gap is 4 mm and amplitude is 20.0 μm .

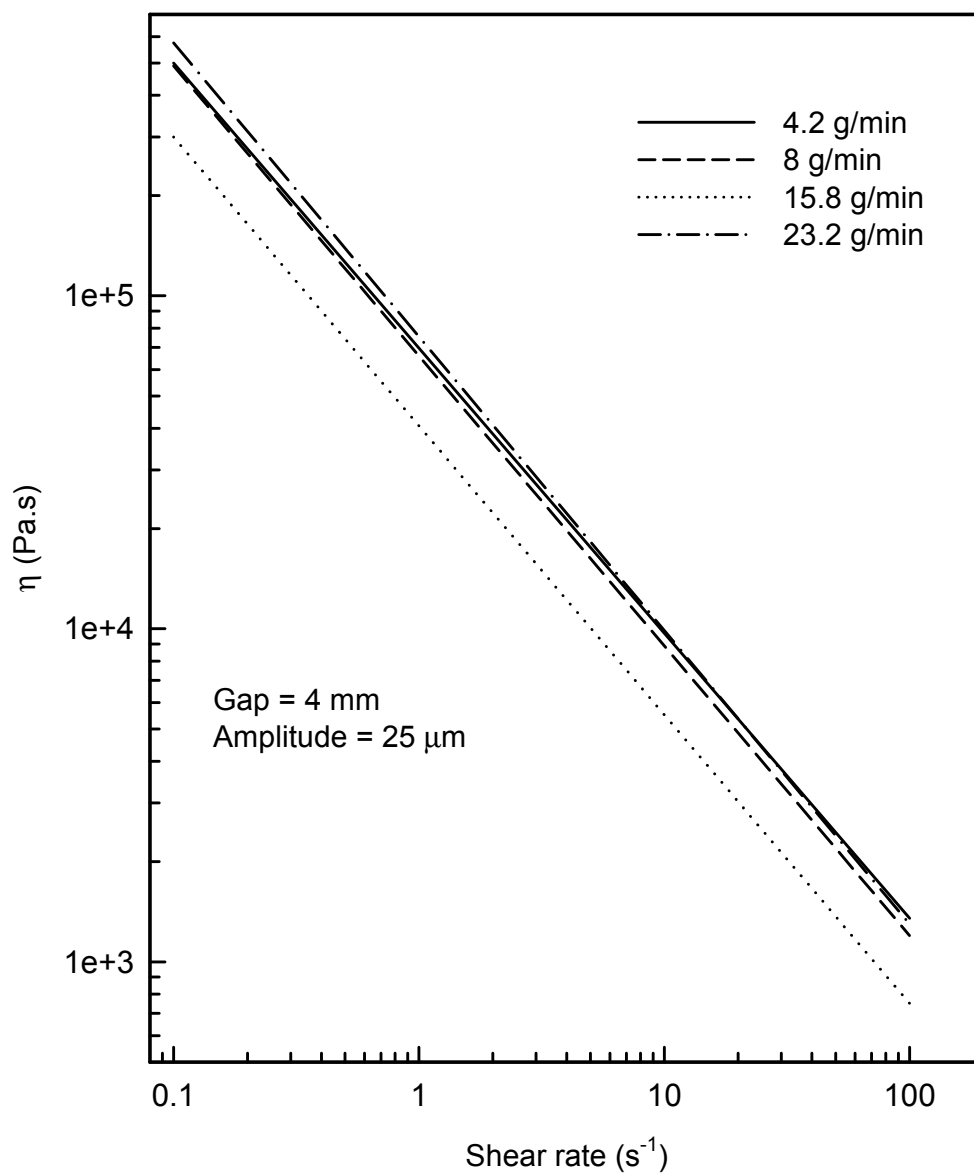


Figure 4.52 Viscosity versus shear rate for samples obtained at various flow rates. Gap is 4 mm and amplitude is 25 μ m.

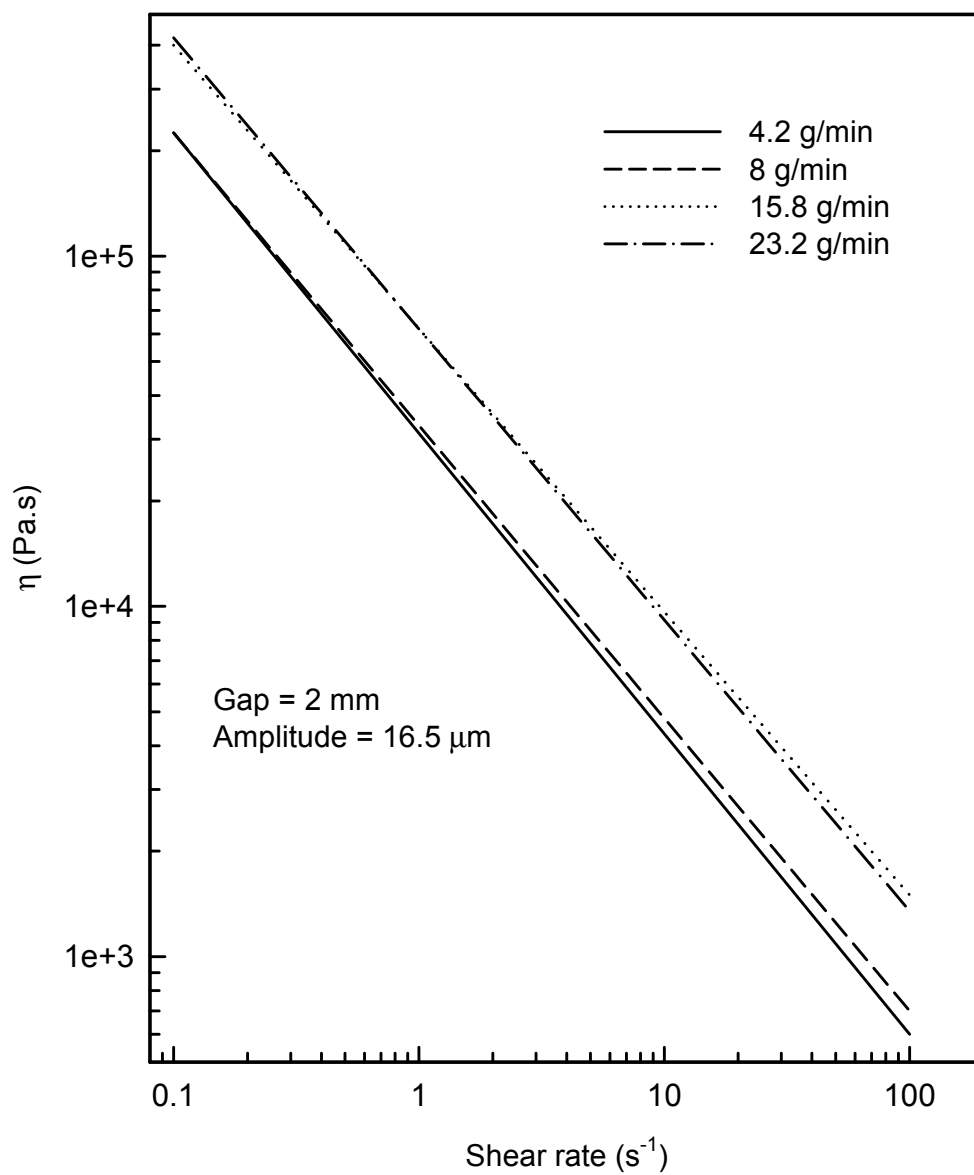


Figure 4.53 Viscosity versus shear rate for samples obtained at various flow rates. Gap is 2 mm and amplitude is 16.5 μm .

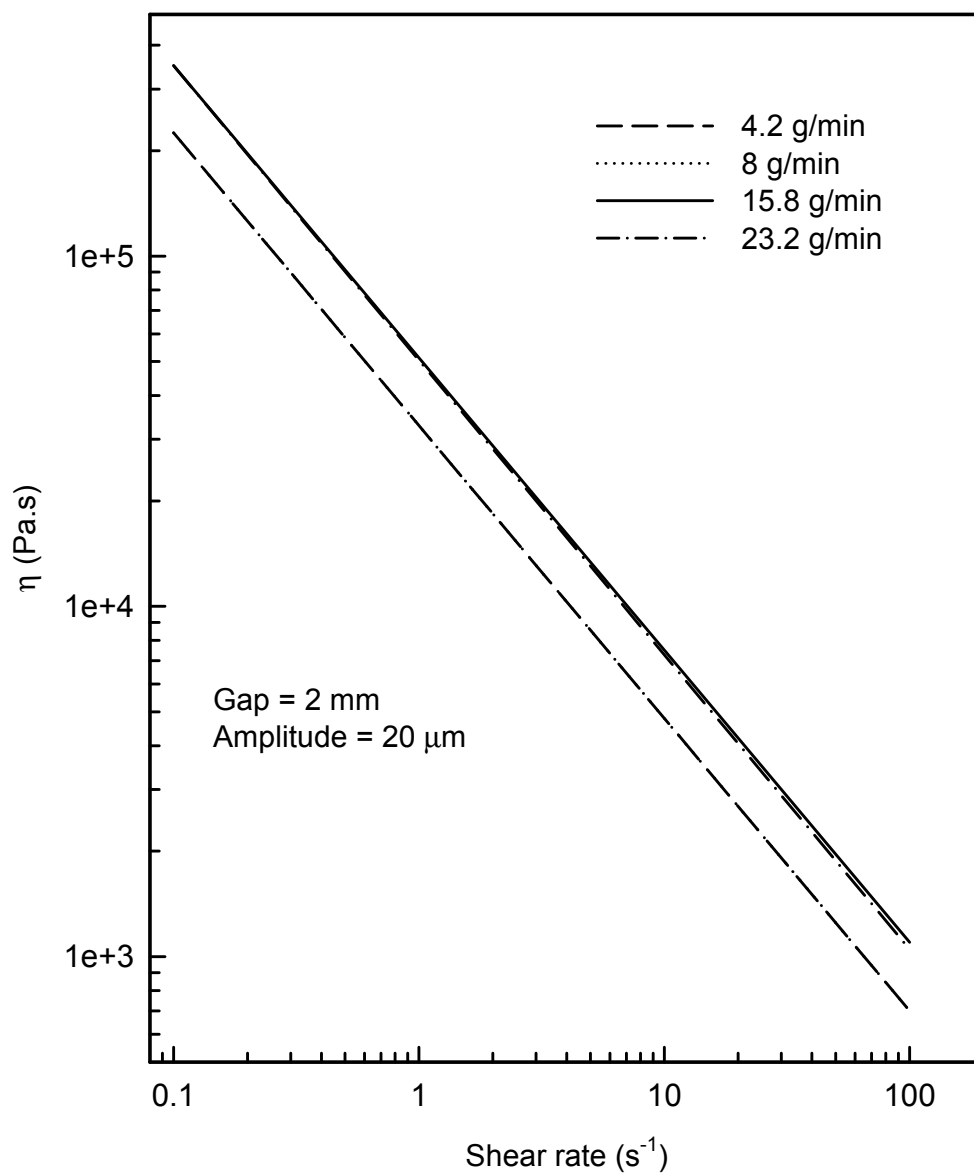


Figure 4.54 Viscosity versus shear rate for samples obtained at various flow rates. Gap is 2 mm and amplitude is 20.0 μ m.

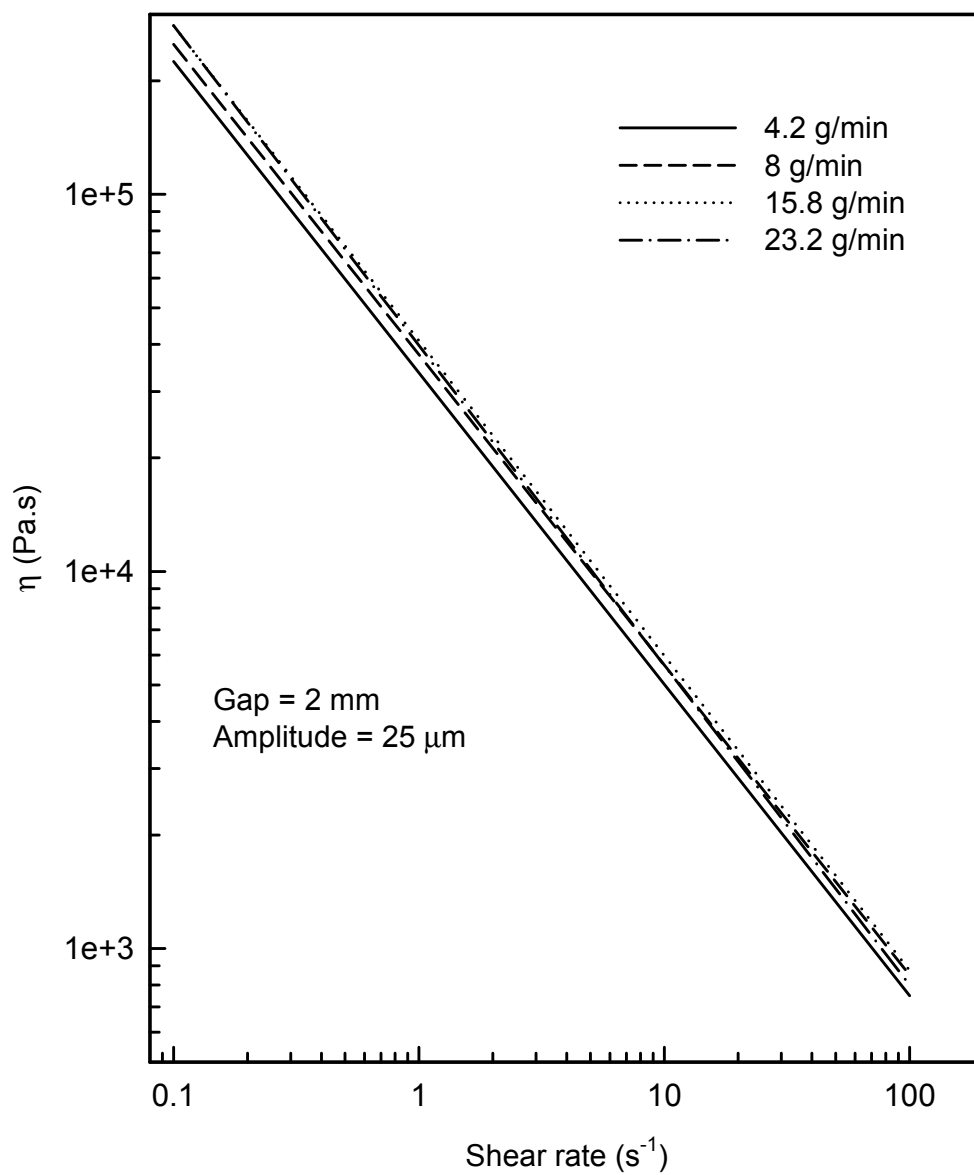


Figure 4.55 Viscosity versus shear rate for samples obtained at various flow rates. Gap is 2 mm and amplitude is 25 μm .

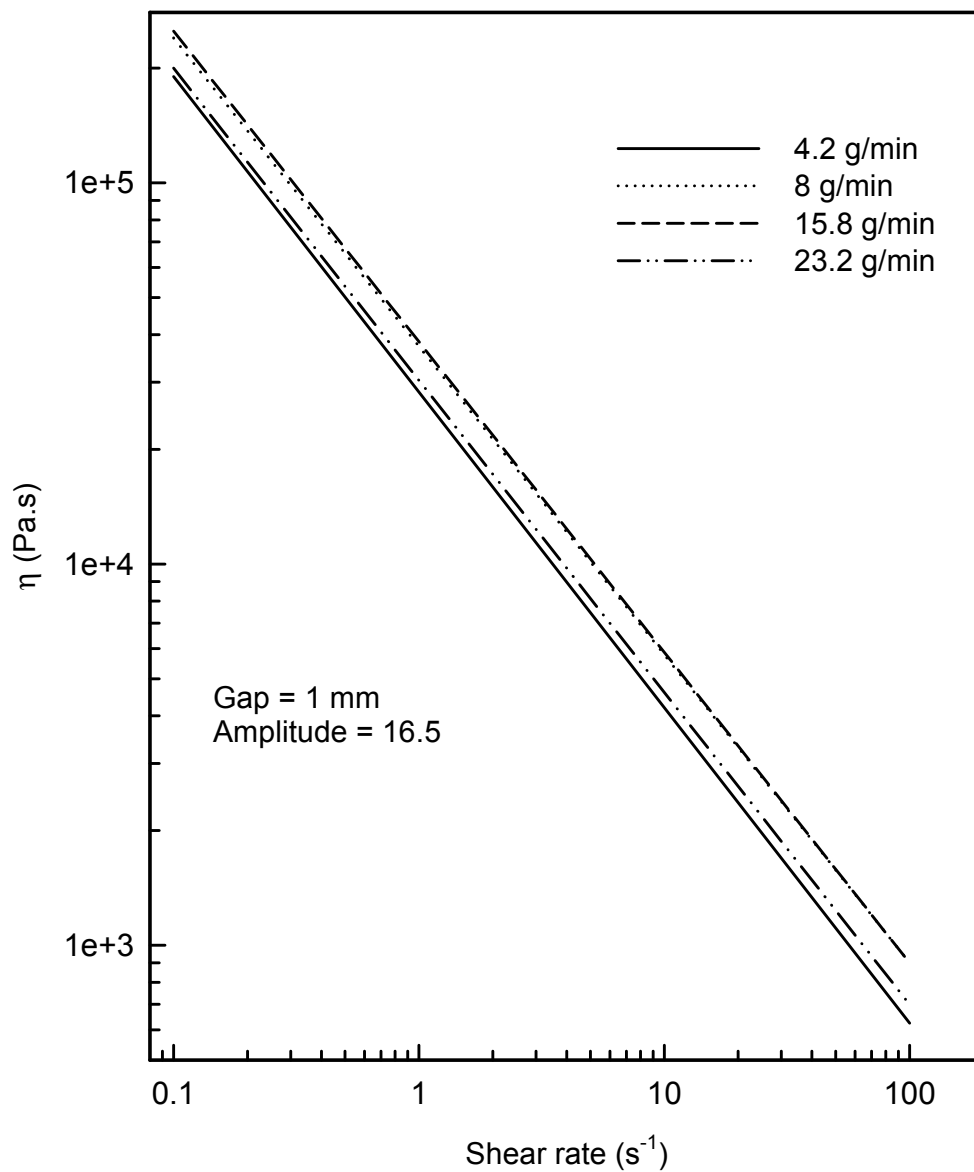


Figure 4.56 Viscosity versus shear rate for samples obtained at various flow rates. Gap is 1 mm and amplitude is 16.5 μm .

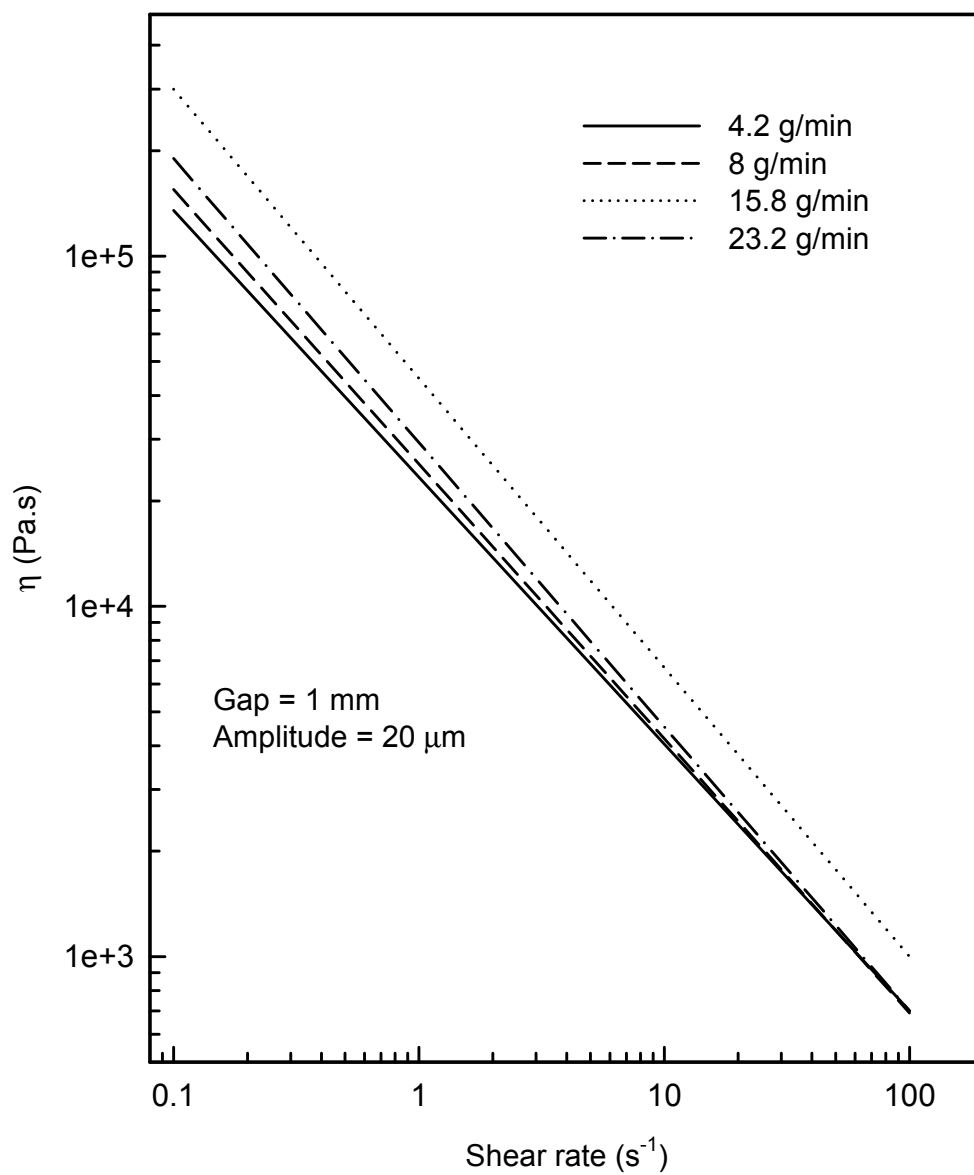


Figure 4.57 Viscosity versus shear rate for samples obtained at various flow rates. Gap is 1 mm and amplitude is 20.0 μ m.

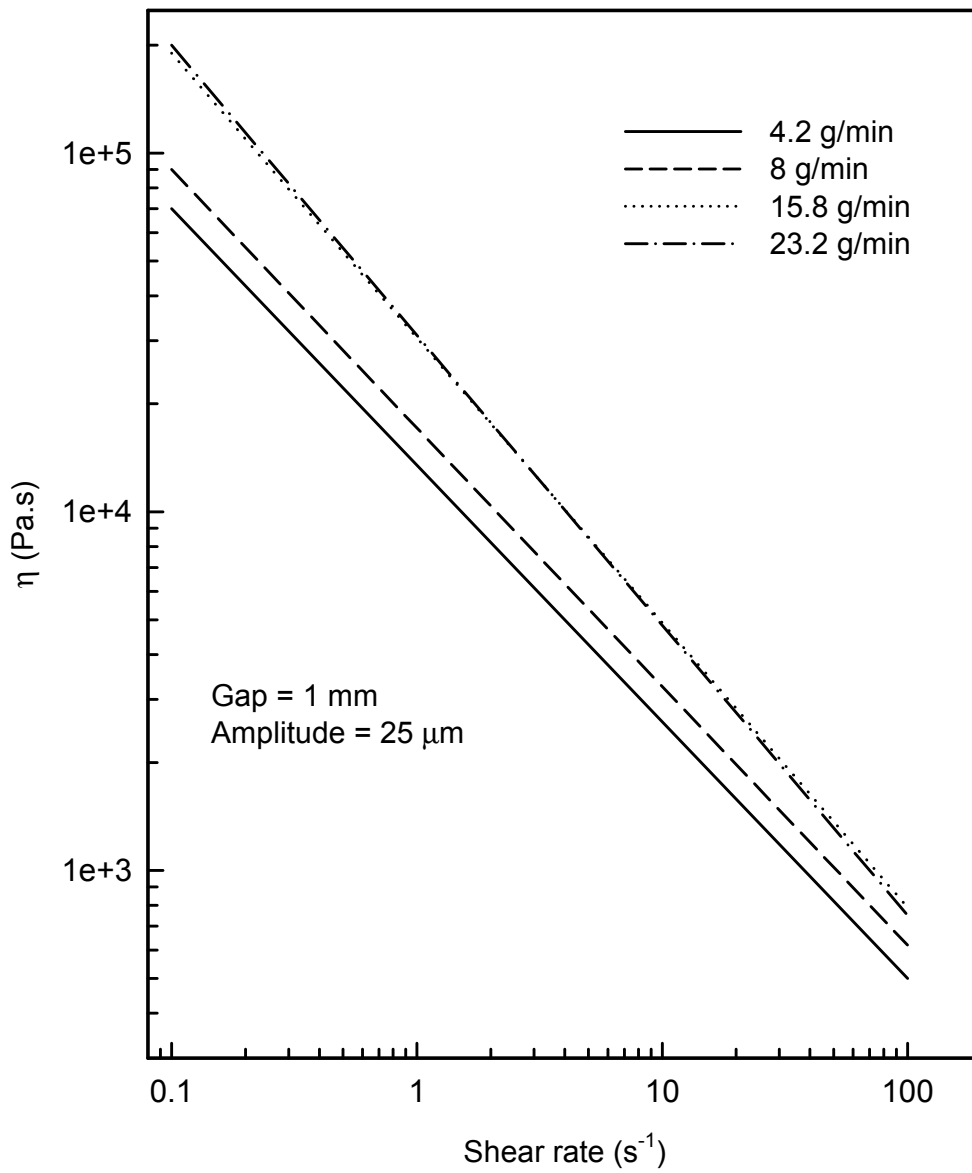


Figure 4.58 Viscosity versus shear rate for samples obtained at various flow rates. Gap is 4 mm and amplitude is 25 μm .

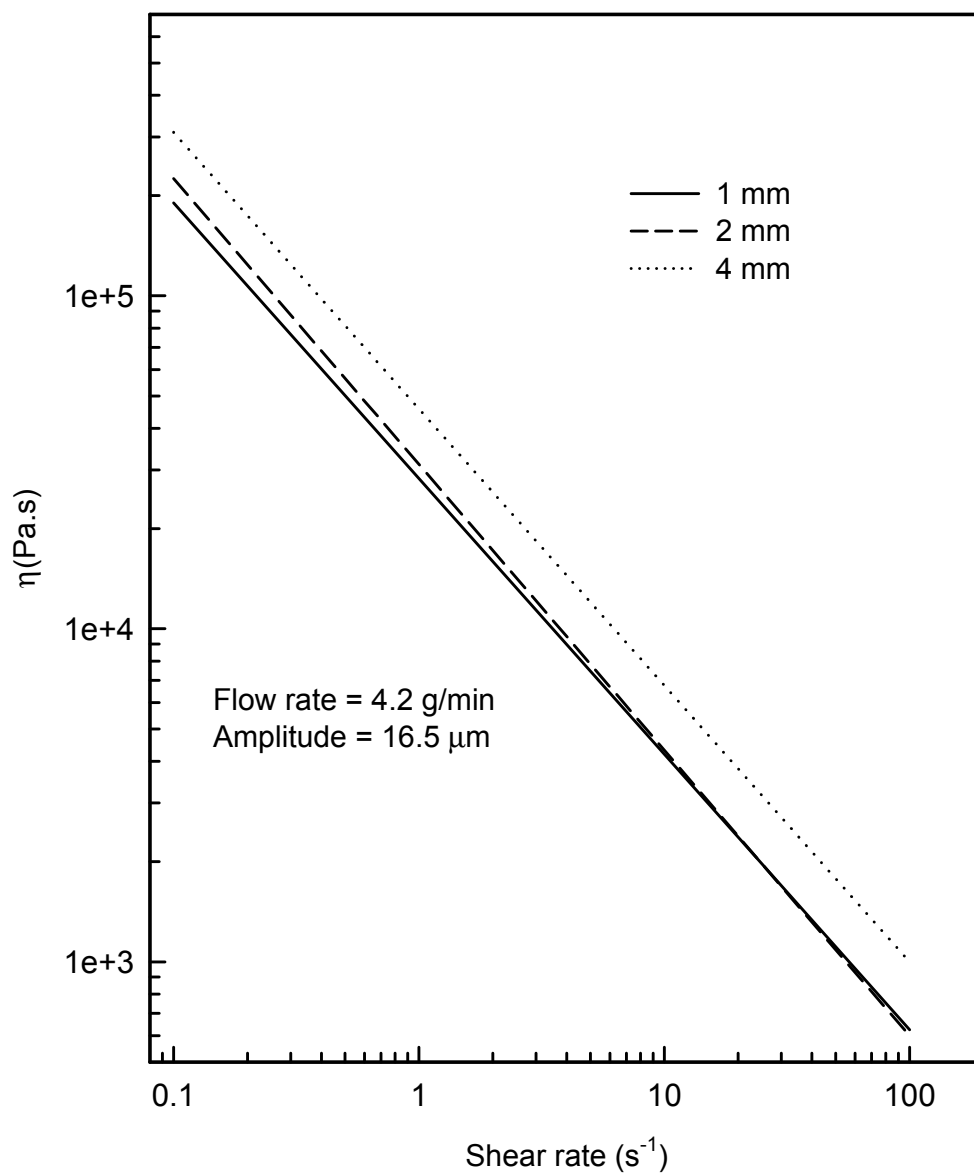


Figure 4.59 Viscosity versus shear rate for samples obtained at various gaps. Flow rate is 4.2 g/min and amplitude is 16.5 μm

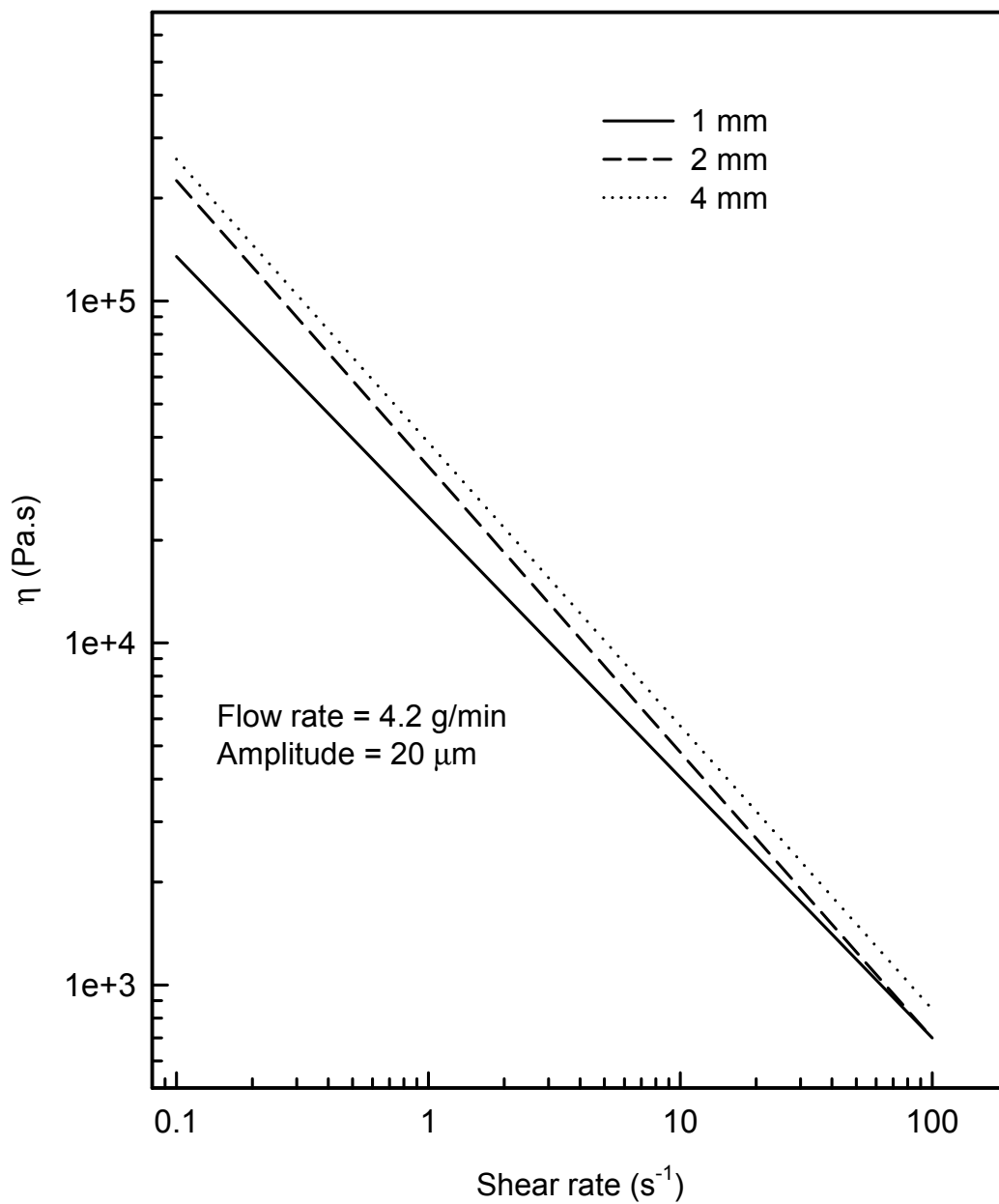


Figure 4.60 Viscosity versus shear rate for samples obtained at various gaps. Flow rate is 4.2 g/min and amplitude is 20.0 μm

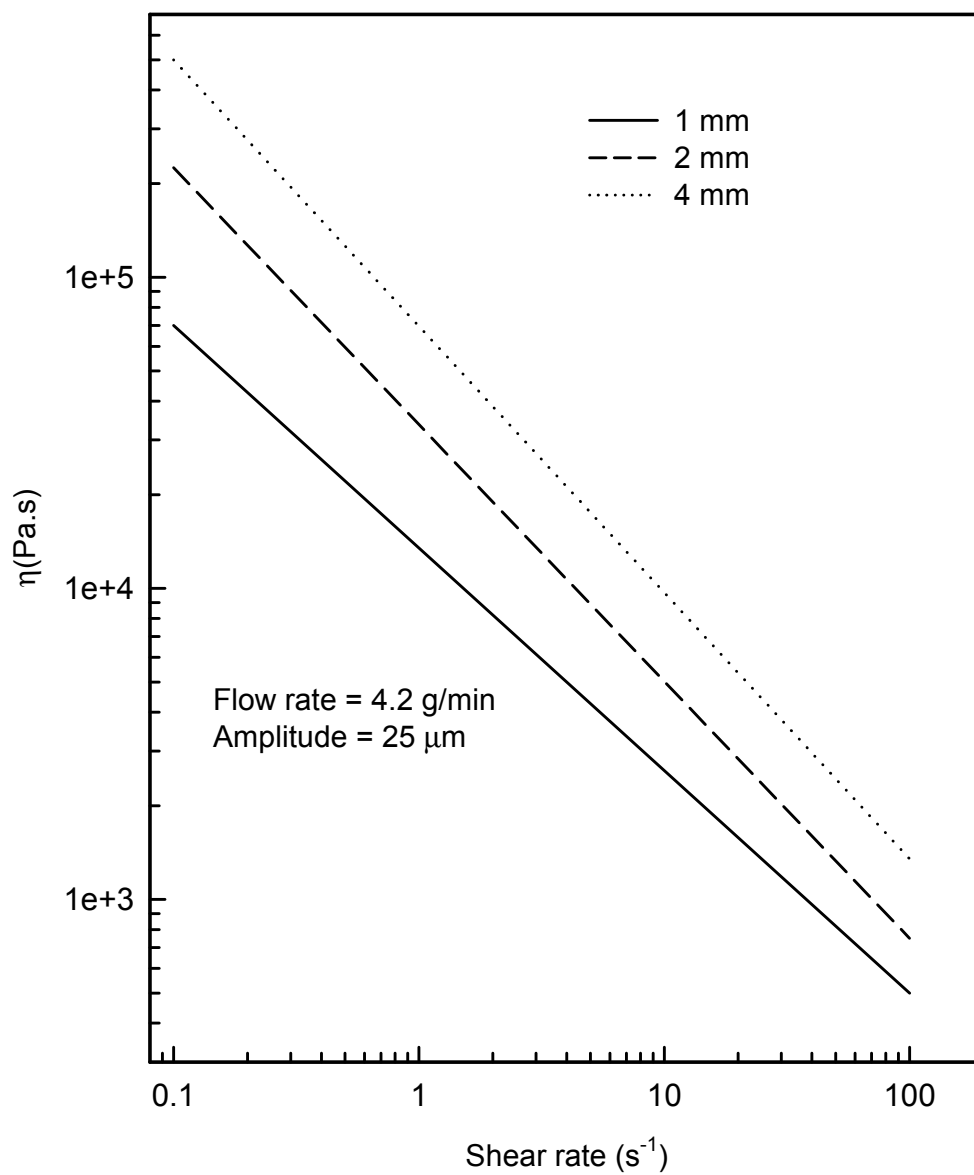


Figure 4.61 Viscosity versus shear rate for samples obtained at various gaps. Flow rate is 4.2 g/min and amplitude is 25.0 μm

Figures 4.56 through 4.58 show the same trend. These materials were all run with a 1 mm gap at different throughputs. The viscosities are very similar in the figures making evaluation difficult. However, Figure 4.58 shows the anticipated trend clearly. A direct relationship between specimen viscosity and throughput can be observed.

Figures 4.59 through 4.70 are four sets of three figures. Each set contains viscosity data that compares materials run at the three ultrasonic treatment levels. Each figure compares materials run at different gaps in the process.

In the first set of figures run at the lowest throughput, Figures 4.59 through 4.61, the data clearly shows a direct relationship between gap thickness and viscosity. As the gap thickness that the sample was run increases, the viscosity of the samples exposed to the same treatment increases. Figure 4.59 results are very close to each other and difficult to evaluate. The results of Figures 4.60 and 4.61 indicate that the viscosity of the materials run at the larger gap is greater than those materials run at the smaller gap. Figures 4.62 through 4.64 show similar results as the previous set and allow the same conclusion to be drawn. They are somewhat easier to interpret because the increased throughput allows more differentiation in treatment levels and the viscosities of the resulting materials are more discrete.

The third set of figures, Figures 4.65 through 4.67, shows the same trend as the previous two sets of data and again, the same conclusion is drawn that viscosities of the materials resulting from treatment are directly related to the gap in the process that they are treated in. Of all the groups of data, this group most clearly demonstrates that there is a direct relationship between the viscosities of the materials and their respective treatment levels. Viscosities of the materials were lowered by the treatment, an obvious effect of de-crosslinking. In each figure, the resulting viscosity of the material was related to the treatment level received in the process by virtue of the gap used in the

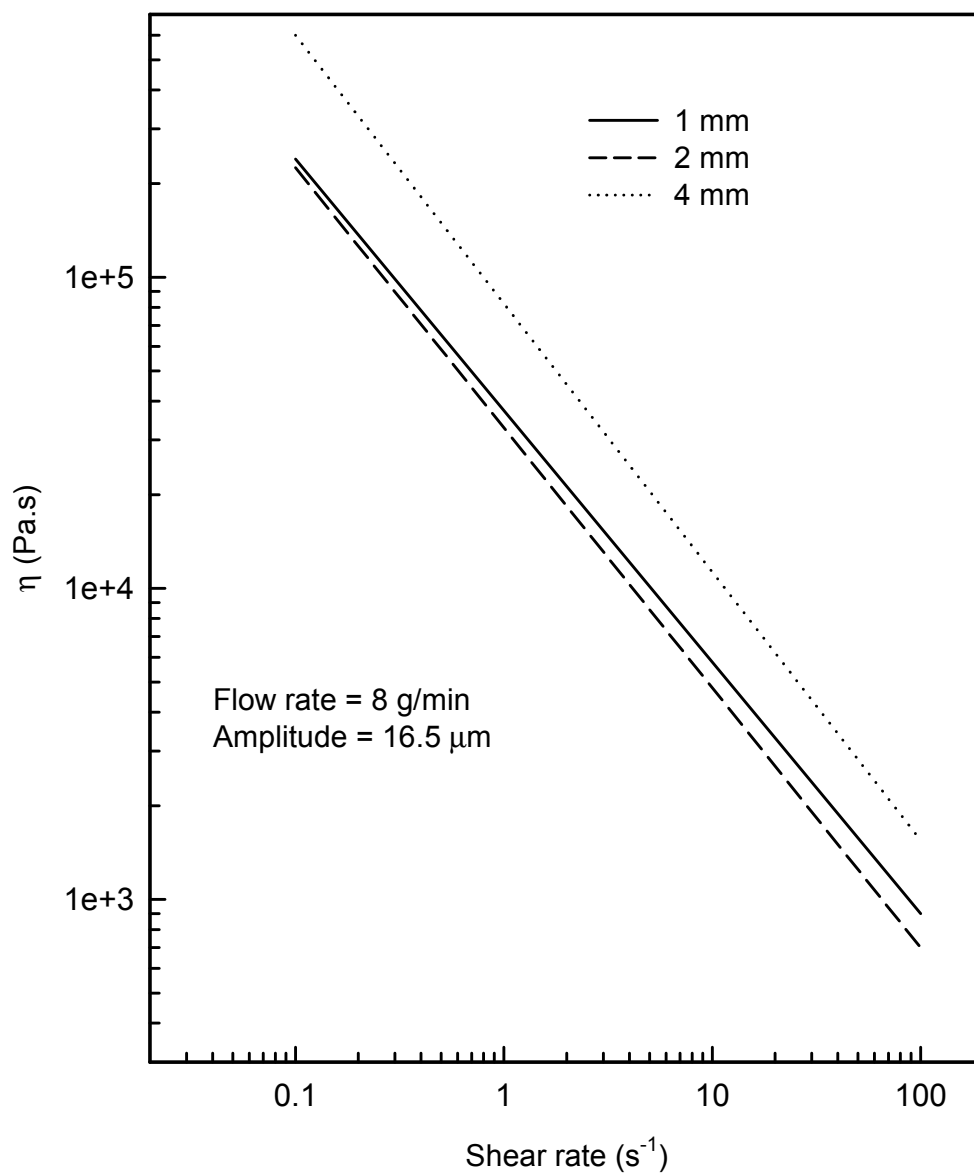


Figure 4.62 Viscosity versus shear rate for samples obtained at various gaps. Flow rate is 8 g/min and amplitude is 16.5 μ m

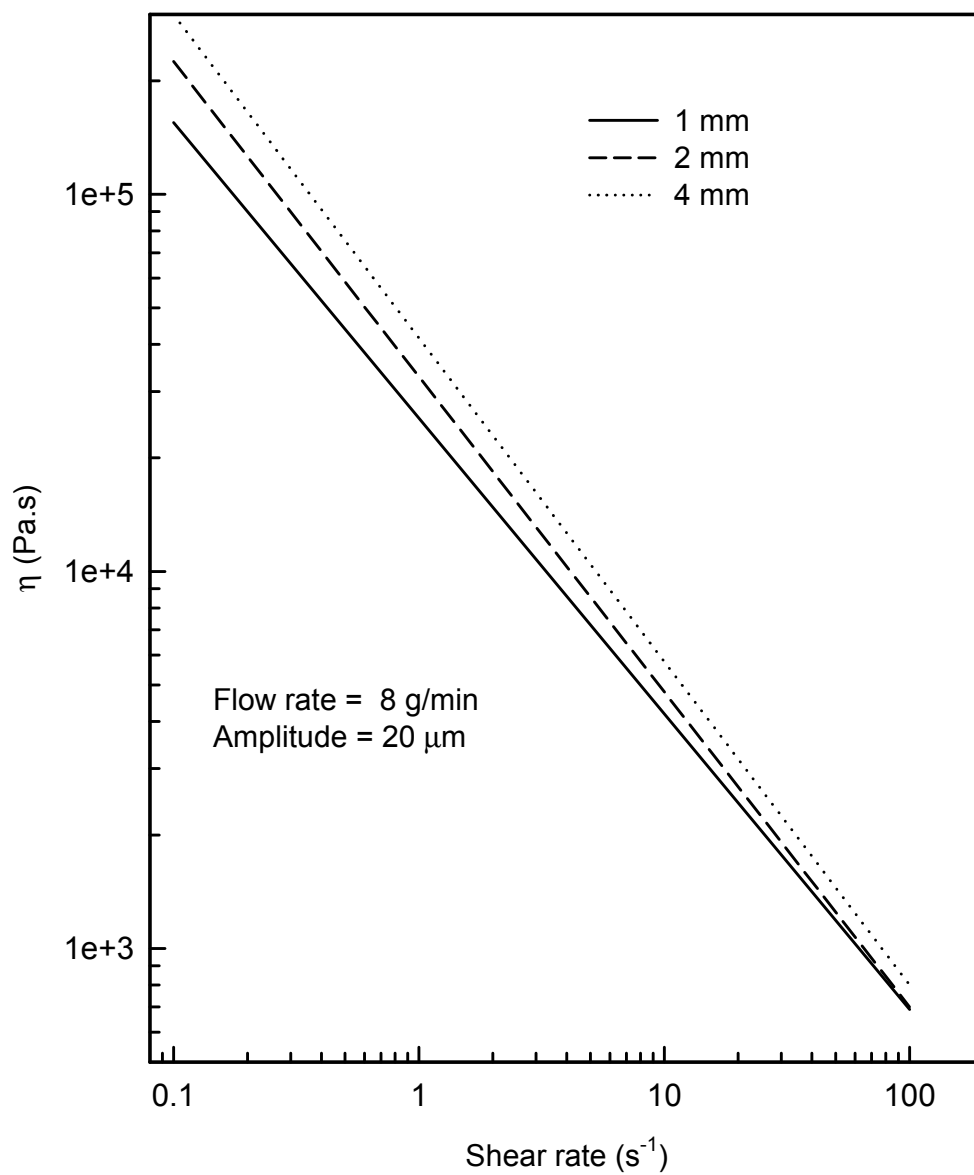


Figure 4.63 Viscosity versus shear rate for samples obtained at various gaps. Flow rate is 8 g/min and amplitude is 20.0 μm

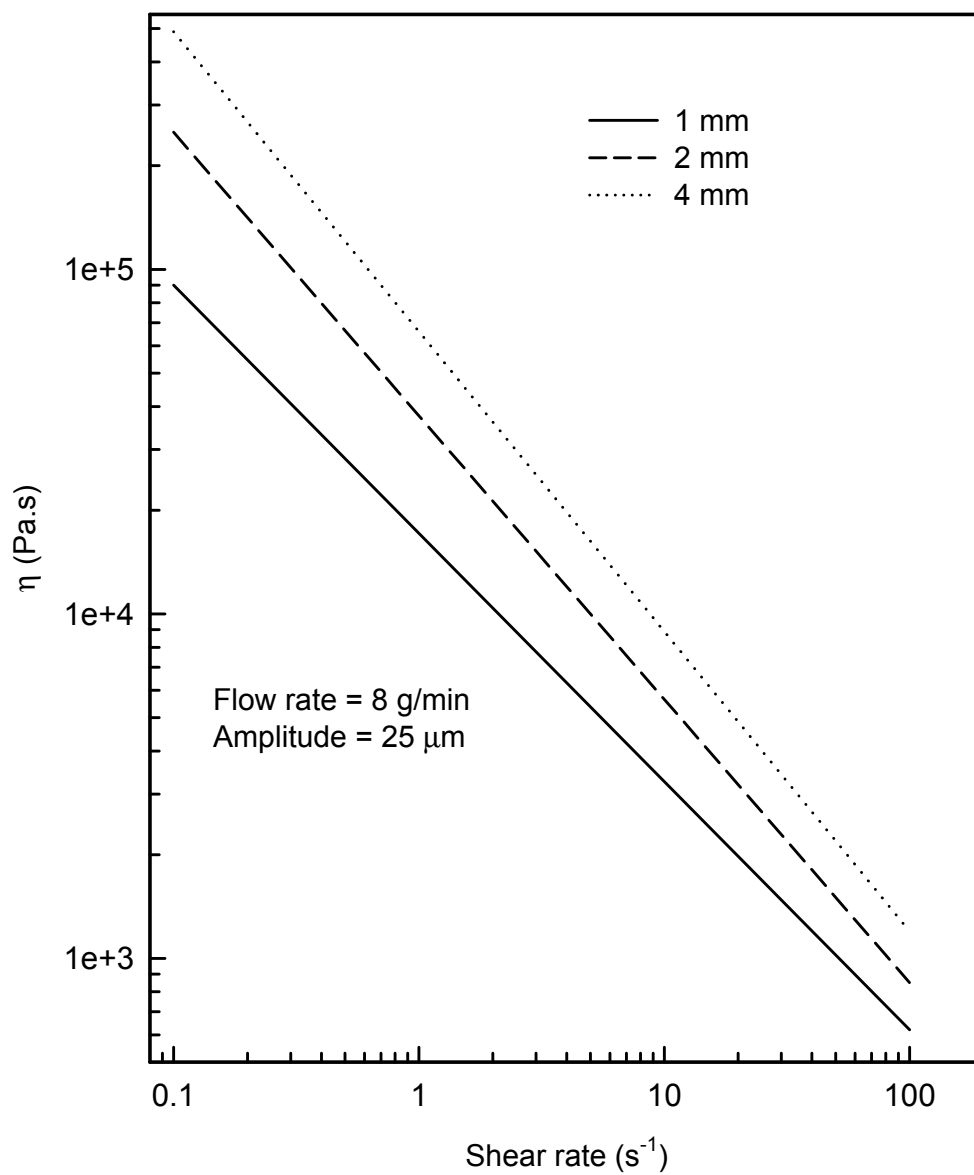


Figure 4.64 Viscosity versus shear rate for samples obtained at various gaps. Flow rate is 8 g/min and amplitude is 25.0 μm

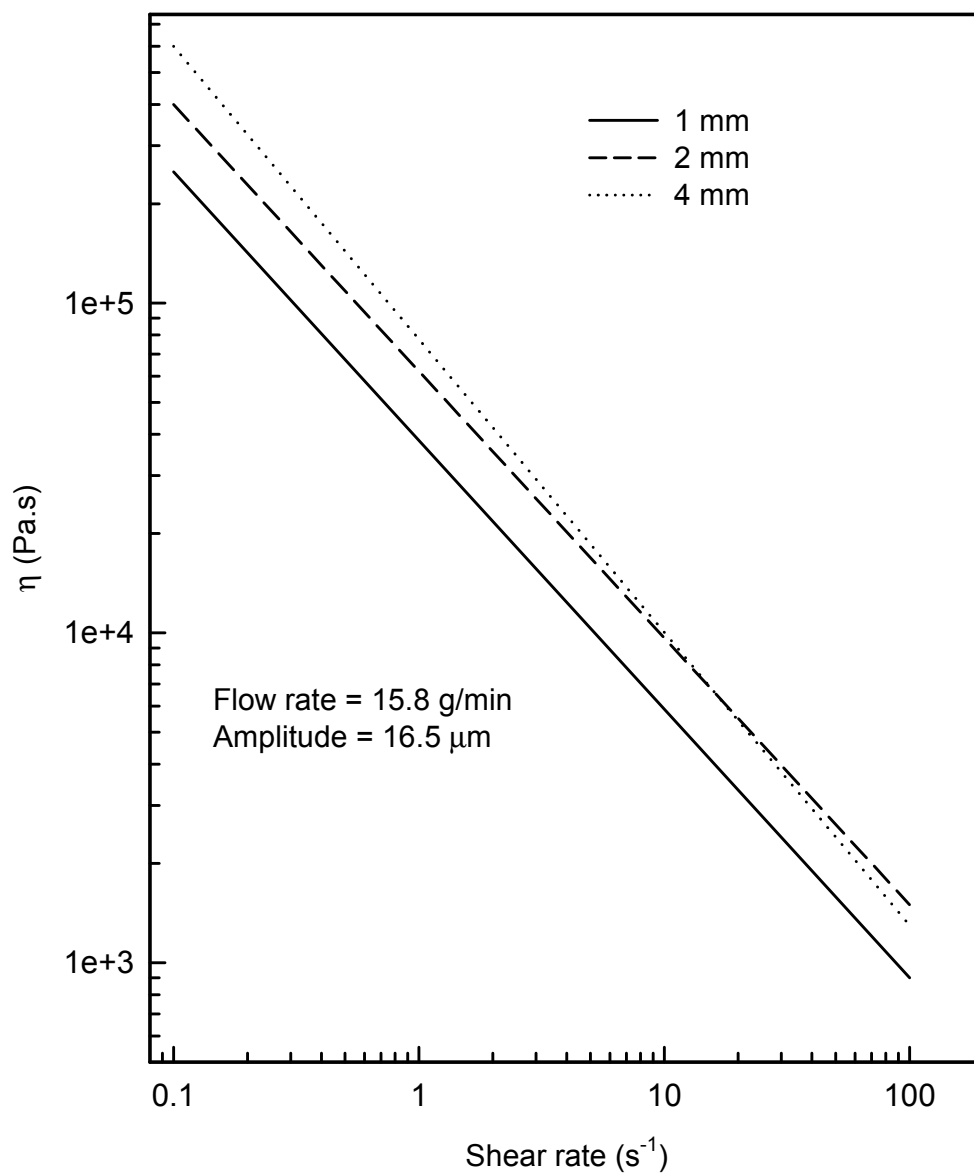


Figure 4.65 Viscosity versus shear rate at various gaps. Flow rate is 15.8 g/min and amplitude is 16.5 μm

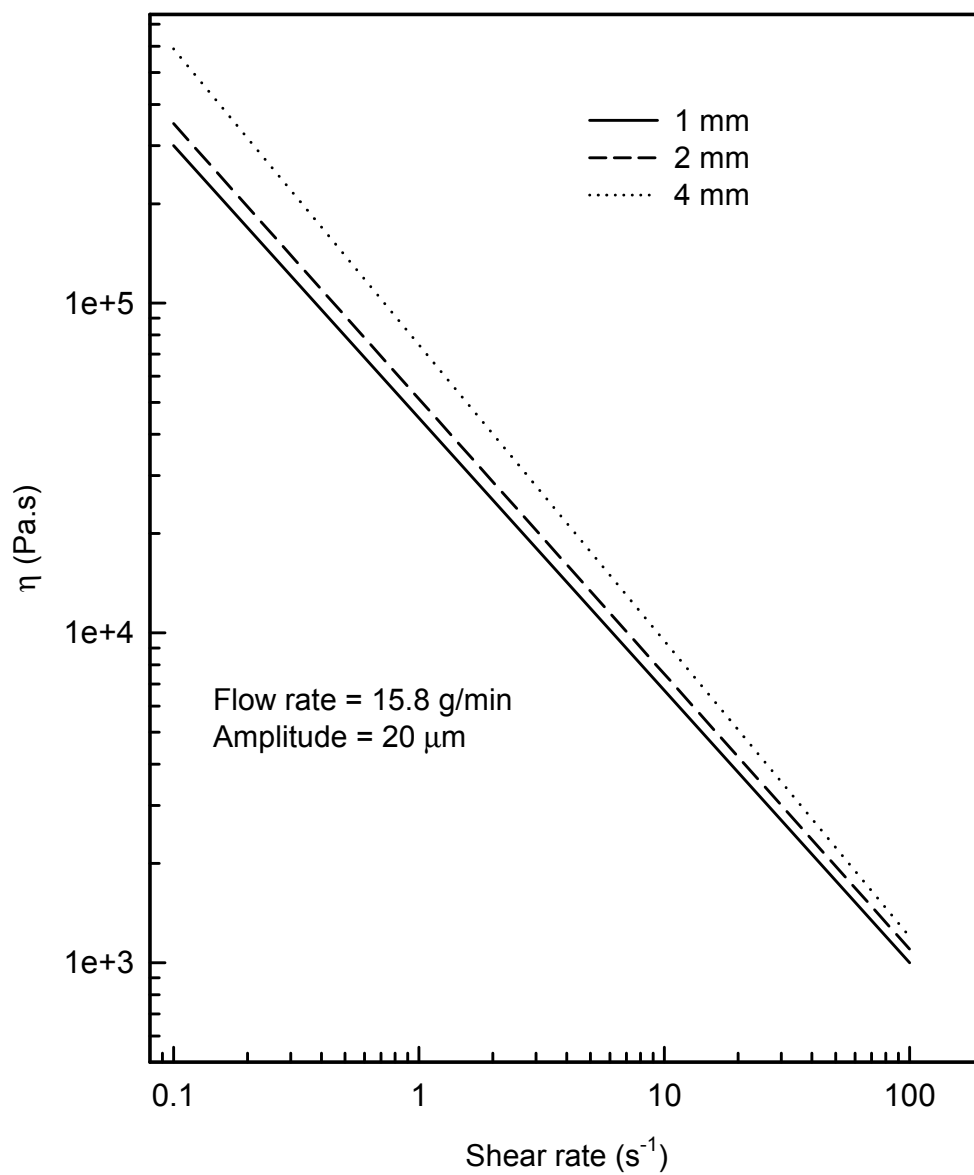


Figure 4.66 Viscosity versus shear rate at various gaps. Flow rate is 15.8 g/min and amplitude is 20.0 μm

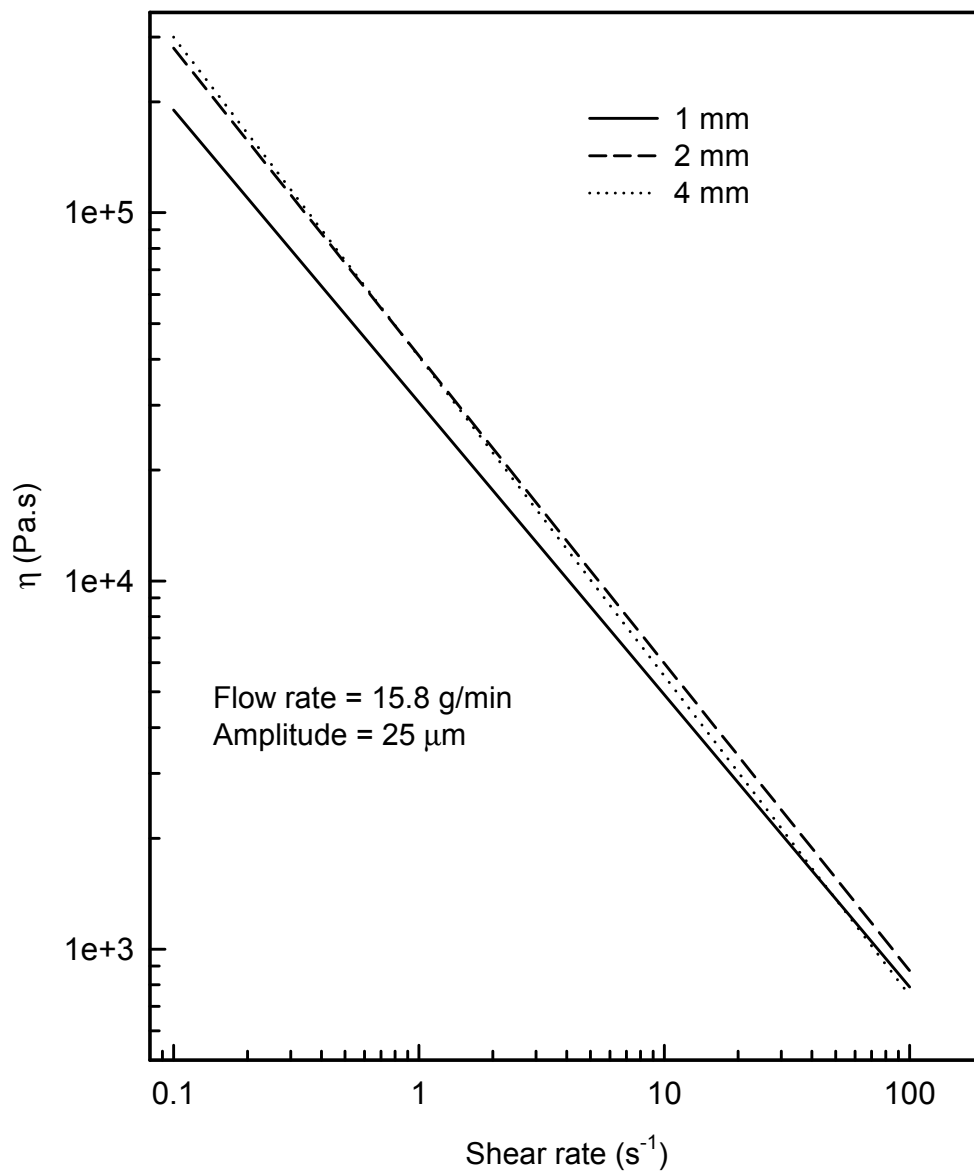


Figure 4.67 Viscosity versus shear rate at various gaps. Flow rate is 15.8 g/min and amplitude is 25.0 μm

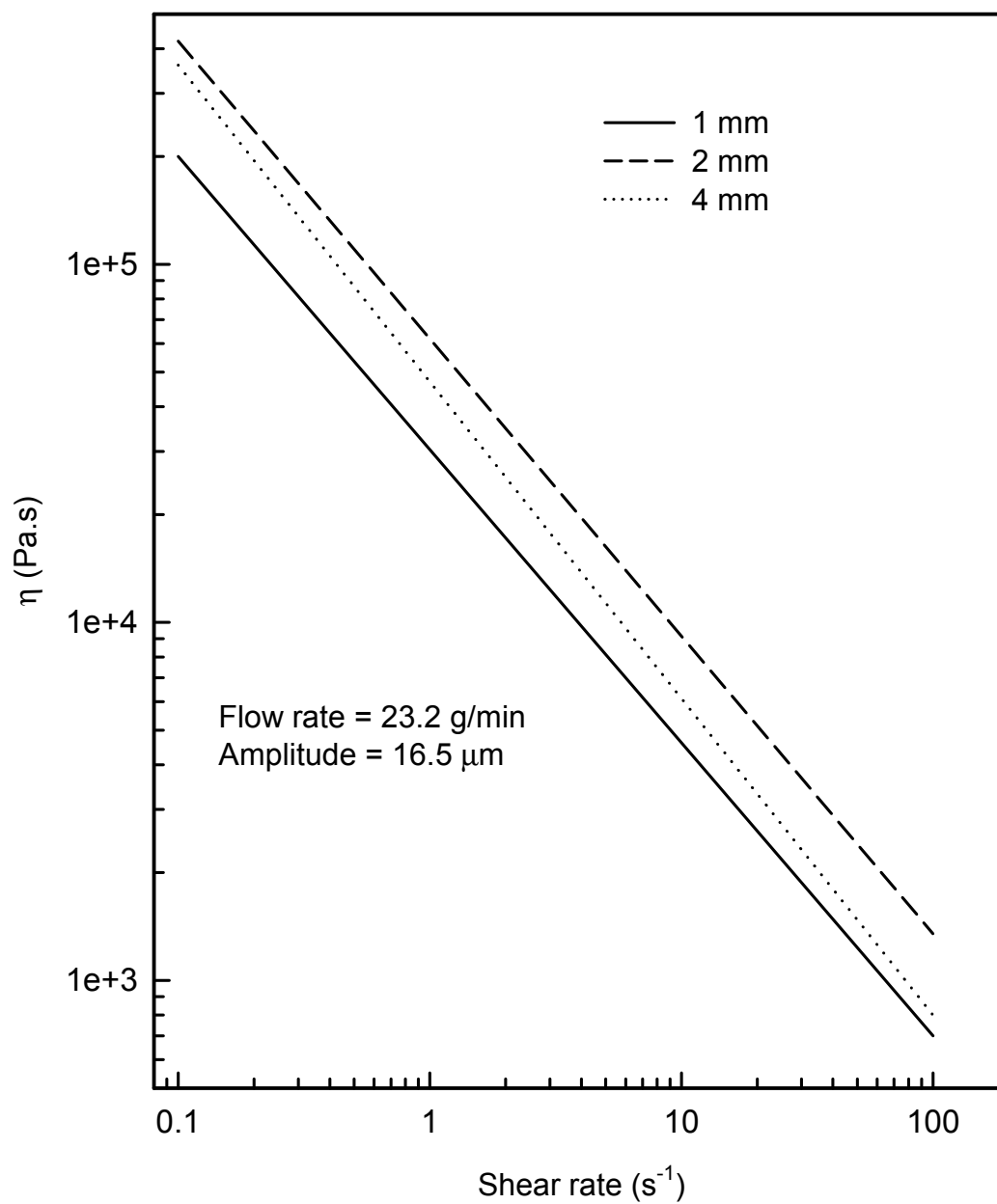


Figure 4.68 Viscosity versus shear rate at various gaps. Flow rate is 23.2 g/min and amplitude is 16.5 μm

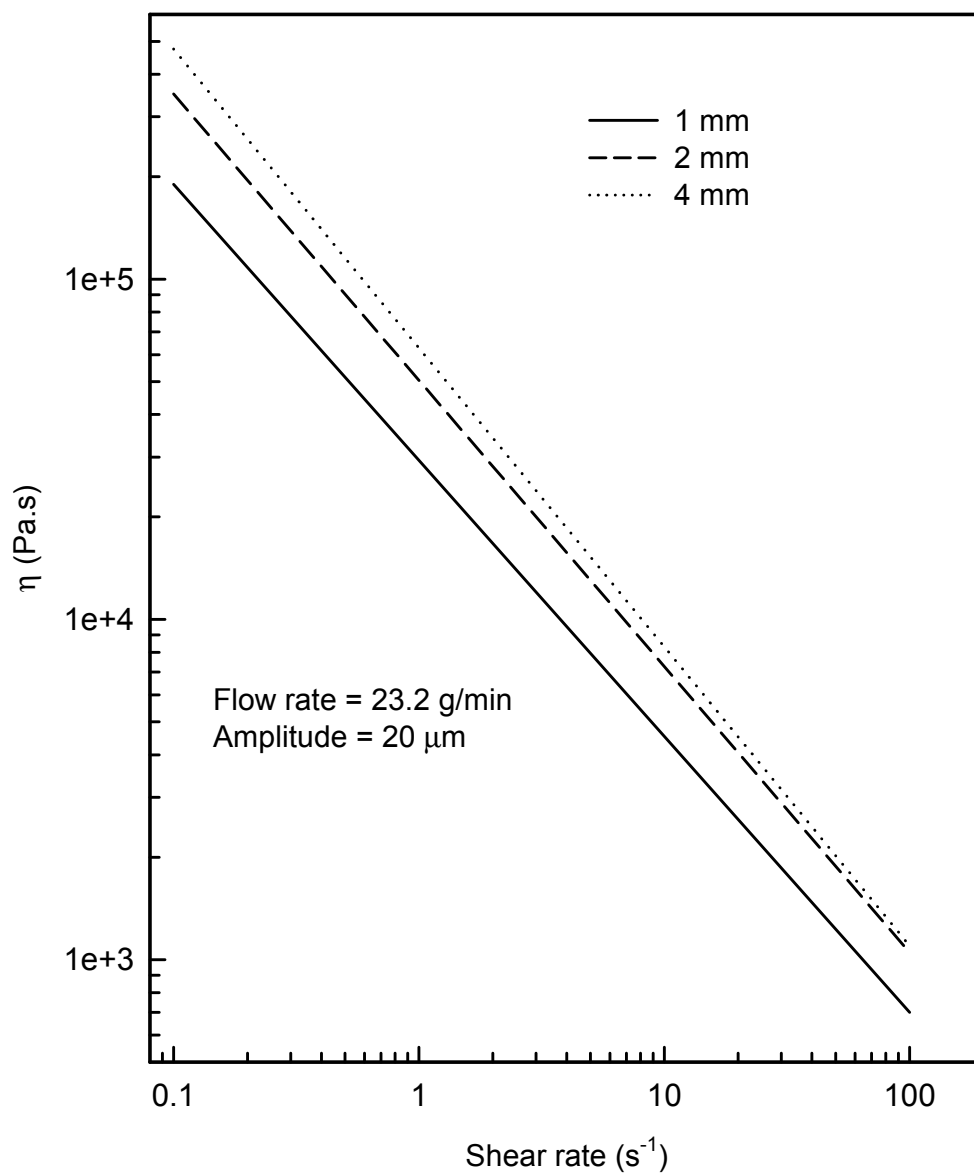


Figure 4.69 Viscosity versus shear rate at various gaps. Flow rate is 23.2 g/min and amplitude is 20.0 μm

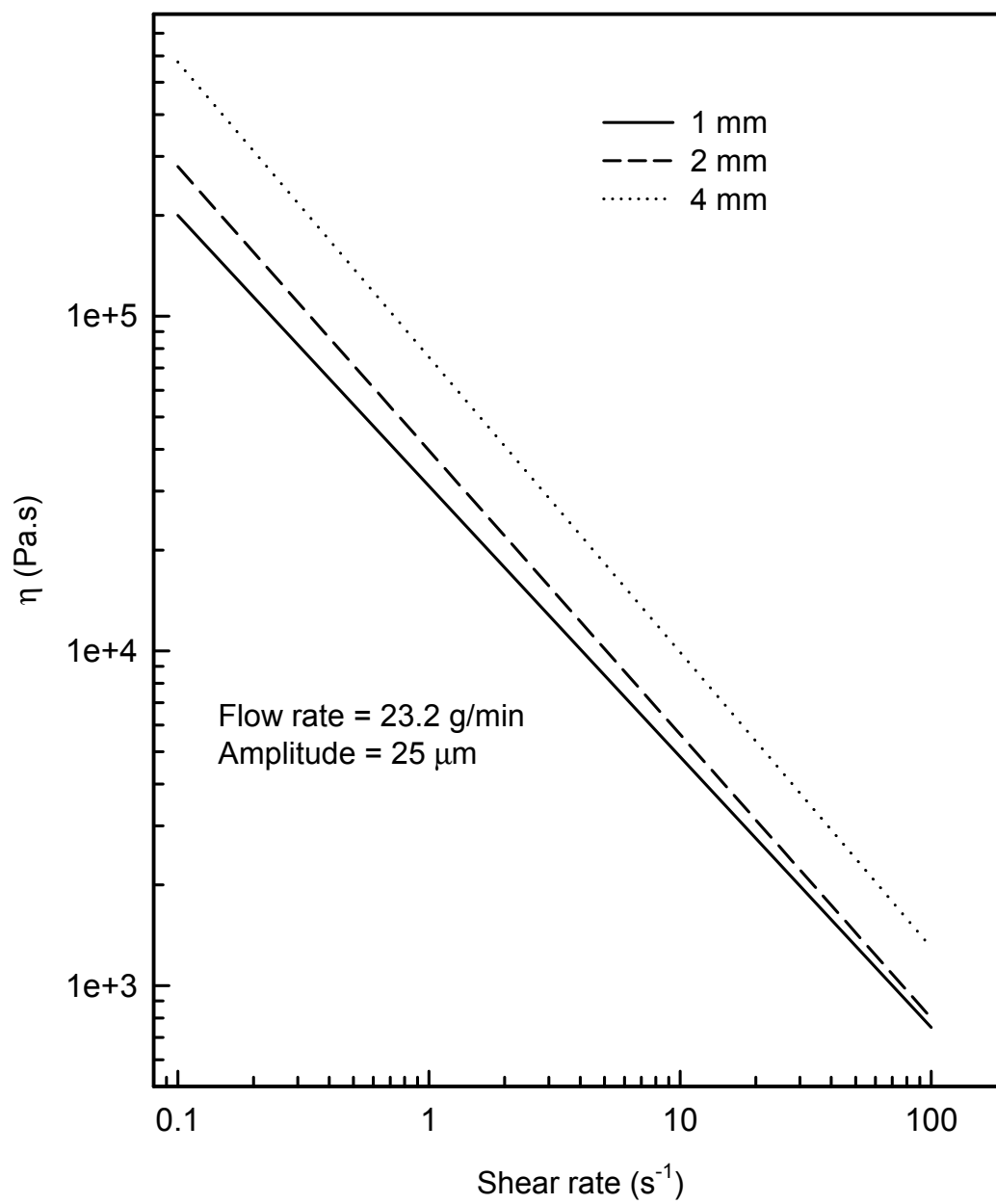


Figure 4.70 Viscosity versus shear rate at various gaps. Flow rate is 23.2 g/min and amplitude is 25.0 μm

process. As the gap size increased, the process less affected the resulting materials and the viscosities were higher.

The table below shows the slopes for the viscosity of the continuous samples. You can compare the slopes at different flow rates and amplitudes for different gap sizes.

Table 4.1 Viscosity Slope Table of Continuous Samples

Flow Rate	Amplitude	n @ 1mm	n @ 2mm	n @ 4mm
4.2	16.5	-.828	-.858	-.830
4.2	20	.762	-.836	-.829
4.2	25	-.715	-.826	-.856
8	16.5	-.809	-.836	-.862
8	20	-.784	-.836	-.858
8	25	-.721	-.823	-.870
15.8	16.5	-.815	-.809	-.888
15.8	20	-.826	-.834	-.897
15.8	25	-.794	-.835	-.867
23.2	16.5	-.819	-.831	-.884
23.2	20	-.811	-.841	-.878
23.2	25	-.809	-.848	-.882

4.4.1 Tensile Properties

Figures 4.71 and 4.72 show elongation at break versus crosslink density and gel fraction respectively. Figures 4.73 and 4.74 show tensile strength at break versus crosslink density and gel fraction respectively. The values for the original sample are not included in the figures because they make the scale too large to read differences that may occur in the treated samples. Original elongations at break values were 400% and the original tensile strength was 3000 psi (20.68 MPa). It can be seen that tensile strength and elongation at break does not correlate with crosslink density or gel fraction. The elongations of the processed materials are all less than ten percent of the original samples value. This is evidence that the tensile results are probably not significantly different enough from each other to consider them identifying characteristics of the material. None of the figures show strong enough trends to justify more detailed analysis. Useful data would show a relationship between the resulting crosslink densities of treated materials and the mechanical properties that spanned a range from very small numbers for the most treated and likely degraded material properties to properties near original values. This data does show a relationship between gel fraction and elongation using different gaps. As the gap increases, the elongation of the materials increases. In typical elongation measurements of polymers elongation is influenced largely by chain entanglement between polymer molecules. As outlined in the experimental part, when the plaques for the tensile tests were made, the treated particles were heated and compression molded, then the samples were cut from the plaques. These measurements are more likely showing an increased mechanical adhesion between treated particles in the specimens. Mechanical adhesion is the phenomenon in which interfacial forces hold surfaces together and occurs under pressure in polymers. This does not necessarily

involve chain entanglement, but more likely a mechanical locking into the microtopography of the surface¹⁹. Spin welding of crosslinked polymers for example does not lead to high degrees of chain entanglement, but does generate enough heat that surfaces of polymers are allowed to bond together more from plastic deformation than chain entanglement. The particles in the materials run with the smaller gaps have been exposed to higher strain amplitude that would make the particle surfaces smoother and less likely to bond together when pressurized. The particles processed with the larger gaps were exposed to lower strain amplitudes and their surfaces were allowed to remain more irregular, and thus more likely to stick together when under heat and pressure. This shows itself with generally higher elongation for specimens treated with the larger gap in the process.

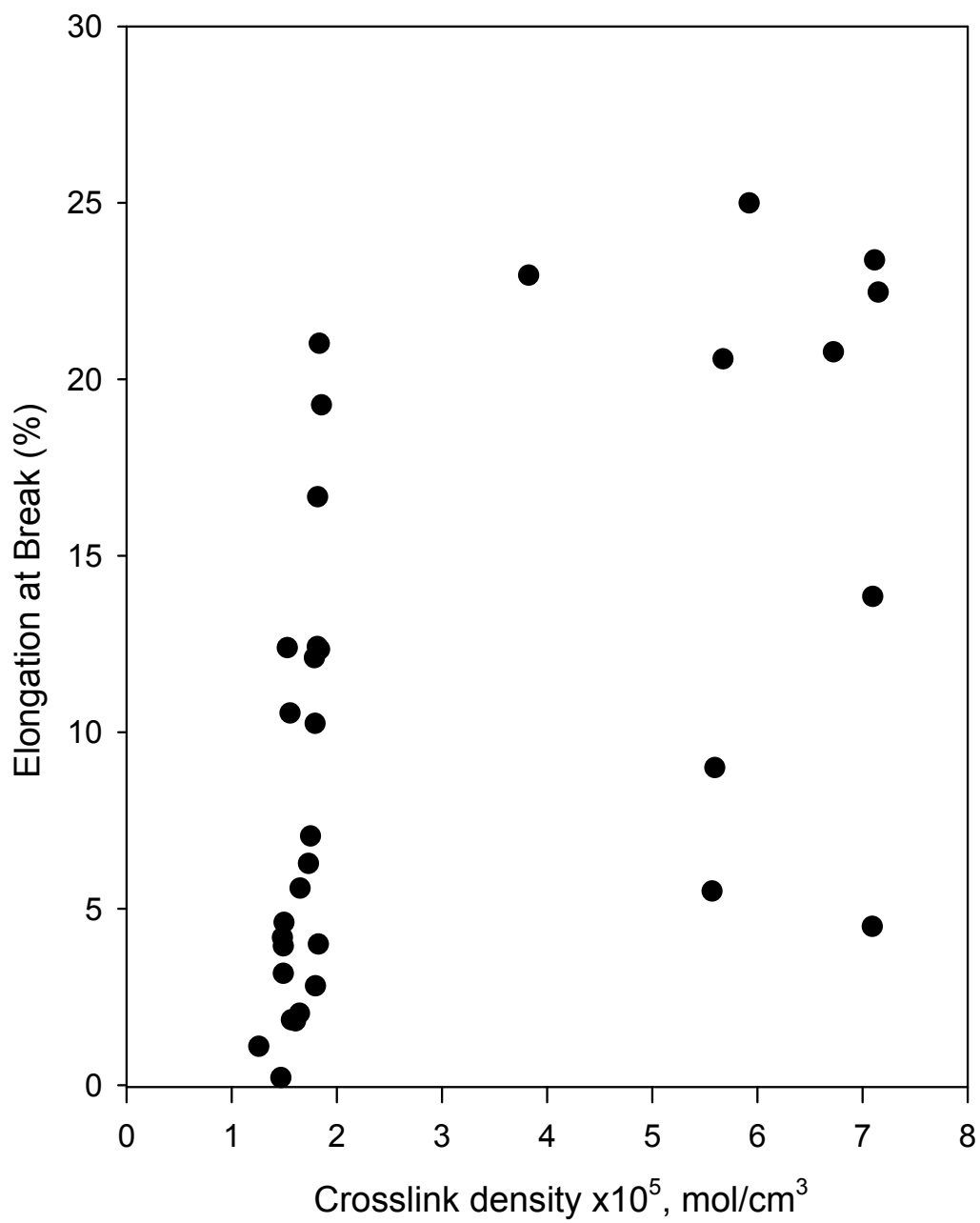


Figure 4.71 Elongation at break as a function of crosslink density for samples treated in continuous decrosslinking process

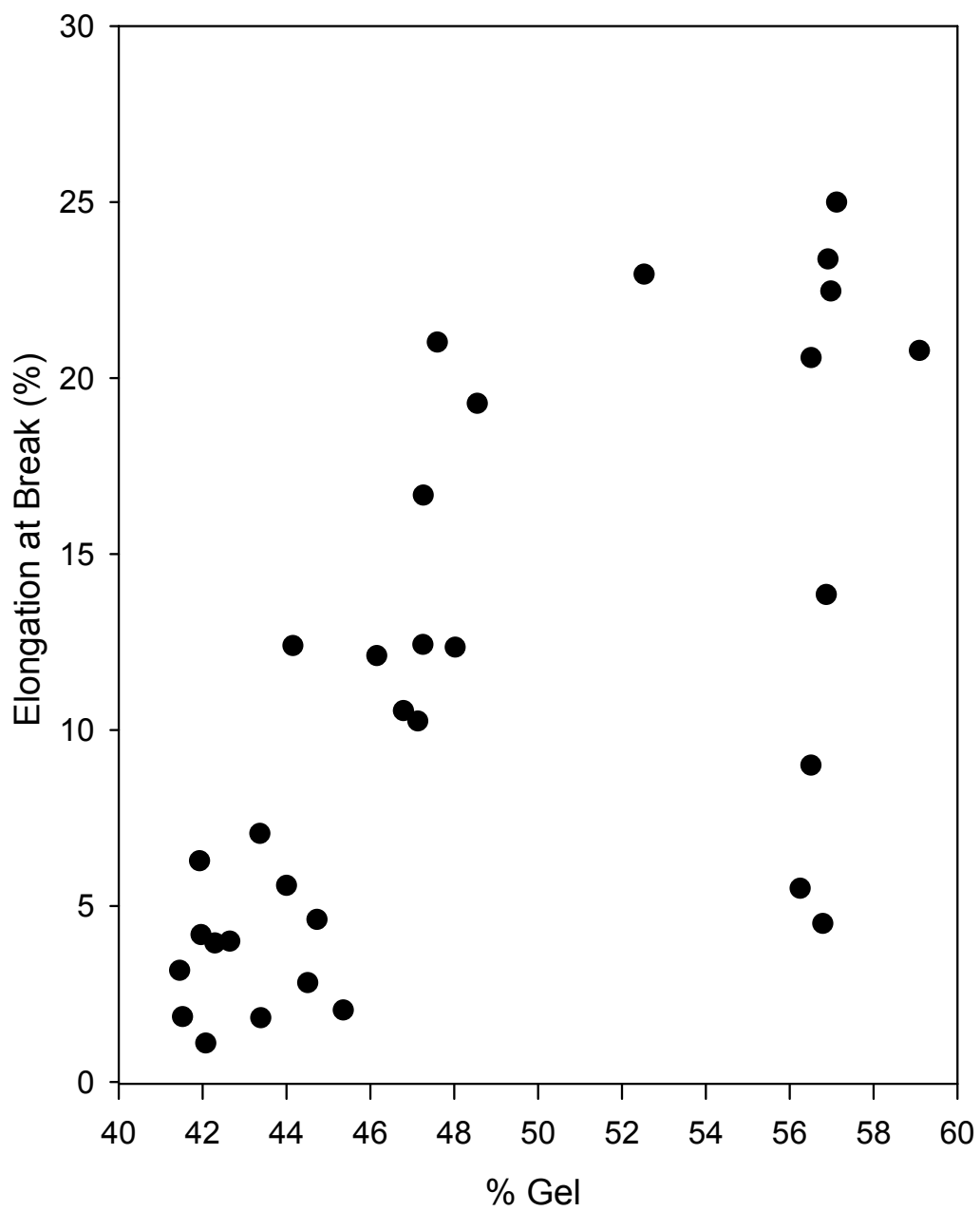


Figure 4.72 Elongation at break as a function of % gel for samples treated in continuous decrosslinking process.

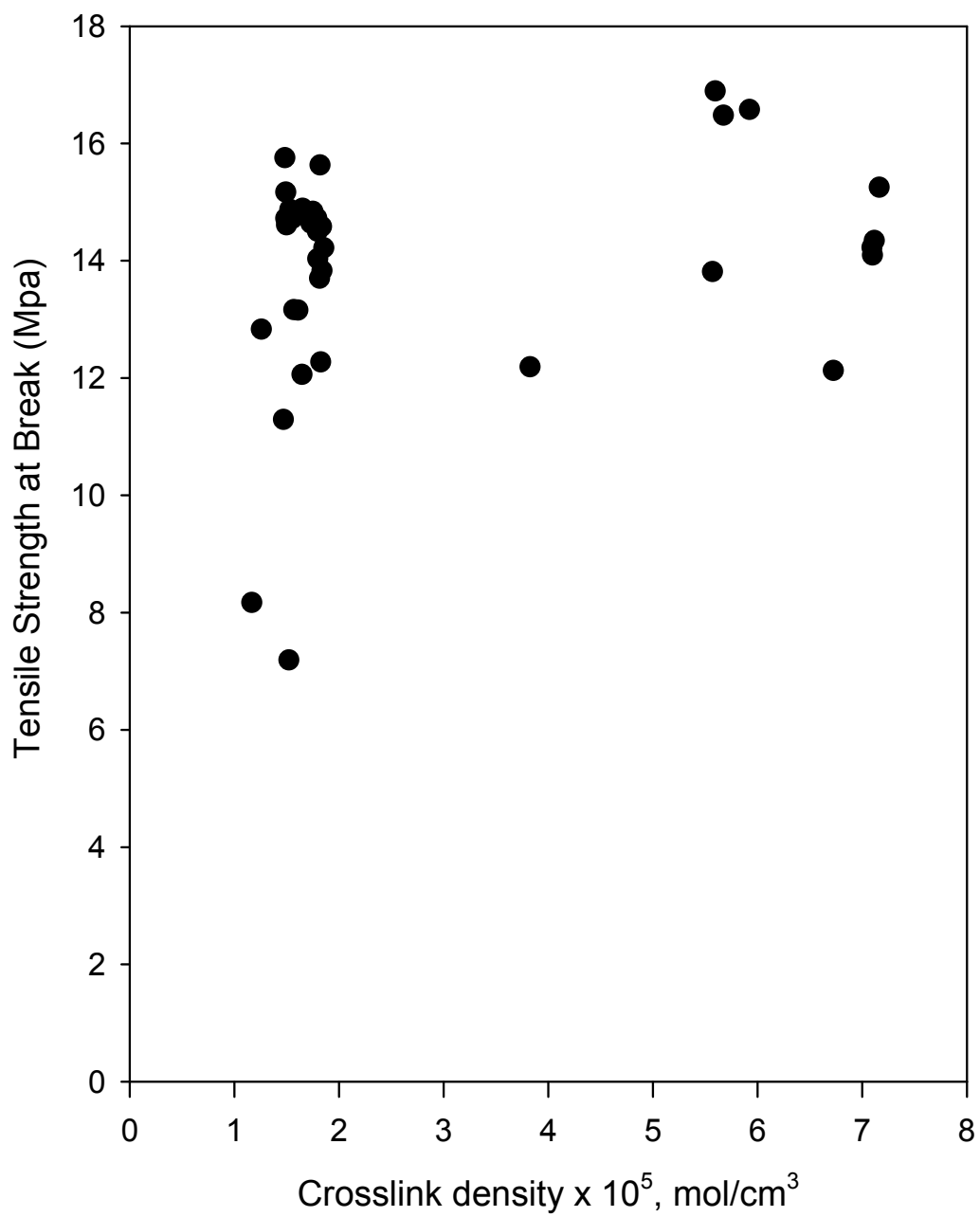


Figure 4.73 Tensile strength at break as a function of crosslink density for samples treated in continuous decrosslinking process.

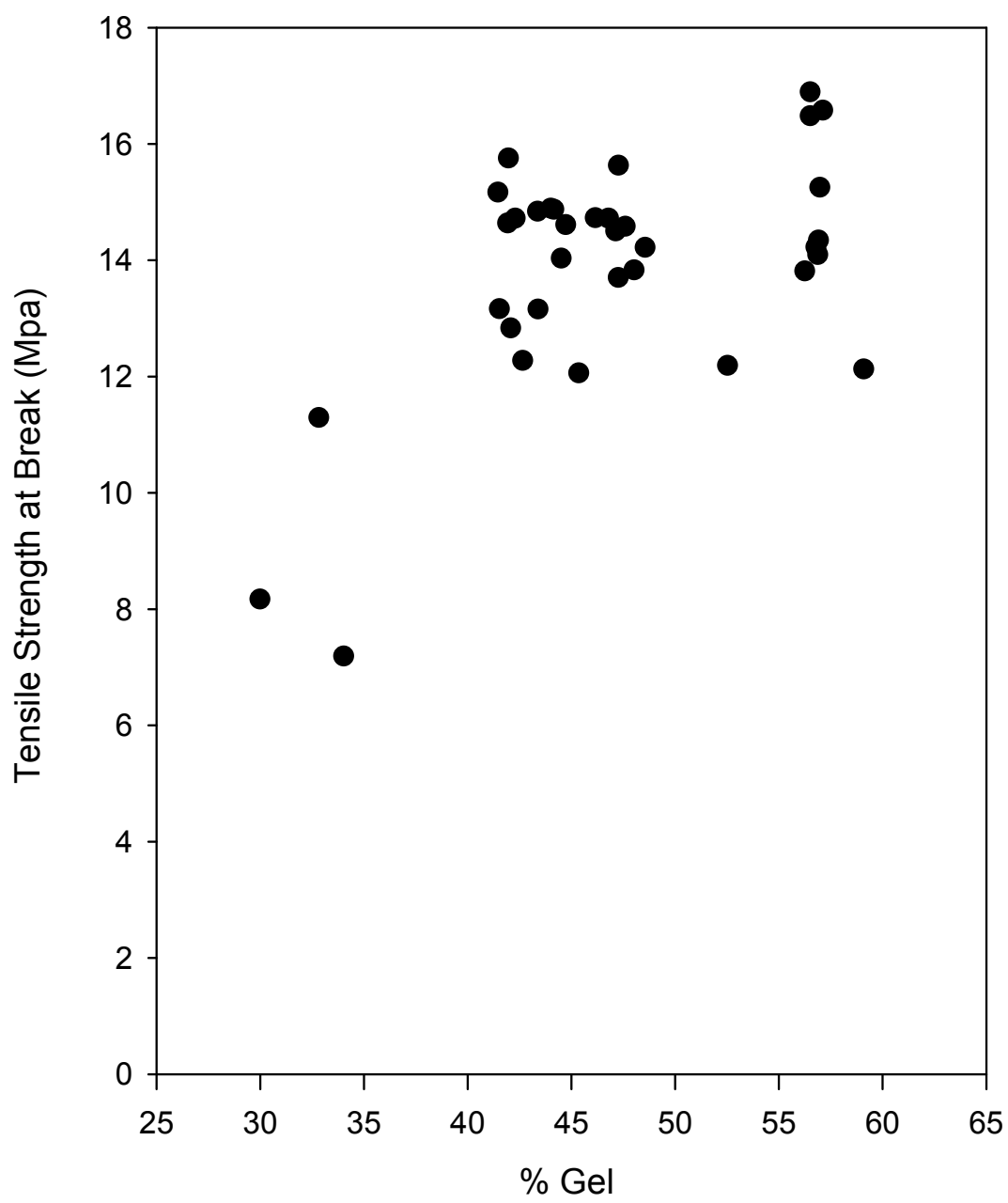


Figure 4.74 Tensile strength at break as a function of % gel for samples treated in continuous decrosslinking process.

CHAPTER V

CONCLUSIONS

This body of work investigates the affect of subjecting crosslinked polyethylene to various levels of ultrasonic energy. The expectation was that as the crosslinked material was exposed to varying ultrasonic energy levels, the crosslinked network would be affected in a manner that made the material useful again for polymer processing. Ideally, the most dramatic affect, or de-crosslinking, would take place at the crosslinked sites and the material could be used in a recycling operation. We found that not only did the introduction of this energy to the network have an affect, but that it was a predictable and repeatable affect that probably has implications on the ability to recycle this material. Static and continuous experiments were performed with results that support this conclusion. In static experiments, crosslinked material was subjected to ultrasonic energy for a controlled amount of time, pressure and energy level. The continuous experiments subjected a ground material to ultrasonic energy with control of the flow rate, energy level, and die gap. The strain amplitude concept was able to be applied to the results found during this examination.

The strain amplitude concept looks at the strain that a molecule is put under as it is subjected to mechanical deformations that occur on the molecular level. The strain amplitude concept says that a crosslinked network can support a certain amount of strain that if exceeded, results in a broken network at its most strained links. In this

experiment, a controlled amount of strain is introduced to the network using an energy source that transmits energy to it through an ultrasonic horn. The strain amplitude concept investigated by comparing the resulting gel fraction of various samples of known thickness exposed to the same ultrasound energy and was shown valid over the range of samples tested. Thicker samples responded less to the process than the thinner samples in both static and continuous experiments. In static sonication experiments, thinner samples also responded more predictably than thick ones. This was understood to occur because of the strain amplitude and perhaps because of a reduction in the material's ability to transmit energy after its surface has been de-crosslinked. The effect on the thicker samples as far as decrosslinking goes is diminished because the strain amplitude over the thicker samples is less, perhaps to a point of ineffectiveness. Increased exposure time and pressure also showed an increased response to the process.

Viscosity of the specimens is affected by forces such as Van Der Waalls bonding, chain entanglement, elasticity, testing temperature and molecular chain length. In this experiment, all properties other than chain length should have been affected to the same degree, if at all, leaving chain length as the primary measurement of viscosity. Viscosity of each specimen treated in continuous ultrasonic process was measured using the RMS 800 viscometer. Since viscosity in this case is primarily a measurement of molecular chain length, and chain length has a direct relationship with viscosity, the reasonable conclusion is reached that the materials with a lower measured viscosity after the treatment had shorter chain lengths than those with higher viscosities. The question on where the chains were shortened remains. If the chains were shortened by random thermal or mechanical degradation, we would expect to see more random viscosity results and an unstable gel fraction versus crosslink density chart. Instead, we recorded predictable viscosity measurements and the normalized gel fraction versus crosslink

density figures were stable and showed strong trends. The non-random reduction in viscosity lead us to the conclusion that the chains were most likely broken in the crosslinked regions which would be the areas exposed to the highest stress in the mechanical vibrations of a network under ultrasonic treatment.

Pressure and time were contributing factors in these experiments when the strain amplitude is at its smallest value for static and continuous experiments. This is an indication that the overall amount of energy that the material is exposed to is important if the strain amplitude is not high enough to break bonds rapidly. For continuous experiments, the time was relatively controlled using flow rate and pressure was not an independent variable. In the case of static experiments, exposure time and pressure were controlled.

Normalized gel fraction versus normalized crosslink density for materials that were exposed to the continuous decrosslinking process showed a strong trend and therefore data that was worth investigation. Since each material is derived from the original material, the differences in gel fractions and crosslink densities could be attributed to the differences in exposure to the continuous decrosslinking process.

Materials exposed to lower strain amplitudes showed a much lower response to the process. Materials run at the higher strain amplitudes showed a measurable and predictable response.

Exposure time to the process showed predictable results but did not have as significant and overall effect as increasing strain amplitude. Indeed, as long as the strain amplitude was great enough, the materials showed the same response to increasing flow rates and therefore decreased exposure times.

Figures comparing the viscosity of the treated materials showed trends for specimens run at 1 and 2 mm gaps. We learned from the static sonication experiments

that these gaps would provide us with material that was suitable for further examination. Specimens run at 1 and 2mm gaps with lowered throughput rates and higher exposure time showed very similar resultant viscosities. This is an indication that there is a limit to the amount of decrosslinking the treatment will impose on the specimens. As the flow rates were increased the affect of flow rates and specific energies became more apparent. These comparisons display very clearly that the materials viscosities are reduced according to exposure to ultrasonic energies. The data collected using the 1 mm gap for the continuous decrosslinking process shows clear differences in viscosities because of exposure to the decrosslinking process. The distribution of viscosities in these same figures becomes narrower as throughput rate is increased. It is important to note that while the first conclusion that can be reached is that material viscosities are reduced according to increased exposure to ultrasound, the gap and therefore strain amplitude that the materials are run at have probably the most significant affect on the results.

Results from tensile testing did not show any trends. Tensile strength is to a large degree a measurement of the weakest part of a specimen. Since the decrosslinked specimens represented materials whose networks were purposely fractured during processing, very irrational results were obtained for elongation at break and tensile strength versus crosslink density and gel fraction.

In all of the evaluations a few themes reoccurred that should be pointed out and considered. The 4 mm gap gave unreliable data in almost each case. It is theorized that the strain amplitude in this case is too small to allow all of the material that passed in front of the horn to be evenly treated. Samples produced with processes that used a smaller gap and therefore higher stain amplitudes, were more successfully treated by the ultrasound processing method. The throughput of the materials also showed a direct effect on the materials. This is an indication that not only is there a strain amplitude

effect, but also a specific energy effect on the materials making time of exposure an important parameter along with gap size.

REFERENCES

- 1 A. I. Isayev, Proceedings of the 23rd Israel Conference on Mechanical Engineering, Technion, Haifa, Paper #5.2.3 (1990).
- 2 A. I. Isayev and S. Mandelbaum, *Polym. Eng. Sci.*, 31, 1051 (1991).
- 3 A. I. Isayev, C. M. Wong, and X. Zeng, SPE ANTEC, 33, 207 (1987).
- 4 A. I. Isayev, C.M. Wong, and X. Zeng, *Adv. Polym. Tech.*, 10, 31 (1990).
- 5 A. I. Isayev, Recycling of Rubber, in Rubber Technologies Handbook, ed. by J. R. White and S. K. De, RAPRA, Shaubury, U.K. (2001).
- 6 D. Adhikari, D. Der. and S. Maiti, *Prog. Polym. Sci.*, 25, 909 (2000).
- 7 R. H. Nurse, SPE ANTEC, Polyethylene Recycling in North America- The Impact on Application Growth and Future Demand, 2357 (1992).
- 8 L. Erwin and J. Dohner, *Polym. Eng. Sci.*, 24, 1277 (1984).
- 9 L. Balamuth, U.S. Pat. 2,580,716, Jan. 1 (1952).
- 10 J. O. Farrer, British Pat. 602,801, June 3 (1948).
- 11 L. Balamuth, SAE Paper No. 650762 presented at the National Aeronautic and Space Engineering and Manufacturing Meeting, Los Angeles, Oct. 4-8 (1965).
- 12 A. Shoh, *Ultrasonics*, 14, 209 (1976).
- 13 D. Ensminger, "Ultrasonics Fundamentals, Technology, Applications", Chap. 12, 1988.
- 14 I. Alig, K. G. Hausler, *Acta Polymerica*, 39, 269 (1988).
- 15 N. E. Weare, J. N. Antonevich, and R. E. Monroe, *Weld. J. Res. Suppl.*, 39, 331 (1960).
- 16 E. H. Halstead and B. T. Vicario, *Can. J. Bot.*, 47, 1638 (1969).

- 17 A. I. Isayev, U.S. Patent 5,258,413 (1993).
- 18 A. I. Isayev and J. H. Chen, U.S. Patent 5,284,625 (1994).
- 19 D. V. Rosato, "Rosato's Plastic Encyclopedia and Dictionary", Hanser Publishers, Barcelona, 1993.
- 20 G. Gruenwald, "Plastics, How Structure Determines Properties", Hanser, Barcelona, 1993.
- 21 F. W. Billmeyer, "Textbook of Polymer Science", John Wiley & Sons, Inc., New York, 1984.
- 22 D. R. Askeland, "The Science and Engineering of Materials", PWS-Kent Publishing Company, Boston, 1984.
- 23 H. Zweifel, "Plastics Additives Handbook", Hanser Gardner Publications, Inc., Cincinnati, 2000.
- 24 E. H. Good, Improving The Marketability of Recycled Plastics, *Retec Proceedings*, Atlanta, GA, 139 (1992).
- 25 ASTM D2765-90, Standard Test Methods for Determination of Gel Content and Swell ratio of Crosslinked Ethylene Plastics.
- 26 P. J. Flory, *J. Chem. Phys.*, 18, 108 (1950).
- 27 A. F. M. Barton, "CRC Handbook of Polymer-Liquid Interaction Parameters and Solubility Parameters", CRC Press, Boca Raton, 1990.

APPENDIX

Table 1: Data for static sonicator, 1 mm thick samples

Sample #	Time (s)	Amp. (μm)	P (MPa)	Ext (%)	Gel (%)	Crosslink Density (mol/cm^3)
1	2	8.5	0.35	58.61	41.39	8.79E-06
2	5			70.69	29.31	3.10E-06
3	10			74.26	25.74	2.16E-06
4	2		0.69	66.91	33.09	4.16E-06
5	5			71.62	28.38	2.84E-06
6	10			79.56	20.44	1.13E-06
10	2	10	0.35	71.57	28.43	2.80E-06
11	5			74.46	25.54	2.02E-06
12	10			80.87	19.13	1.07E-06
13	2		0.69	74.55	25.45	1.74E-06
14	5			75.36	24.64	1.69E-06
15	10			79.08	20.92	1.04E-06
19	2	12	0.35	77.24	22.76	1.37E-06
20	5			78.56	21.44	1.10E-06
21	10			79.39	20.61	1.08E-06
22	2		0.69	77	23	1.49E-06
23	5			79.09	20.91	1.11E-06
24	10			79.95	20.05	1.00E-06

Table 2: Data for static sonicator, 2.1 mm thick samples

Sample #	Time (s)	Amp. (μm)	P (MPa)	Ext (%)	Gel (%)	Crosslink Density (mol/cm^3)
1	2	8.5	0.35	37.82	62.18	5.03E-05
2	5			49.7	50.3	3.00E-05
3	10			54.5	45.5	2.06E-05
4	2		0.69	47.69	52.31	2.87E-05
5	5			58.8	41.2	1.32E-05
6	10			62.32	37.68	1.08E-05
10	2	10	0.35	51.49	48.51	3.50E-05
11	5			55.95	44.05	1.81E-05
12	10			58.8	41.2	1.47E-05
13	2		0.69	54.91	45.09	2.77E-05
14	5			58.94	41.06	1.22E-05
15	10			62.31	37.69	1.09E-05
19	2	12	0.35	56.75	43.25	2.36E-05
20	5			61.21	38.79	1.14E-05
21	10			63.04	36.96	1.04E-05
22	2		0.69	58.31	41.69	2.09E-05
23	5			62.23	37.77	1.03E-05
24	10			63.07	36.93	1.00E-05

Table 3: Data for static sonicator, 3.9 mm thick samples

Sample #	Time (s)	Amp. (μm)	P (MPa)	Ext (%)	Gel (%)	Crosslink Density (mol/cm^3)
1	2	8.5	0.35	16.51	83.49	7.92E-05
2	5			22.63	77.37	6.82E-05
3	10			23.89	76.11	5.80E-05
4	2		0.69	22.28	77.72	7.56E-05
5	5			27.65	72.35	5.04E-05
6	10			31.7	68.3	4.50E-05
10	2	10	0.35	22.73	77.27	6.99E-05
11	5			26.75	73.25	6.28E-05
12	10			29.86	70.14	4.14E-05
13	2		0.69	26.61	73.39	6.59E-05
14	5			29.85	70.15	5.32E-05
15	10			37.04	62.96	5.24E-05
19	2	12	0.35	25.4	74.6	6.50E-05
20	5			30.81	69.19	5.30E-05
21	10			35.66	64.34	4.75E-05
22	2		0.69	28.86	71.14	5.00E-05
23	5			31.25	68.75	4.65E-05
24	10			36.19	63.81	3.16E-05

Table 4: Extrusion samples for 1 mm and 2 mm gap

Sample #	Extract (%)	Gel (%)	Crosslink Density (mol/cm ³)	Elongation at Break (%)	Tensile Strength at Break (psi)	Flow Rate (g/min)	Gap (mm)	Amplitude (μm)
1	65.98	34.02	1.53E-05		1043	4.2	1	16.5
2	67.18	32.82	1.48E-05	0.2148	1638	4.2	1	20
3	70.01	29.99	1.17E-05		1185	4.2	1	25
4	58.07	41.93	1.73E-05	6.282	2123	8	1	16.5
5	58.48	41.52	1.58E-05	1.852	1909	8	1	20
6	60.9	39.1	1.46E-05			8	1	25
7	55.49	44.51	1.80E-05	2.819	2035	15.8	1	16.5
8	56.63	43.37	1.77E-05	7.06	2152	15.8	1	20
9	58.54	41.46	1.50E-05	3.168	2200	15.8	1	25
10	57.35	42.65	1.83E-05	4	1780	23.2	1	16.5
11	57.71	42.29	1.50E-05	3.946	2135	23.2	1	20
12	58.04	41.96	1.49E-05	4.188	2285	23.2	1	25
13	56	44	1.66E-05	5.584	2160	4.2	2	16.5
14	56.61	43.39	1.61E-05	1.825	1908	4.2	2	20
15	57.92	42.08	1.26E-05	1.101	1861	4.2	2	25
16	53.85	46.15	1.80E-05	12.11	2136	8	2	16.5
17	54.64	45.36	1.65E-05	2.04	1749	8	2	20
18	55.27	44.73	1.51E-05	4.617	2119	8	2	25
19	52.74	47.26	1.82E-05	12.43	1987	15.8	2	16.5
20	52.87	47.13	1.80E-05	10.25	2103	15.8	2	20
21	53.21	46.79	1.56E-05	10.55	2135	15.8	2	25
22	51.45	48.55	1.86E-05	19.28	2062	23.2	2	16.5
23	52.4	47.6	1.84E-05	21.02	2115	23.2	2	20
24	52.74	47.26	1.83E-05	16.67	2267	23.2	2	25

Table 5: Extrusion samples for 4 mm gap

Sample #	Extract (%)	Gel (%)	Crosslink Density (mol/cm³)	Elongation at Break (%)	Tensile Strength at Break (psi)	Flow Rate (g/min)	Gap (mm)	Amplitude (μm)
25	55.84	44.16	1.54E-05	12.4	2157	4.2	4	16.5
26	51.98	48.02	1.85E-05	12.35	2006	4.2	4	20
27	47.47	52.53	3.84E-05	22.95	1768	4.2	4	25
28	40.91	59.09	6.76E-05	20.78	1759	8	4	16.5
29	43.75	56.25	5.60E-05	5.5	2003	8	4	20
30	43.49	56.51	5.62E-05	9	2450	8	4	25
31	43.49	56.51	5.70E-05	20.58	2390	15.8	4	16.5
32	42.88	57.12	5.95E-05	25	2404	15.8	4	20
33	43.21	56.79	7.13E-05	4.5	2063	15.8	4	25
34	43.13	56.87	7.13E-05	13.85	2044	23.2	4	16.5
35	43.09	56.91	7.15E-05	23.38	2080	23.2	4	20
36	43.02	56.98	7.19E-05	22.47	2212	23.2	4	25
Original	15.36	84.64	1.93E-04	400	3000			